Historical Deposition and Microbial Redox Cycling of Mercury in Lake Sediments from the Hudson Bay Lowlands, Ontario, Canada

Michelle Brazeau

Thesis submitted to the
Faculty of Graduate and Postdoctoral Studies
in partial fulfillment of the requirements for the
Master of Science, Biology
Ottawa-Carleton Institute of Biology
and
Faculty of Science, University of Ottawa

Thèse soumise à la
Faculté des études supérieures et postdoctorales
dans le cadre des exigences du programme de
Maîtrise ès sciences, Biologie
Institut pour la Biologie Ottawa Carleton
et
Faculté des sciences, Université d'Ottawa

Abstract

The repercussions of climate change are felt worldwide, but Arctic and subarctic regions, where climate warming is expected to be amplified, are especially vulnerable. An episode of mass fish mortality in the Sutton River in the Hudson Bay Lowlands (HBL) of Northern Ontario has elicited the interest of the scientific community. Several lakes were sampled over three years in an effort to better understand and document the changes that may be occurring in these lakes.

This study uses sediment cores to assess the history of mercury (Hg) deposition and to assess changes occurring in autochthonous productivity in these lakes. Sediments deposited after the onset of the industrial revolution contained significantly higher concentrations of Hg, with the highest concentrations found in the most recently deposited sediments. Hg concentrations in these pristine lakes rival those of lakes in heavily urbanized areas, indicating that they are in fact subjected to atmospheric deposition of Hg. There was a large variation in [Hg] of the surface sediments of 13 lakes; underscoring the importance of *in situ* processes in the fate of atmospherically deposited Hg. Methylmercury (MeHg) concentrations were not correlated with total mercury concentrations (THg), demonstrating how THg is a poor predictor of MeHg; the bioaccumulative neurotoxic form of mercury. The S2 fraction of Rock-Eval® Pyrolysis, C:N ratios and $\partial^{13}C$ signatures were used as proxies of autochthonous carbon and all indicated that the lakes have become increasingly productive, presumably due to warmer water temperatures and longer ice-free seasons.

Additionally, I use molecular techniques to detect and quantify the *merA* gene in the sediment; a proxy of bacterial mercury resistance involved in redox transformations. In Aquatuk, Hawley and North Raft Lakes, I observed a subsurface increase in *merA* genes in the sediment core, independently of a control gene and the [THg]. While I have not been able to explain the driving variables of this subsurface increase, I believe that the role of *merA* within remote lake sediments deserves further work.

Lastly, microcosms were used to measure the production of volatile elemental mercury (Hg(0)) from surface sediments of Aquatuk Lake. I used a combination of

analytical and molecular techniques to show that the production of Hg(0) is biogenic and tested the effect of nutrients, pH and ionic strength on the Hg(0) production rates. Ionic strength alone had the greatest impact on Hg(0) production rates, with increased Hg(0) production as ionic strength increases.

Résumé

L'impact des changements climatiques sont perçus dans toutes les régions du monde, mais est amplifié dans l'Arctique et les régions subarctiques où le réchauffement climatique est plus prononcé et où les écosystèmes sont plus vulnérables. Un épisode de mortalité soudaine de populations de poissons dans la rivière Sutton dans la région des Basses-terres de la Baie d'Hudson au nord de l'Ontario, a suscité un intérêt scientifique. Une campagne d'échantillonnage fut donc entreprise durant trois années consécutives afin de documenter les changements ayant lieu dans les lacs de cette région et d'en comprendre les effets.

Cette étude a eut recourt à des carottes de sédiments afin de déterminer les concentrations historiques de mercure (Hg) et les changements ayant lieu au niveau de la productivité primaire des lacs en question. Les sédiments déposés après la révolution industrielle ont une concentration plus élevée en Hg, atteignant un maximum dans les sédiments nouvellement déposés. Les [Hg] sont comparables aux concentrations mesurées dans des sédiments de lacs provenant de régions urbanisées, ce qui indique que les lacs de cette région vierge sont sujets à une déposition atmosphérique de Hg. Les [Hg] dans les sédiments superficiels de 13 lacs étaient très variables, illustrant l'importance des processus *in situ* sur les transformations du Hg de source atmosphérique. Il n'y a pas de corrélation entre les concentrations de méthylmercure (MeHg) et de mercure total (THg) parmi les sédiments superficiels des 13 lacs, démontrant que le THg n'est pas un bon indicateur du MeHg, une neurotoxine bioaccumulatrice. La fraction S2 des analyses de Rock-Eval®, les ratios C:N et la signature de $\partial^{13}C$ ont tous été utilisé comme indice de productivité primaire pour supporter l'hypothèse que les lacs démontrent une productivité primaire accrue.

J'ai utilisé des techniques moléculaires pour détecter et quantifier le gène *merA* parmi les bactéries se trouvant dans les sédiments. Ce gène est utilisé comme indicateur d'une résistance bactérienne au Hg et est impliqué dans sa transformation redox. Dans les lacs Aquatuk, Hawley et North Raft, j'ai mesuré une augmentation du nombre de gène *merA* avec la profondeur dans les sédiments

déposés avant les années 1960s, ce qui ne correspond pas au profil d'un gène de contrôle, ni au profil du Hg.

Finalement, j'ai développé des microcosmes afin de mesurer la production de mercure volatile (Hg(0)) à partir des sédiments superficiels du lac Aquatuk. J'ai utilisé des techniques analytiques et moléculaires pour déterminer que la production de Hg(0) était d'origine biologique et a testé l'impact de nutriments, du pH et de la force ionique sur les taux de production du Hg(0). La force ionique semble avoir le plus grand impact, causant une augmentation du taux de production de Hg(0) avec une augmentation de la force ionique.

Acknowledgements

I must first and foremost thank the two people who contributed the most to this work; my supervisors Dr. Jules Blais and Dr. Alexandre Poulain. Your respective expertises complemented each other perfectly, which yielded a thesis like no other. I thank you both for your support and guidance through this entire process. I feel privileged to have had to opportunity to learn from you. I would also like to thank my committee members Dr. Frances Pick and Dr. Roberto Chica for their guidance.

This project is but a small piece of a much bigger collaboration involving many institutions and world class scientists. I must thank Dr. Andrew Paterson, Dr. Bill Keller and Dr. Kathleen Ruhland without whom I would not have had a project at all. You both spent very long days in the field, battling the elements and swarms of mosquitoes, so that I could have samples to analyse; for that I thank you.

Philip Pelletier was instrumental in the molecular analyses. Phil you went above and beyond your duty and you were always happy to answer my endless pesky questions; for that I thank you. Linda Kimpe's assistance with the radiometric dating was essential to the project and to my comprehension of such a complex method. Linda I couldn't have done it without you; for that I thank you. I am indebted to Dr. Emmanuel Yumvihoze for his help with the mercury analyses and the BioReactor. Emmanu you were always extremely pleasant and very eager to help; for that I thank you. Thank you to the G.G. Hatch Stable Isotope Lab, especially Paul Middlestead, for the help with the carbon and nitrogen analyses.

My experience in the lab would not have been nearly as enjoyable without the people I have met and had the pleasure to work with. Sarah T. we were pioneers in our lab: we shared the challenges, the growing pains and the pleasures of being the first members of a new lab. I'm glad you were the one with whom I shared that experience. Jeffrey Nohra selflessly gave his time to help me process samples. Jeff I owe you one buddy! Xavier Giroux-Bougard contributed to the long and painful battle of establishing the RNA extraction protocol that, after much frustration and many failed attempts, proved successful. Xav; thanks for easing the battle!

To my other lab mates; Hardeep, Charlotte, Dima, Sijmen, Maggie and Julien and all the others, it was great to share this experience with you. But, more

importantly, I consider you all a part of my extended family. We have shared laughter, frustrations, failed PCRs, and yes; even tears. I thank you for enriching my experience in the lab and I wish you all the best in your future endeavours.

To Nic; thank you for putting up with me and sharing my frustrations as well as celebrating my successes. You supported me through the most difficult time in my life; I will always love you for that. Most importantly, thank you for saving me from myself and reminding me of the important things in life.

To my brother Jérémie and my sister Karine, you both are my best friends and my biggest fans. I know that you are behind me 100%, regardless. You encourage me to be the best I can be and to never give up. To my parents, whose love and support have never faltered, you both made me the person that I am today and for that I thank you.

Finally, to my dearest guardian Angel Annik; the battle you faced in your short life dwarfs all challenges that I may encounter in mine. The courage with which you faced your battle inspires me to no end. I hope you are well and have found peace. I miss you every day. I dedicate this thesis to you.

Sincerely,
Michelle Brazeau
Ottawa, January 2012

Table of Contents

Acronyms and Abbreviations

[x]	Concentration of x
AMDE	Atmospheric mercury depletion event
bp	Base pair
C	Carbon
cDNA	Complementary deoxyribonucleic acid
CEPA	Canadian Environmental Protection Act
CIC	Constant Initial Concentration model for ^{210}Pb dating
CRM	Certified reference material
CRS	Constant Rate of Supply model for ^{210}Pb dating
CVAFS	Cold vapour atomic fluorescence spectroscopy
DOM	Dissolved organic matter
DNA	Deoxyribonucleic acid
EA	Elemental analysis
EF	Enrichment factor
EtBr	Ethidium Bromide
GC-AFS	Gas chromatography – atomic fluorescence spectroscopy
HBL	Hudson Bay Lowlands
HCl	Hydrochloric acid
Hg(II)	Divalent mercury
Hg^0	Elemental, volatile mercury
Hg^R	Bacterial mercury resistance
HI	Hydrogen index
HPLC	High performance liquid chromatography
glnA	Gene which encodes the Glutamine synthetase protein
MeHg	Methyl mercury, monomethyl mercury, CH_3Hg
merA	Gene which encodes the Mercuric reductase enzyme
MOPS	3-morpholinopropane-1-sulfonic acid
mRNA	Messenger RNA
N	Nitrogen
OC	Organic carbon

OI	Oxygen index
OM	Organic matter
OMOE	Ontario Ministry of the Environment
P	Phosphorus
PBS	Phosphate Buffered Saline solution
PCBs	Polychlorinated biphenyls
PCR	Polymerase chain reaction
PHg	Particulate mercury
RGM	Reactive gaseous mercury
RNA	Ribonucleic acid
SRB	Sulfate-reducing bacteria
THg	Total mercury

Glossary

Anadromous	Species of fish that live in the sea but breed in freshwater
Anthropogenic	An effect or an object resulting from human activity
Autochthonous	Originating from the place where it is found
Allochtonous	Sediment found in a place other than where their constituents were formed
Bioaccumulation	The build-up of a substance in the tissues of an organism
Biogenic	Originating from a biological, live source
Biomagnification	The non-linear increase in the concentration of a bioaccumulating substance as the food chain is ascended
Bioreactor	Name given to the receptacle of the fresh sediment incubations
Catchment	Also known as drainage basin; a land area from which surface waters converge into a common body of water
Complexation	The bonding of an atom or ion to a surrounding array of molecules
Eutrophic lake	Waters are rich in nutrients with high primary productivity
Extraction	Any procedure designed to separate the components of a mixture
Hypolimnion	The bottom layer of water in a thermally stratified lake
Indigenous	Belonging to a certain place
Isostatic rebound	The rise of land mass once it is released from the pressure of in ice sheet
Ligand	An ion or molecule that binds to a central metal atom or ion
Mer operon	A section of genomic DNA containing a cluster of genes that encode the proteins essential to bacterial mercury resistance
Mercuric Reductase	An enzyme that catalyses the transformation of divalent mercury to elemental mercury
Methylation	The process of adding a methyl group (CH_3) to a substrate
Minamata disease	Methylmercury poisoning
Oligotrophic lake	Waters are nutrient poor and offer little to sustain life

Oxidation	The loss of electrons in a redox reaction and consequent increase in oxidation state
Redox	Reduction-oxidation reactions in which atoms have their oxidation numbers altered; involves the transfer of electrons between species
Reduction	The gain of electrons in a redox reaction and consequent decrease in oxidation state
S1	The Rock-Eval fraction of organic matter which corresponds to volatile, free hydrocarbons
S2	The Rock-Eval fraction of organic matter which corresponds to the hydrogen-rich aliphatic biomacromolecules which form the cell walls of algal matter
Trophic level	The position of a species in the food chain
Volatilization	The process by which a substance is transformed into vapour/gas

List of Tables

List of Figures

Chapter 1

Chapter 2

Chapter 3

Chapter 4

Chapter 1.0: Introduction

1.1 Changes in Arctic and Subarctic Environments

It has become a well-known fact that the Arctic and subarctic regions are currently undergoing drastic climatic changes that have had repercussions on several aspects of the ecosystem (Post *et al.*, 2009). Climate warming is a global phenomenon but changes are expected to be amplified in Polar regions. Arctic sea-ice, permafrost and glaciers have already been radically reduced and changes in the ecosystems are becoming increasingly apparent (Post *et al.*, 2009).

By modifying temperature and precipitation patterns, the changing climate has also led to alterations in the fate and availability of contaminants. For example, Carrie *et al.* (2010) reported a significant increase in concentrations of mercury (Hg) and PCBs in brook charr (*Lota lota*) from the Mackenzie River despite falling or stable atmospheric concentrations. The changing climate is also expected to alter certain limnological characteristics of lakes, such as the occurrence or the strengthening of thermal stratification which can also have repercussions on the fate of contaminants. For example, Driscoll *et al.* (1995) reported an increase in methylmercury in lakes exhibiting anoxic conditions in the hypolimnion during summer stratification.

Most of the scientific attention that has been attributed to the Arctic in the past decades has focused on the Western Arctic and the Canadian Archipelago. The Eastern Arctic and the subarctic are comparatively understudied. The Hudson Bay Lowlands (HBL) in Northern Ontario represent a unique Eastern subarctic ecosystem which is underlain by continuous and discontinuous permafrost with unique characteristics due to the influence of the Hudson Bay (Rouse *et al.*, 1997; Rouse, 1991) (Fig.1.1). The area contains 280 000 km^2 of peatlands, making it the second largest peatland in the world, and is covered by Boreal forest, subarctic open forest (taiga) and tundra (Rouse *et al.*, 1997). It also contains innumerable lakes that vary from shallow ponds to deep, large lakes. The area is inhabited by several First Nations communities who depend on the land for their livelihood. Though the people who have depended on the land for centuries know that significant changes are occurring, very few of these changes

have been scientifically documented.

Sound management of resources and protection of both human and ecosystem health in Arctic regions requires better predictions of the fate of pollutants and the development of novel management strategies. The contaminants of greatest concern fall under the Canadian Environmental Protection Act (CEPA) toxic substance regulations and include many highly toxic elements such as mercury (Hg), cadmium (Cd), lead (Pb) and arsenic (As). Of these, Hg is recognized as a top priority and will be the main focus of this thesis.

1.2. Fish-Kills in the Hudson Bay Lowlands

In 2001, one of the first fish die-offs due to a warming event was recorded in an Eastern Arctic watershed: the Sutton River in the Lowlands of Hudson Bay (Gunn and Snucins, 2010). Several days of very warm air temperatures (>30^{o}C) combined with unusual thermal stratification of the upstream lake led to lethal conditions for the highly productive population of anadromous brook charr (*Salvelinus fontinalis*) that uses these waters for reproduction.

The Sutton River is a renowned angling river that drains into the Hudson Bay. The physical characteristics of the river make it very susceptible to atmospheric changes; for example, the delta area at the mouth of the river is only 20cm deep and extends for about 4 km (Gunn and Snucins, 2010). Fish returning from the sea must cross this delta area and are subjected to a very sharp thermal gradient while undergoing osmotic changes. In 2001, anglers reported major die-offs of brook charr and white suckers (*Catostomus commersoni*) in the warm shallow waters of the lower section of the river.

The headwater lake of the Sutton River is Hawley Lake; a clear oligotrophic lake located on the Precambrian bedrock of the Sutton Ridges (Gunn and Snucins, 2010). At the same time as the fish-kills were reported in August 2001, a detailed fisheries survey was performed on Hawley Lake and a strong thermal stratification was observed (Fig. 1.2). In the past, the lake had been characterized as a cold wind-mixed isothermal lake; however this appears to be changing.

The Ontario Ministry of the Environment has initiated a campaign to study the changing lakes of the Hudson Bay Lowlands. It is through this organization's efforts that the present work was made possible. Three sampling campaigns were executed over the summers of 2009, 2010 and 2011 under the direction of Andrew Paterson (OMOE). Numerous collaborations between governmental and academic institutions have stemmed from this endeavor in an effort to thoroughly study the changes occurring in lakes of the Hudson Bay Lowlands in Northern Ontario.

1.3. Mercury Contamination

Mercury is the only metal to be liquid at room temperature and has a very complex transformation cycle which includes chemical, geological and biological reactions, warranting the need to consider it separately from other heavy metals (Morel *et al.*, 1998). Mercury in its elemental form (Hg(0)) is volatile and accounts for >95% of the mercury in the atmosphere (Lindberg *et al.*, 2007; Gustin *et al.*, 2008). It has an atmospheric residence time of 1-2 years allowing its distribution to areas far removed from any point source, making it a truly global pollutant (Lamborg *et al.*, 2002). The other 5% of Hg in the atmosphere consists of reactive gaseous mercury (RGM) and particulate mercury (PHg) which are more reactive and deposit closer to the point of emission (Lindberg *et al.*, 2007). Hg is naturally occurring in the Earth's crust in a variety of mercury-sulphur (HgS) binary minerals (Barnes and Seward, 1997). The HgS minerals can be solubilized and converted into various forms by natural or anthropogenic processes. The predominant sources of Hg to the atmosphere are due to anthropogenic activities which include the combustion of fossil fuel and coal, the incineration of products containing Hg such as fluorescent light fixtures, batteries, dental restorations, and many others (Barkay *et al.*, 2003). Hg is also heavily used in the mining industry, particularly in gold mining, which has led to the contamination of numerous aquatic ecosystems (Murdoch and Clair, 1986).

The form of Hg that is of greatest biological concern is methylmercury (CH_3Hg or MeHg); a potent bioaccumulative neurotoxin. The main source of

exposure to humans is through consumption of contaminated foods; especially fish and other aquatic mammals. The first documented case of widespread methylmercury poisoning was in Minamata Bay, Japan, in the early 1950s and methylmercury poisoning has since been known as Minamata disease (Takeuchi *et al.*, 1962). The most common symptoms in adults include loss of sensory, visual and auditory functions, muscular weakness and damage to areas of the brain responsible for coordination (Sanfeliu *et al.*, 2001). Developing fetuses are especially at risk as MeHg penetrates the placental barrier and newborns are susceptible to methylmercury when exposed through breast milk. A considerable reduction in brain size, overactive reflexes and severe motor and mental impairments are all common symptoms of pre- and post-natal exposure (Sanfeliu *et al.*, 2001).

1.3.1. The Mercury Cycle

Hg has a very complex biogeochemical cycle because it is readily transformed between the oxidation states of +2, +1 and 0 through biotic and abiotic reactions (Fig. 1.3). Volatile elemental mercury, Hg(0), can be oxidized both biotically and abiotically to ionic mercury, Hg(II), which is rapidly adsorbed to rain, snow and air-borne particles and then deposited onto any surface (Smith *et al.*, 1998; Skov *et al.*, 2004). Hg(II) can then be methylated to methylmercury again through biotic and abiotic processes (Jensen and Jernelov, 1969; Weber, 1993). If MeHg does not get incorporated into the food web, it can be abiotically degraded to methane (CH_4) and Hg(0) by UV rays (Suda *et al.*, 1993). Some bacteria can degrade MeHg into Hg(II) and subsequently into Hg(0) (Barkay *et al.*, 2003). These transformations are catalyzed by an enzymatic complex involved in Hg scavenging, uptake and transformation which is referred to as bacterial mercury resistance (described in section 1.3.4). This resistance plays a major role in the Hg cycle in sediments yet the scale at which this reaction occurs and the fate of the newly formed Hg(0) remains unclear.

1.3.2. Mercury in the Arctic and Subarctic Regions

Because of its volatility, elemental mercury travels over long distances. Hg(0) from lower latitudes follows global air currents and is transported to high latitudes and altitudes (Steffen *et al.*, 2008). As a result of this long-range transport, high levels of Hg can be found in areas far removed from point sources of Hg contamination.

In 1995, unexpectedly low concentrations of Hg(0) were recorded in the Arctic air in the springtime (at polar sunrise) (Steffen *et al.*, 2008). This phenomenon is now known as atmospheric mercury depletion events (AMDEs). They occur at polar sunrise as a result of a series of photochemically initiated reactions involving ozone and halogen compounds of marine origin (Simpson *et al.*, 2007) (Fig. 1.4). AMDEs were observed throughout the high Arctic and in subarctic environments under the influence of marine systems such as northern Quebec (*e.g.,* Kuujjuarapik) or northern Manitoba (*e.g.,* Churchill). To the best of our knowledge, no studies of this phenomenon have been performed in the HBL of Northern Ontario, but AMDEs are hypothesized to occur at this location as well, potentially increasing the Hg burden of this pristine region.

During AMDEs, Hg(0) is depleted from the atmosphere and oxidized to Hg(II), the much more reactive species, which subsequently partitions onto solid surfaces such as aerosols and snow (Steffen *et al.*, 2008). The fate of the newly deposited mercury is still unclear. A variable proportion of it can be re-emitted from the snow pack to the atmosphere, it can undergo reduction and be reemitted as volatile elemental mercury, or it can be methylated (Steffen *et al.*, 2002). Regardless, a portion of it is transported by melt water to streams and lakes, where the potential for methylation is highest. Elevated levels of MeHg have been documented in Arctic marine wildlife which is an important source of food for many Inuit populations (Macdonald and Bewers, 1996). As a result, health problems due to high levels of MeHg in tissues and blood are common in communities across the Arctic (Fontaine *et al.*, 2008). Unfortunately the patterns of contamination remain poorly understood.

1.3.3 Mercury and Organic Matter

The presence of organic and inorganic ligands in water affects the speciation of Hg through complexation (Ravichandran, 2004). Dissolved organic matter (DOM) is a ubiquitous ligand in aquatic environments and empirical evidence has shown that DOM interacts very strongly with Hg, affecting its speciation and bioavailability (Loux, 1998). Mercury has a very strong affinity for sulfur; Skyllberg *et al.* (2006) revealed that reduced organic sulfur and oxygen/nitrogen groups are involved in the complexation of Hg to humic substances (a form of DOM). The impact of DOM on methylation of Hg is ambiguous. Some studies show that an increase in organic matter increases mercury methylation by stimulating the methylating microbial community (Hammerschmidt and Fitzgerald, 2004). However, Ravichandran *et al.* (1999) showed that increases in DOM decreased methylation rates due to the increased complexation of Hg to organic ligands, thus reducing its bioavailability. The fact remains that organic matter (OM) is an important factor to consider when studying the mercury cycle in aquatic environments.

1.3.3.1 Algal-Mercury Scavenging Hypothesis

As mentioned above, lakes in Arctic and subarctic regions are experiencing changes due to global warming. Though the issue is controversial, one fact is clear; lakes that are warming are also experiencing or are expected to experience an increase in autochthonous productivity (Magnuson *et al.*, 1997; Blenckner *et al.*, 2002; Karlsson *et al.*, 2005).

Sedimentary Hg concentrations of lakes far removed from anthropogenic sources of Hg are believed to track delivery of atmospheric Hg, which is likely to be the dominant source of Hg to these lakes. Therefore, lake sediments have been used as historical proxies for atmospheric mercury. However, a recent increase in primary productivity of some aquatic systems has stimulated research on the importance of organic matter in delivery of Hg to the sediment. Hare *et al.* (2010) demonstrated that natural changes in OM composition and dynamics in the Hudson Bay can cause variations in sedimentary Hg concentrations that are just as important as those caused by an increase in anthropogenic Hg emissions. Stern *et al.* (2009) published a study in which they propose and support the

'Algal-Mercury Scavenging hypothesis'. This hypothesis stipulates that a climate-driven increase in aquatic primary productivity is, to a certain extent, controlling the sedimentary accumulation of Hg. The authors suggest that phytoplankton is scavenging Hg from the water column and accelerating its deposition to the sediment. This is supported by the observation that sedimentary Hg concentrations in Arctic and subarctic lakes are steadily increasing despite steady or declining atmospheric Hg concentrations. This hypothesis could imply that using lake sediments as a proxy for historical Hg deposition may result in an overestimation of atmospheric Hg concentrations.

1.3.4 Bacterial Mercury Resistance

There are five known types of bacterial mercury resistance (Hg^R) or detoxification mechanisms however the most studied is the enzymatic reduction of Hg(II) to Hg(0) (Osborn *et al.*, 1997). Hg^R is usually located on conjugative plasmids and/or transposons and is grouped into operons (Radford *et al.*, 1981). An operon is a functioning unit of genomic material containing a cluster of genes under the control of a single regulatory signal or promoter (Madigan *et al.*, 2009). The genes encode polypeptides with regulatory, transport and enzymatic functions. The *mer* operon is responsible for Hg^R in both Gram-negative and Gram-positive bacteria and it can be located on transposons, plasmids or the bacterial chromosomes (Osborn *et al.*, 1997). It consists of MerP; a small periplasmic mercury binding protein, MerT and MerC; inner membrane proteins, and MerB; a protein (organomercurial lyase) that lyses MeHg into CH_3^+ and Hg(II) which is then reduced to Hg(0) by MerA; the mercuric reductase enzyme (Hg:NADP+ oxidoreductase, EC 1.16.1.1) (Barkay *et al.*, 2003; Gopinath *et al.*, 1989). MerR is a metal-responsive regulatory protein which is antagonistically regulated by MerD. These are the most common components of the Gram-negative *mer* operon but other genes have also been identified, such as *merG*, *merE* and *merF* (Barkay *et al.*, 2003).

MerA is arguably the most important part of the *mer* operon. This cytoplasmic enzyme utilizes NADPH as a source of electrons to catalyze the

conversion of Hg(II) to Hg(0) (Furukawa and Tonomura, 1972). Although the *mer* operon can be very diverse among species, it must contain *merA* to be functional (Rosen, 1996). Therefore the presence of *merA* can be used as a reliable proxy to assess the presence of a functional *mer* operon in a particular (meta)genome. The *merA* gene has been extensively studied in mercury contaminated environments; however it is comparatively understudied in non-contaminated areas. This is unfortunate as the *mer* operon reduces the amount of Hg available to methylating bacteria; greatly reducing its toxicity and the potential for bioaccumulation.

1.4 Objectives and Hypotheses

The present research is in collaboration with the Ontario Ministry of the Environment in an effort to understand and document changes occurring in 13 lakes from the Hudson Bay Lowlands.

1.4.1 Mercury Deposition and Organic Matter

The first objective is to determine the history of mercury deposition to lake sediment and how it relates to organic matter. From the results of previous studies, I hypothesize that Hg concentrations in sediments deposited after the onset of the industrial revolution will have higher Hg concentrations than those deposited in a pre-industrial time period. I also hypothesize an increase in organic matter of an autochthonous nature in recent sediments.

1.4.2 Bacterial Mercury Resistance

The second objective is to determine if the *merA* gene, a proxy of bacterial mercury resistance, can be detected in sediment cores from 3 lakes of this pristine region and, if so, to quantify the occurrence of the gene within the indigenous bacterial populations.

1.4.3 In situ Hg(0) Production

The last objective is to assess the potential for biogenic elemental mercury production in sediment from Aquatuk Lake and to determine which factors influence biogenic Hg(0) production.

1.5 References

Barkay, T., S.M. Miller and A.O. Summers. 2003. Bacterial mercury resistance from atoms to ecosystems. Fems Microbiology Reviews, 27(2-3): 355-384.

Barnes, H.L. and T.M. Seward. 1997. Geothermal systems and mercury deposits. In: Geochemistry of hydrothermal ore deposits. John Wiley and Sons, New York: pp: 699-736.

Blenckner, T., A. Omstedt and M. Rummukainen. 2002. A Swedish case study of contemporary and possible future consequences of climate change on lake function. Aquatic Sciences, 64(2): 171-184.

Carrie, J., F. Wang, H. Sanei, R.W. Macdonald, P.M. Outridge and G.A. Stern. 2010. Increasing contaminant burdens in an Arctic fish, burbot (*Lota lota*), in a warming climate. Environmental Science & Technology, 44(1): 316-322.

Driscoll, C.T., V. Blette, C. Yan, C.L. Schofield, R. Munson and J. Holsapple. 1995. The role of dissolved organic-carbon in the chemistry and bioavailability of mercury in remote Adirondack lakes. Water Air and Soil Pollution, 80(1-4): 499-508.

Fontaine, J., E. Dewailly, J.L. Benedetti, D. Pereg, P. Ayotte and S. Dery. 2008. Re-evaluation of blood mercury, lead and cadmium concentrations in the Inuit population of Nunavik (Quebec): A cross-sectional study. Environmental Health, 7: 1-13.

Furukawa, K. and K. Tonomura. 1972. Metallic mercury-releasing enzyme in mercury-resistant *Pseudomonas*. Agricultural and Biological Chemistry, 36(2): 217.

Gopinath, E., Kaaret, T.W. and Bruice, T.C. 1989. Mechanism of mercury (II) reductase and influence of ligation on the reduction of mercury (II) by a water soluble 1,5-dihydroflavin. Proceedings of the National Academy of Science, 86: 3041-3044.

Gunn, J. and E. Snucins. 2010. Brook charr mortalities during extreme temperature events in Sutton river, Hudson Bay Lowlands, Canada. Hydrobiologia, 650(1): 79-84.

Gustin, M.S., S.E. Lindberg and P.J. Weisberg. 2008. An update on the natural sources and sinks of atmospheric mercury. Applied Geochemistry, 23: 482-493.

Hammerschmidt, C.R. and W.F. Fitzgerald. 2004. Geochemical controls on the production and distribution of methylmercury in near-shore marine sediments. Environmental Science & Technology, 38: 1487-1495.

Hare, A.A., G.A. Stern, Z.Z.A. Kuzyk, R.W. Macdonald, S.C. Johannessen and F.Y. Wang. 2010. Natural and anthropogenic mercury distribution in marine sediments from Hudson Bay, Canada. Environmental Science & Technology, 44(15): 5805-5811.

Jensen, S. and A. Jernelov. 1969. Biological methylation of mercury in aquatic organisms. Nature, 223(5207): 753.

Karlsson, J., A. Jonsson and M. Jansson. 2005. Productivity of high-latitude lakes: Climate effect inferred from altitude gradient. Global Change Biology, 11(5): 710-715.

Lamborg, C.H., W.F. Fitzgerald, J. O'Donnell and T. Torgerson. 2002. A non-steady-state compartmental model of global-scale mercury biogeochemistry with interhemispheric atmospheric gradients. Geochim Cosmochim Ac, 66: 1105-1118.

Lindberg, S., R. Bullock, R. Ebinghaus, D. Engstrom, X. Feng, W. Fitzgerald, N. Pirrone and C. Seigneur. 2007. A synthesis of progress and uncertainties in attributing the sources of mercury in deposition. Ambio., 36: 19-32.

Loux, N.T. 1998. An assessment of mercury-species-dependent binding with natural organic carbon. Chem. Spec. Bioavail., 10: 127-136.

Macdonald, R.W. and J.M. Bewers. 1996. Contaminants in the Arctic marine environment: Priorities for protection. Ices Journal of Marine Science, 53(3): 537-563.

Madigan, M.T., J.M. Martinko, P.V. Dunlap and D.P. Clark. 2009. Brock biology of microorganisms. Twelfth Edn., California: Pearson Benjamin Cummings.

Magnuson, J.J., K.E. Webster, R.A. Assel, C.J. Bowser, P.J. Dillon, J.G. Eaton, H.E. Evans, E.J. Fee, R.I. Hall, L.R. Mortsch, D.W. Schindler and F.H. Quinn. 1997. Potential effects of climate changes on aquatic systems: Laurentian great lakes and Precambrian shield region. Hydrological Processes, 11(8): 825-871.

Morel, F.M.M., A.M.L. Kraepiel and M. Amyot. 1998. The chemical cycle and bioaccumulation of mercury. Annual Review of Ecology and Systematics, 29: 543-566.

Murdoch, A. and T.A. Clair. 1986. Transport of arsenic and mercury from gold mining activities through an aquatic system. Science of the Total Environment, 57: 205-216.

Osborn, A.M., K.D. Bruce, P. Strike and D.A. Ritchie. 1997. Distribution, diversity and evolution of the bacterial mercury resistance (*mer*) operon. Fems Microbiology Reviews, 19(4): 239-262.

Post, E., M.C. Forchhammer, M.S. Bret-Harte, T.V. Callaghan, T.R. Christensen, B. Elberling, A.D. Fox, O. Gilg, D.S. Hik, T.T. Hoye, R.A. Ims, E. Jeppesen, D.R. Klein, J. Madsen, A.D. McGuire, S. Rysgaard, D.E. Schindler, I. Stirling, M.P. Tamstorf, N.J.C. Tyler, R. van der Wal, J. Welker, P.A. Wookey, N.M. Schmidt and P. Aastrup. 2009. Ecological dynamics across the Arctic associated with recent climate change. Science, 325(5946): 1355-1358.

Radford, A.J., J. Oliver, W.J. Kelly and D.C. Reanney. 1981. Translocatable resistance to mercuric and phenylmercuric ions in soil bacteria. Journal of Bacteriology, 147(3): 1110-1112.

Ravichandran, M. 2004. Interactions between mercury and dissolved organic matter - A review. Chemosphere, 55(3): 319-331.

Ravichandran, M., G.R. Aiken, J.N. Ryan and M.M. Reddy. 1999. Inhibition of precipitation and aggregation of metacinnabar (mercuric sulfide) by dissolved organic matter isolated from the florida everglades. Environmental Science & Technology, 33(9): 1418-1423.

Rosen, B.P. 1996. Bacterial resistance to heavy metals and metalloids. Journal of Biological Inorganic Chemistry, 1(4): 273-277.

Rouse, W.R. 1991. Impacts of Hudson Bay on the terrestrial climate of the Hudson Bay Lowlands. Arctic and Alpine Research, 23(1): 24-30.

Rouse, W.R., M.S.V. Douglas, R.E. Hecky, A.E. Hershey, G.W. Kling, L. Lesack, P. Marsh, M. McDonald, B.J. Nicholson, N.T. Roulet and J.P. Smol. 1997. Effects of climate change on the freshwaters of Arctic and Subarctic North America. Hydrological Processes, 11(8): 873-902.

Sanfeliu, C., J. Sebastia and S.U. Kim. 2001. Methylmercury neurotoxicity in cultures of human neurons, astrocytes, neuroblastoma cells. Neurotoxicology, 22(3): 317-327.

Simpson, W.R., R. von Glasow, K. Riedel, P. Anderson, P. Ariya, J. Bottenheim, J. Burrows, L.J. Carpenter, U. Friess, M.E. Goodsite, D. Heard, M. Hutterli, H.W. Jacobi, L. Kaleschke, B. Neff, J. Plane, U. Platt, A. Richter, H. Roscoe, R. Sander, P. Shepson, J. Sodeau, A. Steffen, T. Wagner and E. Wolff. 2007. Halogens and their role in polar boundary-layer ozone depletion. Atmospheric Chemistry and Physics, 7(16): 4375-4418.

Skov, H., J.H. Christensen, M.E. Goodsite, N.Z. Heidam, B. Jensen, P. Wahlin and G. Geernaert. 2004. Fate of elemental mercury in the Arctic during atmospheric mercury depletion episodes and the load of atmospheric mercury to the Arctic. Environmental Science & Technology, 38(8): 2373-2382.

Skyllberg, U., P.R. Bloom, J. Qian, C.M. Lin and W.F. Bleam. 2006. Complexation of mercury(II) in soil organic matter: EXAFS evidence for linear two-coordination with reduced sulfur groups. Environmental Science & Technology, 40(13): 4174-4180.

Smith, T., K. Pitts, J.A. McGarvey and A.O. Summers. 1998. Bacterial oxidation of mercury metal vapor, Hg(0). Appl Environ Microb, 64(4): 1328-1332.

Steffen, A., T. Douglas, M. Amyot, P. Ariya, K. Aspmo, T. Berg, J. Bottenheim, S. Brooks, F. Cobbett, A. Dastoor, A. Dommergue, R. Ebinghaus, C. Ferrari, K. Gardfeldt, M.E. Goodsite, D. Lean, A.J. Poulain, C. Scherz, H. Skov, J. Sommar and C. Temme. 2008. A synthesis of atmospheric mercury depletion event chemistry in the atmosphere and snow. Atmospheric Chemistry and Physics, 8(6): 1445-1482.

Steffen, A., W. Schroeder, J. Bottenheim, J. Narayan and J.D. Fuentes. 2002. Atmospheric mercury concentrations: Measurements and profiles near snow and ice surfaces in the Canadian Arctic during Alert 2000. Atmospheric Environment, 36(15-16): 2653-2661.

Stern, G.A., H. Sanei, P. Roach, J. Dalaronde and P.M. Outridge. 2009. Historical interrelated variations of mercury and aquatic organic matter in lake sediment cores from a subarctic lake in Yukon, Canada: Further evidence toward the algal-mercury scavenging hypothesis. Environmental Science & Technology, 43(20): 7684-7690.

Suda, I., M. Suda and K. Hirayama. 1993. Degredation of methyl and ethyl mercury by singlet oxygen generated from sea-water exposed to sunlight or ultraviolet-light. Archives of Toxicology, 67(5): 365-368.

Takeuchi, T., N. Morikawa, H. Matsumoto and Y. Shiraishi. 1962. A pathological study of Minamata disease in Japan. Acta Neuropathol, 2: 40-57.

Weber, J.H. 1993. Review of possible paths for abiotic methylation of mercury(II) in the aquatic environment. Chemosphere, 26(11): 2063-2077.

1.6 List of Figures

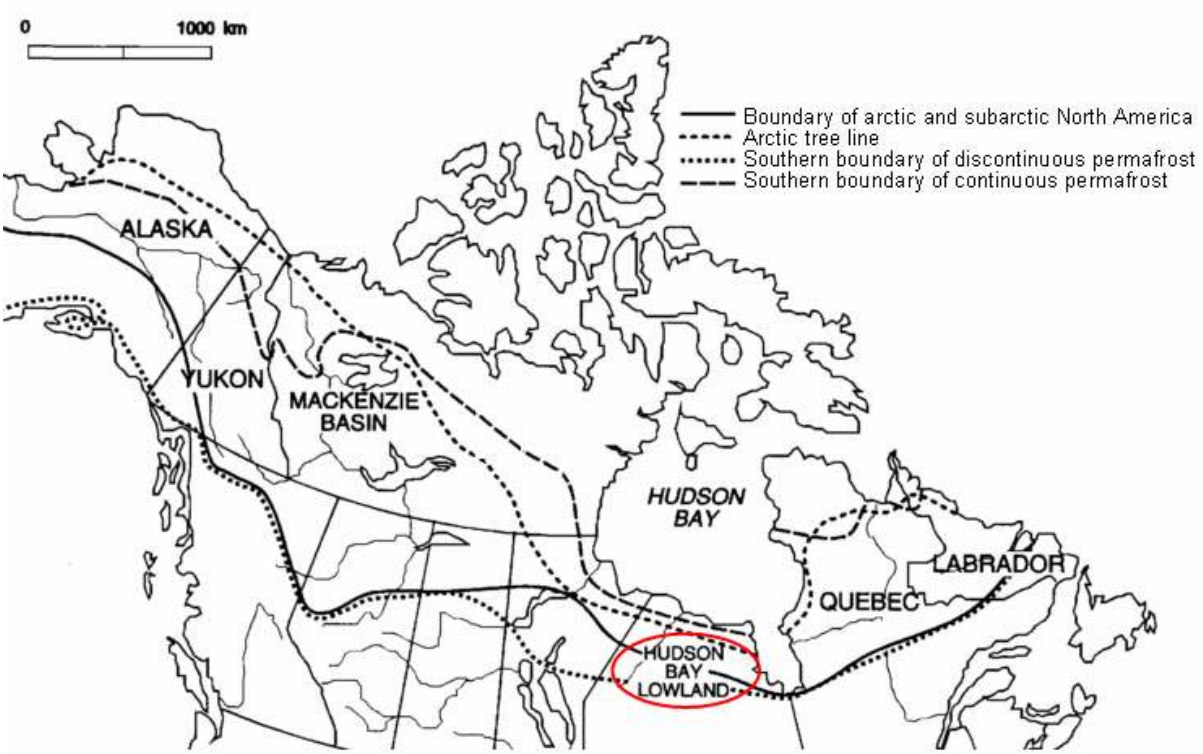

Figure 1.1: Map of Arctic and subarctic regions of North America showing the location of continuous and discontinuous permafrost, Arctic tree line and the location of the Hudson Bay Lowlands (modified with permission from Rouse *et al*., 1997).

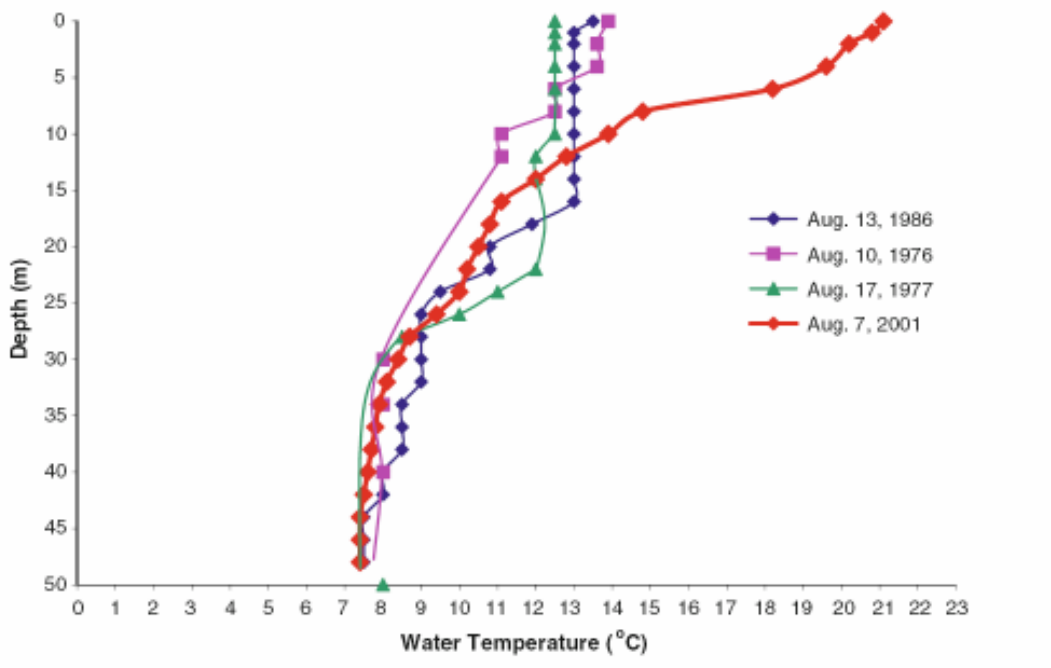

Figure 1.2: Water column temperature (^{o}C) profiles of Hawley Lake located in the Hudson Bay Lowlands of Ontario, Canada (Gunn and Snucins, 2010).

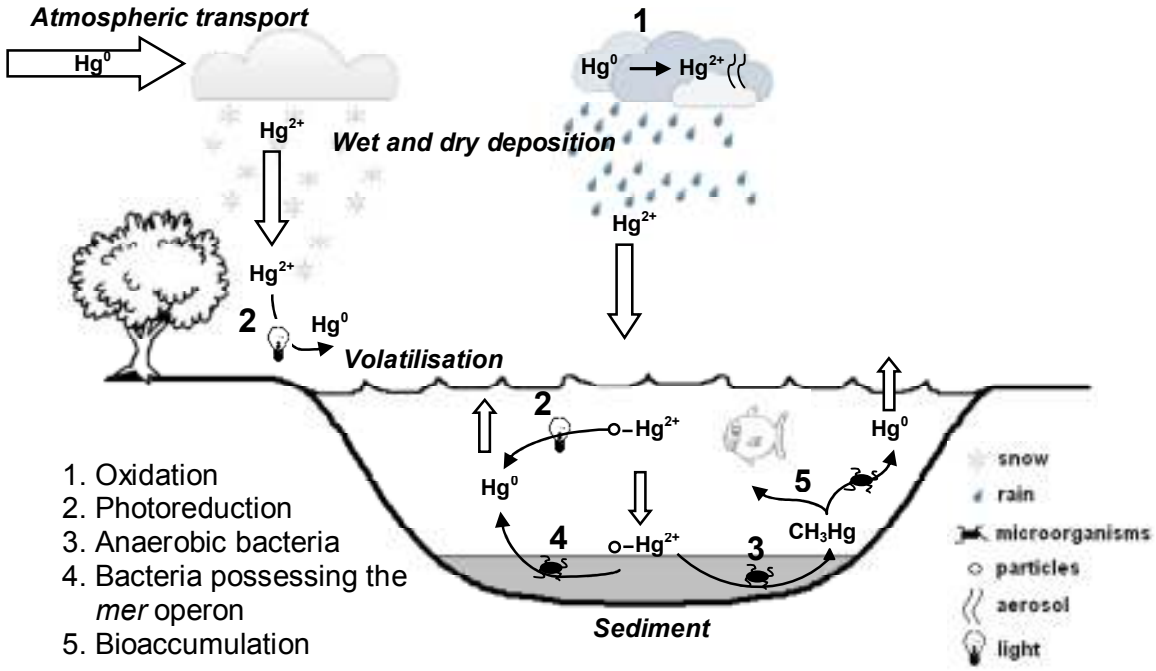

Figure 1.3: Schematic summary of the mercury (Hg) cycle in terrestrial and aquatic environments.

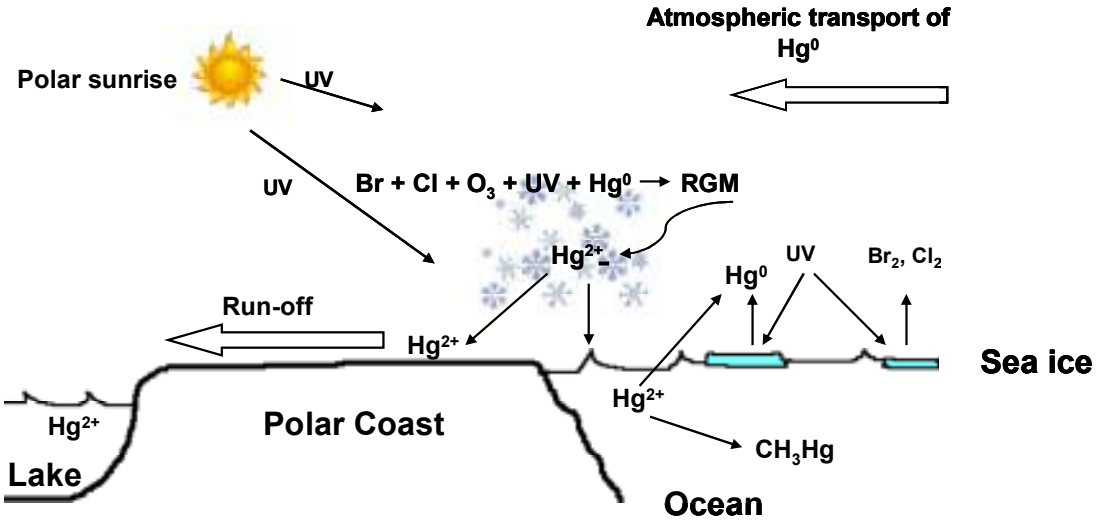

Figure 1.4: Simplified schematic representation of atmospheric mercury depletion event (AMDE) in coastal Polar Regions. Hg^0: elemental mercury, Hg^{2+}: ionic mercury, UV: ultraviolet light, Br: bromine, Cl: chlorine, O_3: ozone, RGM: reactive gaseous mercury, CH_3Hg: methylmercury

Chapter 2.0: Recent Changes in Mercury Deposition and Primary Productivity Inferred from Sediments of Lakes from the Hudson Bay Lowlands, Ontario, Canada

2.1 Abstract

Consequences of climate change have recently become apparent in Northern Ontario's aquatic ecosystems where warming waters are believed to have caused episodes of elevated fish mortality in lakes from the Hudson Bay Lowlands; a pristine environment far removed from industrial activities. The synthesis of methylmercury (MeHg) by methylating bacteria in lake sediments is mainly controlled by the availability of the ionic mercury substrate and organic matter to sustain bacterial activity. We use a paleolimnological approach to analyze changes in mercury (Hg) concentrations and organic carbon (OC) on a temporal and spatial level. Sediment cores show a steady increase of Hg post-1900 while OC increases are only seen in recent decades. Surface sediments of 13 lakes had a large variation in [Hg], ranging from 6.13 ± 0.7 ng g^{-1} to 125.4 ± 0.9 ng g^{-1} (dw), emphasizing the importance of post-depositional *in situ* processes in Hg cycling. There was no significant relationship between total Hg and MeHg in the surface sediments which illustrates how total Hg is a poor predictor of MeHg; the bioaccumulative neurotoxic form of Hg. Primary productivity was assessed with four different proxies; organic carbon, S2 C (algal-derived OC), C:N and $\partial^{13}C$. Each proxy supports an increase in autochthonous productivity of the lakes in recent decades and S2 was significantly correlated with Hg in both sediment cores. The use of paleolimnological proxies allowed us to identify a short-lived sedimentation event in Hawley Lake where a large amount of inorganic sediment was introduced into the lake between 1950 and 1960, presumably due to a disturbance in the catchment such as a forest fire. Hg, MeHg, sedimentation rate, OC, water content, hydrogen index and oxygen index profiles all show variations that coincide at the same core depth supporting the occurrence of a sedimentation event, demonstrating how lake sediments can be effective historical archives.

2.2 Introduction

Mercury (Hg) is a ubiquitous contaminant that is emitted through natural and anthropogenic processes and is identified as a priority chemical by the

United Nations Environment Programme (UNEP). It has a very complex transformation cycle which includes chemical, geological and biological reactions, warranting the need to consider it separately from other heavy metals (Morel *et al.*, 1998). Typically, the volatile from, Hg^0, has an atmospheric residence time of 1-2 years allowing for a global distribution and the contamination of areas far removed from point sources of Hg (Lamborg *et al.*, 2002). Hg is of special concern in Arctic and subarctic ecosystems where populations are exposed to dangerous levels of methylmercury, the organic form of Hg which is a potent bioaccumulative neurotoxin, through the consumption of traditional foods (Macdonald and Bewers, 1996). In a review of Hg trends in the Arctic, Riget *et al.* (2011) demonstrated that Hg bioaccumulation in the Canadian and Greenland regions of the Arctic is significantly increasing when compared to the North Atlantic Arctic. Numerous studies have focused on Hg in the Canadian Archipelago and the Canadian Western Arctic, but the Eastern Arctic and subarctic remain comparatively understudied (Carrie *et al.*, 2010; Kirk *et al.*, 2011). Northern Ontario represents a unique eastern subarctic ecosystem with particular characteristics due to the influence of the Hudson Bay (Rouse, 1991). The Hudson Bay Lowlands (HBL) contain countless lakes that have experienced warming in recent decades and are displaying symptoms of significant ecological changes. Gunn and Snucins (2010) reported one of the first fish die-offs due to a warming event in the Sutton River in the HBL in 2001. Large populations of anadromous brook charr (*Salvelinus fontinalis*) and white suckers (*Catostomus commersoni*) were reported to have died suddenly and the warming waters of the river are hypothesized to be the cause of the observed mortality.

Climate warming has led to an increase in primary productivity in northern lakes which presents a new challenge for the study of Hg in these systems (Grant *et al.*, 2011). Atmospheric deposition through oxidization of volatile elemental mercury (Hg^0) is presumed to be the only source of Hg to environments removed from industrial areas. Hg concentrations in lake sediments have therefore been used as historical archives to elucidate atmospheric mercury concentrations for areas where modern monitoring

techniques are unavailable. However, as Outridge *et al.* (2007) proposed, increases in phytoplankton communities could scavenge Hg from the water column and accelerate its deposition to the sediment, in which case, sediment concentrations of Hg may not accurately reflect mercury delivery via the atmosphere. The authors of this hypothesis argue that Hg concentrations in Arctic and subarctic lakes are steadily increasing despite stable or even declining atmospheric concentrations while lakes in temperate areas, where warming impacts are buffered, do not display this increase in sediment Hg concentrations.

The objective of this study is to determine the history of Hg deposition to lakes of the Hudson Bay Lowlands in Northern Ontario and to determine the relationship between sedimentary concentrations of mercury and organic matter. We also use lake sediment archives to document increases in primary productivity as a result of a warming climate. In addition, we examine the algal-mercury scavenging hypothesis by characterizing the type of organic matter found in the sediment with the use of Rock-Eval analyses.

2.3 Materials and Methods

2.3.1 Site Description

The Hudson Bay Lowlands (HBL) area includes the continuous belt of land with an elevation of less than 200m, which surround the western side of Hudson Bay and James Bay. The area is mostly flat, very wet with countless lakes and ponds, and is traversed by the southern boundaries of continuous and discontinuous permafrost as well as the Arctic tree line (Rouse *et al.*, 1997). The region is still responding to the last glacial retreat and exhibits a very rapid isostatic rebound of approximately 1.2m $100yr^{-1}$ (Klinger and Short, 1996).

2.3.2 Sample Collection

For this study, efforts were concentrated in the HBL area in Northern Ontario. Seventeen lakes were sampled over the summers of 2009 to 2011 and range in longitude from 53 to 55^{o}N and 84 to 85 ^{o}W in latitude. The experimental design was devised to include a spatial and a temporal aspect.

Dissolved oxygen and temperature in lakewater was measured using a YSI 55 dissolved oxygen probe and meter (YSI Inc., Yellow Springs, OH) and water chemistry was collected using a composite sampling technique.

Sediment cores were taken using a MiniGlew KB gravity corer (Glew, 1991). Complete cores were taken from North Raft (NRT), Hawley (HWL) and Aquatuk (AQT) Lakes. The complete cores were sectioned into 0.5 cm intervals over the first 10 cm (20 samples) and every 2 cm for the remaining fraction of the core. Only the surface and bottom 0.5 cm fractions were retained from the cores of 10 other lakes. Upon collection, core samples were divided into two. Half of the interval was put into a 50mL polypropylene centrifuge tube with 10mL of RNAlater® solution (Life Technologies, Inc.) and shaken to allow the solution to properly penetrate the sample, which was dedicated to molecular analyses. The other half of the interval was placed into a Whirl-Pak® bag and dedicated to Hg and radiometric analyses. All samples were kept at 4^{o}C and in the dark until frozen at -20^{o}C.

Surface water for total Hg analyses was collected in triplicate in 100 mL white cap, Teflon lined, acid washed glass bottles. Bottles were rinsed three times with lake water before sampling. Each sample was spiked with 0.5mL of ultra pure trace metal grade hydrochloric acid (HCl). Surface water for MeHg analyses was collected in triplicate in 1L HDPE bottles and spiked with 5mL trace metal grade HCl. The bottles were rinsed three times with lake water before sampling. All water samples were kept at 4^{o}C and protected from light.

2.3.3 Radiometric Dating

Sediment cores from AQT, HWL and NRT were radiometrically dated using gamma (γ) spectrometry and analyzed for the activity of ^{210}Pb, ^{137}Cs and ^{226}Ra in an Ortec germanium crystal well detector (DSPec, Ortec, model # GWL-120230) following the method by Appleby (2001). Analysis of ^{210}Pb was performed on 14 -18 selected depth intervals of the sediment cores to determine the sediment age, and the sediment accumulation rate. Samples were lyophilized, homogenized, hermetically sealed and left to reach secular

equilibrium for a minimum of 21 days before being counted for 23 hours (82,800 seconds). The resulting spectrum files showed ^{210}Pb activity with a peak at 46.5 keV, and ^{137}Cs at 662 keV. ^{226}Ra activity was determined by γ-ray emissions of its daughter isotope ^{214}Pb, resulting in peaks at 295 and 352 keV. Long-term sedimentation rates were determined for each core using methods in Appleby and Oldfield (1978). ^{137}Cs activity (from atmospheric fallout of nuclear weapons, peaking in 1963) was measured to verify ^{210}Pb dates.

2.3.4 Mercury Analyses

2.3.4.1 Total Mercury

Water samples were preserved with bromine chloride. Total mercury was analyzed in water samples using dual gold trap pre-concentration and cold vapour atomic fluorescence spectroscopy (CV-AFS). The analysis was conducted using a Tekran 2600 system control module equipped with a Tekran 2610 liquid handling module and Tekran model 2620 auto-sampler, following the modified U.S. EPA Method 1631. The instrument was calibrated with a stock standard of mercuric chloride ($HgCl_2$) for a calibration curve with a R^2 value of 0.999. Field and travel blanks as well as standard checks were performed to insure that there was no THg contamination during sampling, extraction and analysis.

Frozen sediments were transferred from Whirl-Pak® bags into 50mL sterile high density polypropylene Falcon® tubes. Samples were lyophilized for a period of 72 hours under a vacuum of 5 atm and homogenized. Total Hg in sediments was analyzed with Nippon Instruments Corporation's Mercury SP-3D Analyzer (CV-AAS) by thermal decomposition with gold trap amalgamation and cold vapour atomic absorption method (UOP Method 938-00, detection limit of 0.01ng Hg and range up to 1000ng Hg; Fox *et al.*, 2005). The instrument was calibrated with Mercury Reference Solution 1000ppm ± 1% (Fisher CSM114-100) and MESS-3 (91±9 ng g^{-1}, National Research Council of Canada) which is a marine sediment reference material for trace elements and other constituents was used

as reference material with a minimum 90% recovery. Blanks were also performed as suggested by the manufacturer.

2.3.4.2 Methylmercury

Organomercury concentrations in both sediments and water were determined by capillary gas chromatography coupled with atomic fluorescence spectrometry (GC-AFS) using the Analytical Mercury System Model PSA 10.723, as described by Cai (1996) and Cai (1997) for water and soil, respectively. For sediments, initial extracts are subjected to sodium thiosulfate clean-up and the organomercury species are isolated as their bromide derivatives by acidic KBr and $CuSO_4$ and subsequent extraction into a small volume of dichloromethane. Duplicates were performed when sample amounts were sufficient. Recovery of certified reference material ERM580 was between 93 -109% (n = 8). Processing of water samples involved an adsorbent pre-concentration of the organomercurials onto sulfhydryl cotton fibers followed by elution with acidic KBr and $CuSO_4$ and extraction in methylene chloride. Field and travel blanks were performed to insure samples were free of MeHg contamination.

2.3.5 Organic Geochemistry (Rock-Eval® 6 Pyrolysis)

Rock-Eval® 6 (Vinci Technologies, France) pyrolysis analyses were performed by the Geological Survey of Canada in Calgary, Alberta, on selected depth intervals of NRT and HWL Lake sediment cores. This technique utilizes the degree of thermal degradation of various organic compounds to elucidate the quantity and type of organic matter present within the sample. The first step occurs in a pyrolysis oven in which the S1 and S2 fractions are recorded. S1 is geochemically identified as volatile, free hydrocarbons in the sample corresponding to amorphous organic matter, including pigments and oils/lipid products (Lafargue *et al.*, 1998). S2 is classified as a kerogen fraction which corresponds to hydrogen-rich aliphatic biomacromolecules that form the cell walls of algal matter; it is therefore referred to as algal-derived OC (Sanei *et al.*, 2005). An oxidation step follows in which highly refractory residual organic carbon (RC) is quantified. In addition to the various organic matter fractions, the analysis also

yields an oxygen index (OI; mg CO_2 g^{-1} TOC) and a hydrogen index (HI; mg HC g^{-1} TOC). A higher OI is characteristic of the kerogen contained in land-derived terrestrial plants and oxidized organic matter whereas algal-derived kerogen is characterized by a higher HI value (Wehlan, 1993).

2.3.6 Carbon and Nitrogen Isotopes

Elemental and isotopic analyses of all samples were performed at the G.G. Hatch Stable Isotope Laboratory at the University of Ottawa. Prior to the analyses, lyophilized sediment samples were re-hydrated with HPLC water and desiccated with HCl to remove carbonates. Samples were lyophilized again under a vacuum of 5 atm for 24 hours.

Samples were submitted to an elemental analysis (EA) to determine the elemental composition of organic carbon using the CE EA1110. Between 3-5 mg of lyophilized sediment was measured into tin capsules along with the proper reagents. Calibrated EA standards were also prepared in a range of weights. The prepared capsules were loaded into the carousel of the AS128 autosampler. Samples fall down into the top of a column of solid chemicals at 1000°C, and are flash combusted at 1800°C (Dumas combustion) with the addition of oxygen. Ultra-pure helium is used to carry the resulting gases through the column of chemicals to obtain N_2, CO_2, H_2O, and SO_2, then through a gas chromatograph column to separate the gases which are measured by a thermoconductivity detector. Eager 200 software for Windows is used to control the EA, as well as process the results from the thermoconductivity detector using either the Linear Fit or K-factor method. The analytical precision (2 sigma) for the analyses is +/- 0.1% for N, H and S and +/- 0.3% for C (Pella, 1990).

Amounts needed for the isotopic analyses are based on the results of the EA. Sediments were weighed accordingly into tin capsules (0.5-17 mg) with 2 parts tungsten oxide (WO_3). Calibrated internal standards were prepared as a reference with every batch of samples. The isotopic composition of organic carbon and nitrogen was determined by the analysis of CO_2 and N_2, produced by combustion on a VarioEL III Elemental Analyzer (Elementar, Germany) followed

by "trap and purge" separation and on-line analysis by continuous-flow with a DeltaPlus XP Plus Advantage isotope ratio mass spectrometer coupled with a ConFlo II (Thermo, Germany). The data are reported in Delta notation δ, the units are per mil (‰) and defined as δ = ((Rx-Rstd))/Rstd)*1000 where R is the ratio of the abundance of the heavy to the light isotope, x denotes sample and std is an abbreviation for standard. The routine precision of the analyses is 0.20‰ (Pella, 1990).

2.3.7 Flux Calculations and Statistical Analyses

Mercury fluxes (HgF), S2 fluxes (S2F), anthropogenic fluxes (ΔHgF, ΔS2F), flux ratios (FR) and Hg enrichment factors (EF) were calculated as in Muir *et al.* (2009).

1. Flux (F) (ng or mg m^{-2} y^{-1}) = Concentration (ng g^{-1} or mg g^{-1}) × ^{210}Pb-derived sedimentation rates (g m^{-2} y^{-1}) for each core horizon.
2. Anthropogenic flux (ΔF) (ng or mg m^{-2} y^{-1}) = $F_{recent} - F_{pre\text{-}ind}$.
3. Flux ratio (FR) = $F_{recent}/ F_{pre\text{-}ind}$.
4. Enrichment factor (EF) = recent (post-1990) / pre-industrial (pre-1900) concentrations.

The samples from lakes of which only surface and deep sediments were collected could not be radiometrically dated; however, we presume that the deep sediments were deposited before the atmospheric levels of Hg were significantly altered due to anthropogenic activities (Mills *et al.*, 2009). Therefore we use the deep sediments as pre-industrial and the surface sediment as recent to determine the Hg EF.

Sediment particle focusing factors (FF) were estimated for the three dated sediment cores. We multiplied each core's cumulative unsupported ^{210}Pb inventory (Bq m^{-2}) by the ^{210}Pb decay constant (0.03114 y^{-1}) and then divided this observed ^{210}Pb flux (Bq m^{-2} y^{-1}) by the predicted ^{210}Pb flux for this latitude (150 Bq m^{-2} y^{-1}; Omelchenko *et al.*, 1995).

Statistical analyses such as general linear models and correlations were performed using Systat Software Inc. 2008. All of the data for which p-values are reported passed the normality (Shapiro-Wilk) and constant variance tests.

2.4 Results and Discussion

2.4.1 Spatial Hg Distribution

A wide range of total mercury (Hg) concentrations was found throughout the lakes with the lowest in SRT Lake (surface: 6.13 (± 0.7) and depth: 4.96 (± 0.2) ng g^{-1} dw) and highest in RFT Lake (surface: 125.4 (± 0.9) and depth: 91.4 (± 2) ng g^{-1} dw) (Table 2.1or Fig. 2.2, panel A). The Hg concentration in the surface sediment is significantly higher than in the deep sediments ($p = 0.004$). The wide range of Hg concentrations recorded in lake sediments emphasizes the importance of other physical and chemical parameters as well as within lake processes in the fate of Hg deposited from the atmosphere. For example, there is a significant positive correlation ($p < 0.05$) between lake water colour and Hg in surface sediments while a significant negative correlation exists between Cl in water and Hg in surface sediments of these lakes (Fig. S2.1 and S2.2).

Methylmercury (MeHg) concentrations were lowest in SRT lake surface (0.0772 ng g^{-1} dw) and SPC deep sediments (0.0202 ng g^{-1} dw) and highest in WGN surface (1.83 ng g^{-1} dw) and RFT deep (0.466 ng g^{-1} dw) sediments (Table 2.1 or Fig.2.2 (panel D)). There is no significant correlation between Hg and MeHg in surface sediment ($p = 0.54$) underscoring that Hg concentration is a poor predictor of MeHg concentration and its biological importance in sediments.

In surficial lakewater, Hg concentrations varied from 0.659 to 2.72 ng L^{-1} and MeHg varied from 0.00508 to 0.0745 ng L^{-1}. These concentrations are below the Water Quality Guidelines for Mercury for the Protection of Aquatic Life that were established by Environment Canada in 2003, although these guidelines may not protect wildlife that consume aquatic species (Environment, 2003).

When considering Hg concentrations in the environment, it is important to consider the proportion of Hg that is in the methylated form; the Hg fraction that is biologically relevant and of most concern (([MeHg]/[THg])*100). The Canadian

Council of Ministers of the Environment (2003) report that MeHg in water of undisturbed systems should represent less than 10% of the total Hg which was the case for all water samples (0.22 to 6.4%). In surface sediment, 0.17 to 2.9% of Hg is present as MeHg while 0.078 to 0.95% of Hg is in a methylated form in deep sediments. MeHg degradation is common in subsurface sediments which is why we observe a decrease in MeHg concentrations and MeHg:Hg proportions as we get into deeper, older sediments (Fig 2.2, panel D) (Rydberg *et al.*, 2008).

The Hg enrichment factor (EF) represents the increase in Hg concentrations due to anthropogenic emissions of Hg as a result of the industrial revolution. The Hg EF for the 13 lakes vary between 1.24 in SRT and 4.30 in WGN which suggests that these lakes are in fact subjected to anthropogenic inputs of Hg through atmospheric deposition. These values are also consistent with the average global enrichment factor of 3 that has been recorded in areas around the globe (Yang, 2010). Hg is known to be highly correlated with organic matter (OM) due to the formation of Hg-OM complexes (Lindberg and Harriss, 1974). Interestingly, no significant correlation exists between Hg and organic carbon (OC), neither in surface sediment, nor in deep sediments and there is also no significant relationship between DOC (dissolved organic carbon) and either Hg or MeHg in lake water ($p > 0.1$). However, there is a significant correlation between MeHg and OC in surface and deep sediments ($p = 0.0001$ and 0.0161, respectively) suggesting that MeHg production in these lakes is greater in organic-rich sediments. Delongchamp *et al.* (2010) observed higher MeHg concentrations in sediment of the St. Lawrence River where anaerobic OM decomposition and methane emissions were highest due to methanogenic bacteria which are known MeHg producers (Avramescu *et al.*, 2011). When Hg concentrations are corrected for OC, surface sediments in NRT lake and deep sediments in HWL lake have the highest Hg content while surface sediments of SAM and deep sediments of JLN have the lowest amount of Hg g^{-1} OC (Fig.2.2, panel B).

2.4.2 Temporal Hg Distribution

Radiometric dating revealed that most excess ^{210}Pb and ^{137}Cs is concentrated in the top 2 cm of accumulated dry mass for all three cores suggesting a very low sediment accumulation rate (Fig 2.3). As a result, background was achieved early in the NRT and AQT cores, limiting dating to the top 9 cm intervals. The constant rate of supply model (CRS) was used in the three cores to achieve dating with decadal resolution. Table 2.2 contains a few key characteristics of the study lakes.

The Hg depth profiles of the sediment cores form AQT, HWL and NRT lakes are consistent with those reported by others in the Arctic and subarctic (Kirk *et al.*, 2011). In all three cores, Hg concentrations steadily increase towards the surface of the core, with the highest concentrations in the most recently deposited sediments (Fig. 2.4). Radiometric dating of the cores revealed that the deepest sediments may have been deposited after the onset of the industrial revolution, however they were deposited before industrial-scale anthropogenic emissions of Hg reached their peak (Roos-Barraclough *et al.*, 2002). For the sake of discussion, we consider sediments deposited before the 1900s to be historical/preindustrial. In AQT Lake, the historical [Hg] is 68.8 ± 5 ng g^{-1} (dw) from 10.25 to 22.25cm depth and the recent [Hg] is 108.6 ± 1 ng g^{-1} (dw) yielding an EF of 1.58 (Fig. 2.4). Historical concentration of Hg in HWL sediments from 22.25 to 24.25 cm is 44.8 ± 0.5 ng g^{-1} (dw) and the recent sediments have a concentration of 92.7 ± 5 ng g^{-1} (dw) for an enrichment factor of 2.07. NRT Lake historical concentrations are 62.3 ± 3 ng g^{-1} (dw) between the depths of 9.25 to 29.75 cm and reach a maximum of 112.5 ± 11 ng g^{-1} (dw) in recent sediments resulting in an EF of 1.80.

We calculated the Hg flux (HgF) which accounts for variations in sedimentation rates. The AQT core has a relatively constant sedimentation rate therefore the Hg and HgF profiles are similar (Fig. 2.4). The sedimentation rate of the NRT core could only be inferred for the top 9 cm intervals due to the rapid loss of excess ^{210}Pb therefore we cannot calculate the HgF, the FR and the ΔF for the complete core. However, the HgF peaks at 2770 ng m^{-2} y^{-1} at 6.25 cm depth (1938) then decreases to 1090 ng m^{-2} y^{-1} in 2009. Hg in the HWL lake core

diminishes between 1950 and 1960 which is likely a dilution due to a large input of allochthonous inorganic matter. The cause of this large allochthonous input from the catchment is still under review but is hypothesized to have been the result of a localized landslide due to erosion of the catchment after a forest fire (personal communication with A. Paterson). Several different proxies corroborate the event including the sedimentation rate profile which increases drastically at the corresponding depth of the Hg decrease. We also register a decrease in TOC and water content of the sediment at the corresponding depths due to a dilution by inorganic clays and silts from the catchment (Fig. 2.4). The HgF is highest in the HWL core when [Hg] is at its lowest (17600 ng m^{-2} y^{-1} and 28.5 ng g^{-1} dw), suggesting that the allochthonous matter that was introduced into the lake contained elevated levels of Hg. However, the HgF is likely artificially inflated by the drastic rise in sedimentation rate at this interval. The HgF in recent sediments of HWL and NRT is decreasing as opposed to AQT where it is increasing (Fig. 2.4). The anthropogenic Hg flux (ΔHgF) for AQT is 2510 ng m^{-2} y^{-1} and the HgFR is 2.72. For HWL, the ΔHgF is 620 ng m^{-2} y^{-1} and the HgFR is 1.69. In NRT, the ΔHgF is 778 ng m^{-2} y^{-1} and the HgFR is 2.36.

In contrast to the spatial analyses of lakes from various latitudes, Hg is significantly correlated with OC for all three sediment cores (p value: AQT = 0.007; HWL and NRT < 0.001), indicating that the catchment of these lakes may have been an important contributor of OM-bound Hg. In all three cores, Hg g^{-1} OC is increasing in recent sediments, suggesting an increasing input of Hg bound to OM (Fig. 2.4). This effect can be expected to intensify as the integrity of the underlying permafrost of the catchment is compromised by progressive climate warming (Anisimov, 2007).

MeHg analyses were limited to 5 depth intervals. As anticipated, MeHg concentrations are highest in surface sediment and decrease steadily with depth in all cores most likely due to MeHg degradation (Fig. 2.4). MeHg is correlated with OC in all three depth profiles (p values: AQT = 0.033; HWL = 0.022; NRT = 0.026) and as a result the MeHg profiles remain similar once corrected for OC.

MeHg was also diluted by the input of allochthonous matter in the HWL core at 5 cm depth (1950-1960).

2.4.3 Algal-Derived Carbon

Rock-Eval analyses were performed on HWL and NRT sediment cores. S2 concentrations, or algal-derived OC, varied from 2.84 to 12.4 mg HC g^{-1} (dw) with an average of 6.87 ± 2 mg HC g^{-1} (dw) in HWL and 9.43 to 12.1 mg HC g^{-1} (dw) and an average of 10.2 ± 0.6 mg HC g^{-1} (dw) in NRT. These concentrations are consistent with those found in other subarctic lakes (Kirk *et al*. 2011). S2 rises sharply towards the surface of both cores and there is a significant positive relationship between S2 and Hg (HWL: $R^2 = 0.81$, $p < 0.001$; NRT: $R^2 = 0.44$, $p = 0.007$) supporting the hypothesis that Hg and algal productivity are increasing in tandem (Fig. 2.5).

The S2F in HWL has a similar profile as the HgF, where concentrations increase up to 1997 mg HC m^{-2} y^{-1} between 6 and 8 cm due to the increase in the sedimentation rate. The HWL S2EF is 2.05, the ΔS2F is 65.7 mg HC m^{-2} y^{-1} and the S2FR is 1.54. The S2F in NRT also increases slightly at 5 cm depth to 382.3 mg HC m^{-2} y^{-1} due to the slight increase in sedimentation rate. The NRT S2EF is 1.20, the ΔS2F is 52.7 mg HC m^{-2} y^{-1} and the S2FR is 1.63.

The average hydrogen index (HI) is lower than the oxygen index (OI) in the HWL core (205 ± 30 mg HC g^{-1} TOC and 219 ± 10 mg CO_2 g^{-1} TOC respectively) but we observe the opposite for the NRT core (212 ± 5 mg HC g^{-1} TOC and 201 ± 10 mg CO_2 g^{-1} TOC, respectively). The HI and OI fluctuate in the HWL core and in recent sediments the OI decreases and the HI increases, indicating that algal derived OC is increasingly present in sediment (Fig. 2.5). Surprisingly, the NRT core shows a different trend where the average HI is higher than the OI. This would suggest that autochthonous carbon is more important than allochthonous inputs of carbon which is unlikely. Figure 2.7 shows that NRT C:N is higher than HWL and the $\partial^{13}C$ signature is less depleted in ^{13}C, both supporting a more allochthonous origin of OM. Chlorophyll a concentrations have been measured in NRT lake in another study and concentrations fluctuated

around the detection limit of the analysis (personal communication with K. Ruhland). We believe that the high HI index in the NRT core may be erroneous and irrelevant.

In HWL, we see a sharp increase in OI and a decrease of HI at the depth which corresponds to the sedimentation event of 1950 – 1960 (Fig. 2.5). Stern *et al*. (2009) characterized increases in OI as being caused by factors such as inputs of reworked-oxidized organic carbon, the cellulosic remains of higher terrestrial plants, and/or airborne residues of carbonized organic matter such as char and ash from wildfires, further corroborating the hypothesis of a landslide due to a wildfire in the HWL catchment during this time period.

Diagrams which plot S2 as a function of TOC are employed to illustrate the source and composition of organic matter by representing the proportion of hydrogen-rich organic matter dominantly composed of autochthonous matter (S2) relative to the total organic carbon in the sediments (Fig 2.6) (Langford and Blanc-Valleron, 1990). The solid lines on the diagrams indicate the boundaries between kerogen types, where high S2/TOC is classified as Type I, with Type II and Type III having descending S2/TOC values (Yalçin-Erik *et al.*, 2006). The Van Krevelen diagram serves a similar purpose where HI and OI are plotted together and the curves indicate maturity paths for the kerogen (Yalçin-Erik *et al.*, 2006). In both HWL and NRT, the kerogen is Type III to Type II-III which is characterized as terrigenous and reworked organic matter and is typical of such systems (Fig 2.6) (Carrie *et al.*, 2009).

2.4.4 Carbon and Nitrogen

The elemental and stable isotope compositions of OM in lake sediments have been shown to be useful paleolimnological variables related to changes in primary productivity (Vreca and Muri, 2010). In the 13 lakes studied here, there is a significant difference between the C:N ratio of the surface and deep sediments ($p = 0.01$). The average C:N ratio in deep sediments is 12.9 ± 3 and 10.5 ± 1 in surface sediments. A decrease in C:N ratio can also be seen in the three sediment cores (Fig. 2.7). The AQT C:N ratio decreases from 11.3 at 22 cm

depth to 9.23 in surface sediment. The ratio of HWL sediments at 24 cm depth is 10.20 and decreases to 9.21 at the surface while NRT decreases from 13.3 at 29.5cm to 10.7 at the surface. Algae and phytoplankton are characterized by high protein content and the absence of cellulose, and show low atomic C:N ratios (4-12) whereas terrestrial plants have higher C:N ratios due to their low protein content and abundance of cellulose (Meyers, 1994). Therefore the observed decrease in the C:N ratio in surface sediments provides some support to the hypothesis of increasing algal productivity within these lakes. However, the lability of carbon and nitrogen in oligotrophic lakes remains an outstanding issue. Several studies have shown the presence of active bacterial and archaeal populations in sub-surface sediments which consume various forms of carbon through diverse metabolic pathways (Lay *et al.*, 1996; Scholten *et al.*, 2000; Biderre-Petit *et al.*, 2011). Xia *et al.* (2008) demonstrated the impact of microbial populations on the carbon nitrogen ratio in a bioreactor where the diversity of microbial community structure was positively correlated with C:N ratio. Therefore the higher C:N ratio in subsurface sediments could be due to microbial consumption of nitrogen; further studies are needed to assess the impact of microbial populations on the C:N ratios in these lakes.

The carbon isotope is fractionated, to varying degrees, during photosynthesis due to the inherent kinetics of enzymatic reactions (Farquhar, 1989). The two major terrestrial plant groups, C3 and C4, have $\partial^{13}C$ of approximately -26 to -28 ‰ and -12 to -14 ‰, respectively (Hecky and Hesslein, 1995). A combination of physiological and environmental influences can modify the carbon isotopic composition of plankton communities resulting in a large range in stable carbon isotope ratios of algae (France *et al.*, 1997, and references therein). In addition to a literature review, France *et al.* (1997) studied 52 Canadian Shield lakes to elucidate the environmental and ecophysiological determinants of $\partial^{13}C$ signatures of phytoplankton. They demonstrated that, in oligotrophic lakes, rates of respiration can exceed those of photosynthesis leading to an oversaturation of CO_2 and depletion of the $\partial^{13}C$ signature of the plankton community. Lakes with high DOC and high colour are also known to be

heterotrophically dominated and exhibit considerable rates of decomposition of allochthonous organic matter which may also lead to a depletion of the $\partial^{13}C$ signature of plankton (Hessen, 1992). All of our study lakes are oligotrophic with high DOC values (> 5 mg/L) therefore we expect the plankton community to exhibit depleted $\partial^{13}C$ signatures. Surface sediment $\partial^{13}C$ signatures vary between -32.0‰ and -25.7‰ with an average of -29.0 ± 2‰ whereas deep sediments vary between -30.4‰ and -24.1‰ with an average of -27.9 ± 2‰. The temporal depletion of the $\partial^{13}C$ signature is also seen in the three sediment cores. The average $\partial^{13}C$ of the sediment at 22 cm depth from AQT is -29.3‰ (± 0.06) and -30.4‰ (± 0.04) in the surface sediment. HWL sediments at 24 cm depth have an average $\partial^{13}C$ of -30.6‰ (± 0.04) while the surface sediment have a $\partial^{13}C$ of -31.3‰ (± 0.04). Sediment from 29.5 cm depth from NRT have a $\partial^{13}C$ of -28.5‰ (± 0.2) and -29.2‰ (± 0.1). The slight depletion of the $\partial^{13}C$ signature in the surface sediment compared to deep sediment is not significant ($p = 0.12$), however we believe that it could be an additional indicator of increasing primary productivity in these lakes over recent decades.

2.5 Conclusions

Three lake sediment cores and sediment from surface and deep intervals of 10 additional lakes from the Hudson Bay Lowlands were analysed to determine the history of Hg deposition and the changes occurring in organic carbon concentrations in lakes of this region. Despite the remote location of the lakes, sediments revealed that they are impacted by atmospheric deposition of Hg. After the onset of the industrial revolution, when atmospheric concentrations of Hg began to rise, sedimentary concentrations of Hg increased in all three cores and reached concentrations equating those found in lakes subjected to industrial activity and anthropogenic stressors (Lockhart *et al.*, 1998). There is also a wide range in Hg concentrations is surface sediments, ranging from 6.13 ± 1 to 125.4 ± 1 ng g^{-1} dw, which emphasizes the importance of *in situ* and post-depositional processes in the Hg cycle. Total Hg and MeHg were not correlated in surface sediments, indicating that total Hg is a poor predictor of MeHg; the

form of greatest biological concern. There was a significant correlation between Hg and OC in all three sediment depth profiles however there was no significant relationship between Hg and OC in surface sediments from all the lakes. MeHg and OC were positively correlated in surface sediments of the lakes, suggesting that the production of MeHg in these lakes may be limited by the availability of OC. Rock-Eval analyses were applied to two of the sediment cores and significant relationships were found between S2 (algal-derived organic carbon) and Hg, supporting the hypothesis that [Hg] and algal productivity are increasing in tandem. Rock-Eval, OC, C:N ratios and $\partial^{13}C$ signatures all provide evidence to support an increase in primary productivity in these lakes, which is assumed to be a consequence of a warming climate.

2.6 References

Anisimov, O.A. 2007. Potential feedback of thawing permafrost to the global climate system through methane emission. Environmental Research Letters, 2(4): 1-7.

Appleby, P.G. 2001. Chronostratigraphic techniques in recent sediments. In: Tracking environmental changes in lake sediments: Physical and chemical techniques, W. M. Last and J. P. Smol, (Eds.). Kluwer Academic Publishers, Dordrect.

Appleby, P.G. and F. Oldfield. 1978. The calculation of lead-210 dates assuming a constant rate of supply of unsupported 210pb to the sediment. Catena, 5(1): 1-8.

Avramescu, M.L., E. Yumvihoze, H. Hintelmann, J. Ridal, D. Fortin and D.R.S. Lean. 2011. Biogeochemical factors influencing net mercury methylation in contaminated freshwater sediments from the st. Lawrence river in cornwall, ontario, canada. Science of the Total Environment, 409(5): 968-978.

Biderre-Petit, C., D. Jezequel, E. Dugat-Bony, F. Lopes, J. Kuever, G. Borrel, E. Viollier, G. Fonty and P. Peyret. 2011. Identification of microbial communities involved in the methane cycle of a freshwater meromictic lake. Fems Microbiol Ecol, 77(3): 533-545.

Cai Y, J.R., Alli A, Jones RD. 1996. Determination of organomercury compounds in aqueous samples by capillary gas chromatography-atomic fluorescence spectrometry following solid-phase extraction. Analytica Chimica Acta, 334: 251-259.

Cai Y, T.G., Jaffé R, Jones RD. 1997. Evaluation of some isolation methods for organomercury determination in soil and fish samples by capillary gas chromatography -atomic fluorescence spectrometry. International Journal of Environmental Analytical Chemistry, 68(3): 331-345.

Carrie, J., H. Sanei, F. Goodarzi, G. Stern and F.Y. Wang. 2009. Characterization of organic matter in surface sediments of the mackenzie river basin, canada. International Journal of Coal Geology, 77(3-4): 416-423.

Carrie, J., F. Wang, H. Sanei, R.W. Macdonald, P.M. Outridge and G.A. Stern. 2010. Increasing contaminant burdens in an Arctic fish, burbot (lota lota), in a warming climate. Environmental Science & Technology, 44(1): 316-322.

CFEP, C.F.E.U. 2011. Progress report – aquatic ecosystem studies in the hawley lake/sutton river area of the hudson bay lowlands, 2009 – 2010. Editor. Sudbury.

Delongchamp, T.M., J.J. Ridal, D.R.S. Lean, L. Poissant and J.M. Blais. 2010. Mercury transport between sediments and the overlying water of the st. Lawrence river area of concern near cornwall, ontario. Environmental Pollution, 158(5): 1487-1493.

Canadian Council of ministers of the Environment. 2003. Canadian water quality guidelines for the protection of aquatic life: Inorganic mercury and methylmercury. Editor. Winnipeg.

Farquhar GD, E.J., Hubick KT. 1989. Carbon isotope discrimination and photosynthesis. Annual Review of Plant Physiology, 40: 503-537.

Fox, B.S., Mason, K.J., McElroy, F.C., 2005. Determination of total mercury in crude oil by combustion cold vapor atomic absorption spectrometry (CVAAS), in: Nadkarni, R.A.K. (Ed.), Elemental Analysis of Fuels and Lubricants: Recent Advances and Future Prospects, pp. 196-206.

France, R.L., P.A. delGiorgio and K.A. Westcott. 1997. Productivity and heterotrophy influences on zooplankton delta c-13 in northern temperate lakes. Aquatic Microbial Ecology, 12(1): 85-93.

Glew, J. 1991. Miniature gravity corer for recovering short sediment cores. J. Paleolimn., 5(3): 285.

Grant, R.F., E.R. Humphreys, P.M. Lafleur and D.D. Dimitrov. 2011. Ecological controls on net ecosystem productivity of a mesic Arctic tundra under current and future climates. Journal of Geophysical Research-Biogeosciences, 116.

Gunn, J. and E. Snucins. 2010. Brook charr mortalities during extreme temperature events in sutton river, hudson bay lowlands, canada. Hydrobiologia, 650(1): 79-84.

Hecky, R.E. and R.H. Hesslein. 1995. Contributions of benthic algae to lake food webs as revealed by stable isotope analysis. Journal of the North American Benthological Society, 14(4): 631-653.

Hessen, D.O. 1992. Dissolved organic carbon in a humic lake - effects on bacterial production and respiration. Hydrobiologia, 229: 115-123.

Kirk, J.L., D.C.M. Muir, D. Antoniades, M.S.V. Douglas, M.S. Evans, T.A. Jackson, H. Kling, S. Lamoureux, D.S.S. Lim, R. Pienitz, J.P. Smol, K. Stewart, X.W. Wang and F. Yang. 2011. Climate change and mercury accumulation in canadian high and subarctic lakes. Environmental Science & Technology, 45(3): 964-970.

Klinger, L.F. and S.K. Short. 1996. Succession in the hudson bay lowland, northern ontario, canada. Arctic and Alpine Research, 28(2): 172-183.

Lafargue, E., F. Marquis and D. Pillot. 1998. Rock-eval 6 applications in hydrocarbon exploration, production, and soil contamination studies. Revue De L'Institut Français Du Pétrole, 53(4): 421-437.

Lamborg, C.H., W.F. Fitzgerald, J. O'Donnell and T. Torgerson. 2002. A non-steady-state compartmental model of global-scale mercury biogeochemistry with interhemispheric atmospheric gradients. Geochim Cosmochim Ac, 66: 1105-1118.

Langford, F.F. and M.M. Blanc-Valleron. 1990. Interpreting rock-eval pyrolysis data using graphs of pyrolyzable hydrocarbons vs total organic carbon. American Association of Petroleum Geology Bulletin, 74: 799-804.

Lay, J.J., T. Miyahara and T. Noike. 1996. Methane release rate and methanogenic bacterial populations in lake sediments. Water Research, 30(4): 901-908.

Lindberg, S.E. and R.C. Harriss. 1974. Mercury-organic matter associations in estuarine sediments and interstitial water. Environmental Science & Technology, 8(5): 459-462.

Lockhart, W.L., P. Wilkinson, B.N. Billeck, R.A. Danell, R.V. Hunt, G.J. Brunskill, J. Delaronde and V. St Louis. 1998. Fluxes of mercury to lake sediments in central and northern canada inferred from dated sediment cores. Biogeochemistry, 40(2-3): 163-173.

Macdonald, R.W. and J.M. Bewers. 1996. Contaminants in the Arctic marine environment: Priorities for protection. Ices Journal of Marine Science, 53(3): 537-563.

Meyers, P.A. 1994. Preservation of elemental and isotopic source identification of sedimentary organic-matter. Chemical Geology, 114(3-4): 289-302.

Mills, R.B., A.M. Paterson, J.M. Blais, D.R.S. Lean, J.P. Smol and G. Mierle. 2009. Factors influencing the achievement of steady state in mercury contamination among lakes and catchments of south-central ontario. Canadian Journal of Fisheries and Aquatic Sciences, 66(2): 187-200.

Morel, F.M.M., A.M.L. Kraepiel and M. Amyot. 1998. The chemical cycle and bioaccumulation of mercury. Annual Review of Ecology and Systematics, 29: 543-566.

Muir, D.C.G., X. Wang, F. Yang, N. Nguyen, T.A. Jackson, M.S. Evans, M. Douglas, G. Kock, S. Lamoureux, R. Pienitz, J.P. Smol, W.F. Vincent and A. Dastoor. 2009. Spatial trends and historical deposition of mercury in eastern and northern canada inferred from lake sediment cores. Environmental Science & Technology, 43(13): 4802-4809.

Omelchenko, A., W.L. Lockhart and P. Wilkinson. 1995. Study of the depositional characteristics of the lake sediments across canada with 210-pb and cs-137. Editor. Winnipeg, MB, Canada.

Outridge, P.M., H. Sanei, G.A. Stern, P.B. Hamilton and F. Goodarzi. 2007. Evidence for control of mercury accumulation rates in canadian high Arctic lake sediments by variations of aquatic primary productivity. Environmental Science & Technology, 41(15): 5259-5265.

Pella, E. 1990. Elemental organic analysis. Instruction Manual for the EA 1110.

Riget, F., B. Braune, A. Bignert, S. Wilson, J. Aars, E. Born, M. Dam, R. Dietz, M. Evans, T. Evans, M. Gamberg, N. Gantner, N. Green, H. Gunnlaugsdottir, K. Kannan, R. Letcher, D. Muir, P. Roach, C. Sonne, G. Stern and O.

Wiig. 2011. Temporal trends of hg in Arctic biota, an update. Science of the Total Environment, 409(18): 3520-3526.

Roos-Barraclough, F., A. Martinez-Cortizas, E. Garcia-Rodeja and W. Shotyk. 2002. A 14 500 year record of the accumulation of atmospheric mercury in peat: Volcanic signals, anthropogenic influences and a correlation to bromine accumulation. Earth and Planetary Science Letters, 202(2): 435-451.

Rouse, W.R. 1991. Impacts of hudson-bay on the terrestrial climate of the hudson-bay lowlands. Arctic and Alpine Research, 23(1): 24-30.

Rouse, W.R., M.S.V. Douglas, R.E. Hecky, A.E. Hershey, G.W. Kling, L. Lesack, P. Marsh, M. McDonald, B.J. Nicholson, N.T. Roulet and J.P. Smol. 1997. Effects of climate change on the freshwaters of Arctic and Subarctic North America. Hydrological Processes, 11(8): 873-902.

Rydberg, J., V. Galman, I. Renberg, R. Bindler, L. Lambertsson and A. Martinez-Cortizas. 2008. Assessing the stability of mercury and methylmercury in a varved lake sediment deposit. Environmental Science & Technology, 42(12): 4391-4396.

Sanei, H., L.D. Stasiuk and F. Goodarzi. 2005. Petrological changes occurring in organic matter from recent lacustrine sediments during thermal alteration by rock-eval pyrolysis. Organic Geochemistry, 36(8): 1190-1203.

Scholten, J.C.M., R. Conrad and A.J.M. Stams. 2000. Effect of 2-bromo-ethane sulfonate, molybdate and chloroform on acetate consumption by methanogenic and sulfate-reducing populations in freshwater sediment. Fems Microbiol Ecol, 32(1): 35-42.

Vreca, P. and G. Muri. 2010. Sediment organic matter in mountain lakes of north-western slovenia and its stable isotopic signatures: Records of natural and anthropogenic impacts. Hydrobiologia, 648(1): 35-49.

Wehlan JK, T.-R.C. 1993. Chemical methods for assessing kerogen and protokerogen types and maturity. In: Organic geochemistry. Plenum Press, New York: pp: 289-353.

Xia, S., J. Li and R. Wang. 2008. Nitrogen removal performance and microbial community structure dynamics response to carbon nitrogen ratio in a compact suspended carrier biofilm reactor. Ecol. Eng., 32(3): 256-262.

Yalçin-Erik, N., O. Ozcelik and M. Altunsoy. 2006. Interpreting rock-eval pyrolysis data using graphs of s-2 vs. Toc: Middle triassic-lower jurassic units,

eastern part of se turkey. Journal of Petroleum Science and Engineering, 53(1-2): 34-46.

Yang, H., Engstrom, DR., Rose, NL. 2010. Recent changes in atmospheric mercury deposition recorded in the sediments of remote equatorial lakes in the rwenzori mountains , uganda. Environmental Science & Technology, 44: 6570-6575.

2.7 List of Tables

Table 2.1: Total mercury, methylmercury and mercury present as methylmercury (%) in surface water (ng L^{-1}) and surface and deep sediment (ng g^{-1} dw) from lakes in the Hudson Bay Lowlands of Ontario, Canada.

	THg ng L^{-1}, ng g^{-1} dw, (SD)			MeHg ng L^{-1}, ng g^{-1} dw, (SD)			Hg as MeHg (%)		
Lake	Surface water	Surface sediment	Deep sediment	Surface water	Surface sediment	Deep sediment	Surface water	Surface sediment	Deep sediment
AQT '09	1.31 (0.1)	104 (5)	63.1 (6)	0.060 (0.006)	0.212	0.0797	4.6	0.20	0.13
AQT '10	0.87 (0.2)	110 (2)	63.2 (3)	0.025 (0.005)	0.305	0.0745	2.8	0.28	0.12
BLB	2.7 (0.2)	61.9 (1)	24.8 (1)	0.021 (0.004)	0.755	0.236	0.78	1.2	0.95
CSE	0.95 (0.06)	68.3 (1)	20.8 (1)	0.041 (0.002)	0.718	0.0246	4.3	1.1	0.12
HWL '09	1.1 (0.08)	98.2 (5)	45.2 (1)	0.056 (0.01)	0.415	0.0938	5.2	0.42	0.21
HWL '10	0.71 (0.01)	-	-	0.026 (0.004)	-	-	3.7	-	-
JLN	0.93 (0.06)	28.8 (1)	13.9 (1)	0.020 (0.02)	0.513	0.0402	2.2	1.8	0.29
KSO	1.3 (0.2)	93.9 (4)	54.5 (2)	0.020 (0.02)	0.747	0.171	1.6	0.80	0.31
NRT	1.9 (0.5)	120 (3)	57.7 (3)	0.052 (0.03)	0.204	0.130	2.7	0.17	0.23
NWG	1.3 (0.1)	-	-	-	-	-	-	-	-
OPE	1.7 (0.3)	92.2 (0.2)	47.9 (2)	0.040 (0.005)	1.12	0.117	2.4	1.2	0.24
OPU	2.3 (0.01)	-	-	0.0051 (0.009)	-	-	0.22	-	-

RFT	1.7 (0.04)	125 (1)	91.4 (2)	0.056 (0.06)	1.76	0.466	3.3	1.4	0.51
SAM	0.66 (0.1)	45.2 (1)	34.3 (1)	0.031 (0.006)	0.883	0.0990	4.6	1,9	0.29
SPC	1.4 (0.09)	56.2 (5)	25.8 (5)	0.038 (0.003)	0.185	0.0202	2.8	0.33	0.078
SRT	1.2 (0.03)	6.1 (1)	4.96 (0.2)	0.046 (0.01)	0.0772	0.0241	3.9	1.3	0.49
STN	1.2 (0.2)	-	-	0.075 (0.01)	-	-	6.4	-	-
WCU	1.2 (0.1)	-	-	0.0073 (0.009)	-	-	0.61	-	-
WGN	0.77 (0.04)	62.9 (2)	14.6 (3)	0.030 (0.01)	1.83	0.0205	3.9	2.9	0.14

AQT = Aquatuk; BLB = Billbear; CSE = Cassie; HWL = Hawley; JLN = Julison; KSO = Kinushseo; NRT = North Raft; NWG = North Washagami; OPE = Opinnagau East; OPU = Opinnagau; RFT = Raft; SAM = Sam; SPC = Spruce; SRT = Stuart; STN = Sutton; WCU = Warchesku; WGN = Wolfgang.

Table 2.2: Characteristics of three lakes of the Hudson Bay Lowlands of Ontario, Canada.

Name	Sampling Year	Latitude Longitude	Observed ^{210}Pb flux (Bq m^{-2} y^{-1})	Predicted ^{210}Pb flux ▲ (Bq m^{-2} y^{-1})	Focusing Factor (FF)	Average sedimentation rate (g m^{-2} y^{-1}) (SD) *	Depth at sampling location (m)
Aquatuk (AQT)	2010	54°21'11.8" 84°34'29.8"	117	150	0.782	21.3 (8)	12.2
Hawley (HWL)	2009	54°31'38.7" 84°37'46.5"	98.1	150	0.654	120.6 (105) †	35.2
North Raft (NRT)	2009	54°32'4.0" 84°45'21.6"	49.9	150	0.333	23.5 (9)	10.5

*According to the constant rate of supply model.
† Note that the average sedimentation rate is inflated by the sedimentation event in 1950-1960.
▲ Omelchenko *et al*. 1995

2.8 List of Figures

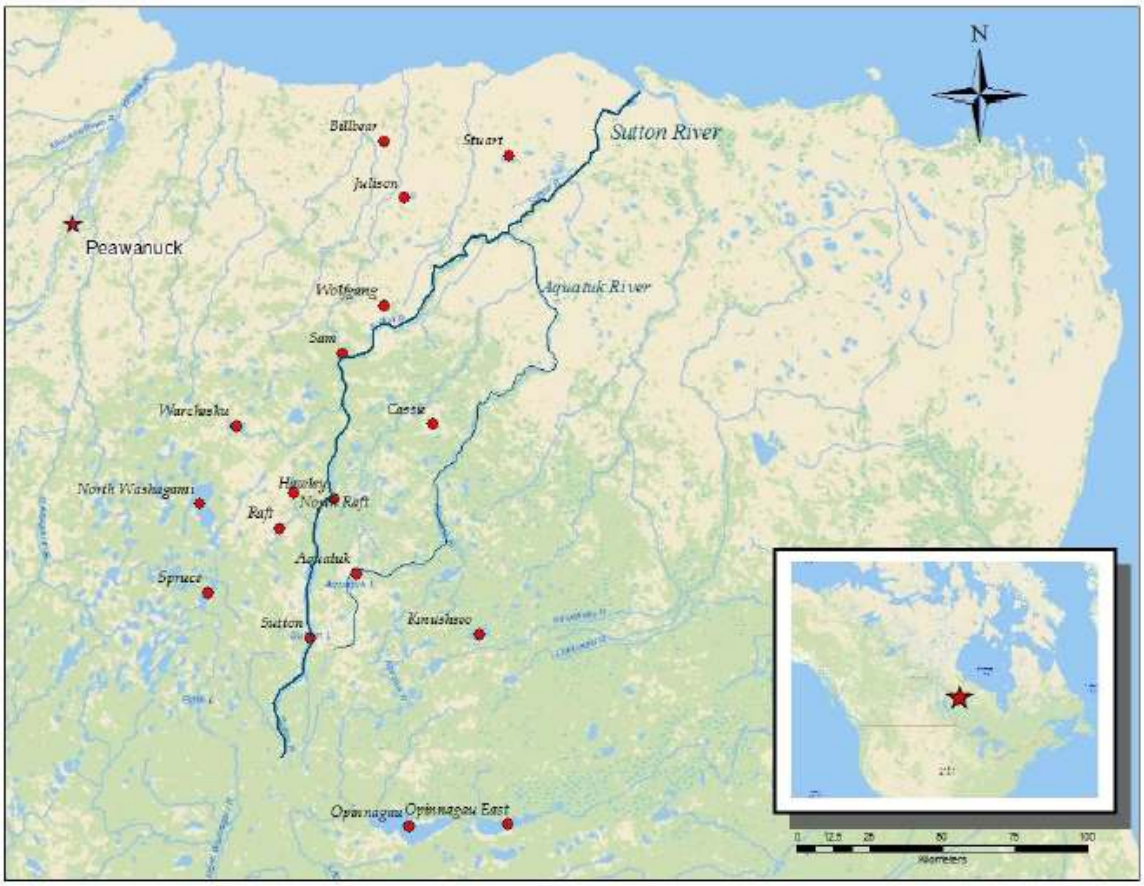

Figure 2.1: Map of Northern Ontario showing the location of the study lakes in the Hudson Bay Lowlands (CFEP, 2011).

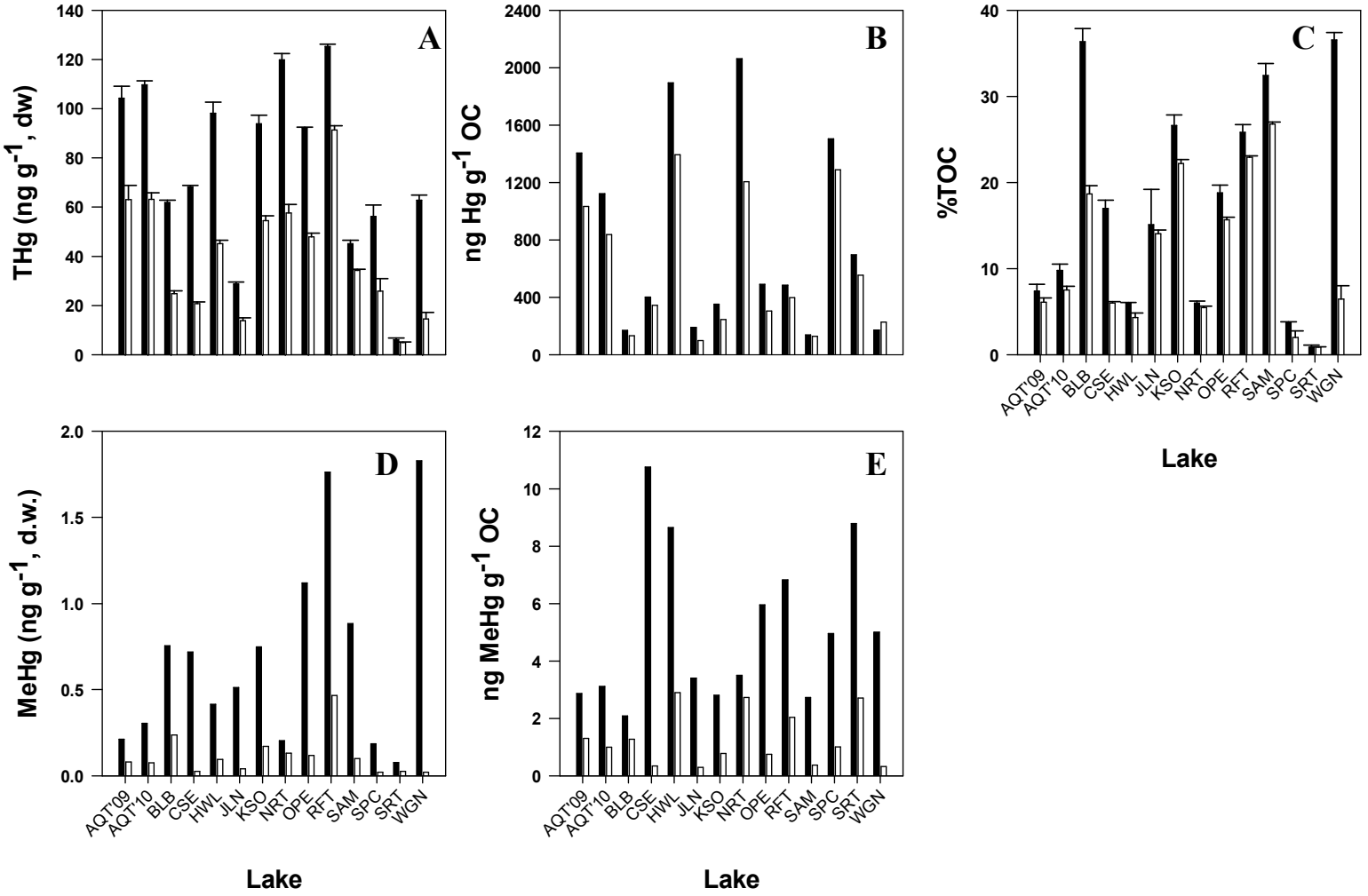
A
THg (ng g-1, dw)
0
20
40
60
80
100
120
140
B
ng Hg g-1 OC
0
400
800
1200
1600
2000
2400
C
%TOC
0
10
20
30
40
AQT'09
AQT'10
BLB
CSE
HWL
JLN
KSO
NRT
OPE
RFT
SAM
SPC
SRT
WGN
Lake
D
MeHg (ng g-1, d.w.)
0.0
0.5
1.0
1.5
2.0
Lake
E
ng MeHg g-1 OC
0
2
4
6
8
10
12
Lake

Figure 2.2: A) Mean total mercury ± SD (ng g^{-1}, dw), B) total mercury corrected for organic content (ng g^{-1} OC), C) mean total organic content ± SD (%), D) methylmercury (ng g^{-1}, dw) and E) methylmercury corrected for organic content (ng MeHg g^{-1} OC) in surface (black bars) and deep (white bars) sediments from lakes in the Hudson Bay Lowlands. AQT'09 = Aquatuk 2009; AQT'10 = Aquatuk 2010, BLB = Billbear; CSE = Cassie; HWL = Hawley; JLN = Julison; KSO = Kinushseo; NRT = North Raft; OPE = Opinnagau East; RFT = Raft; SAM = Sam; SPC = Spruce; SRT = Stuart and WGN = Wolfgang.

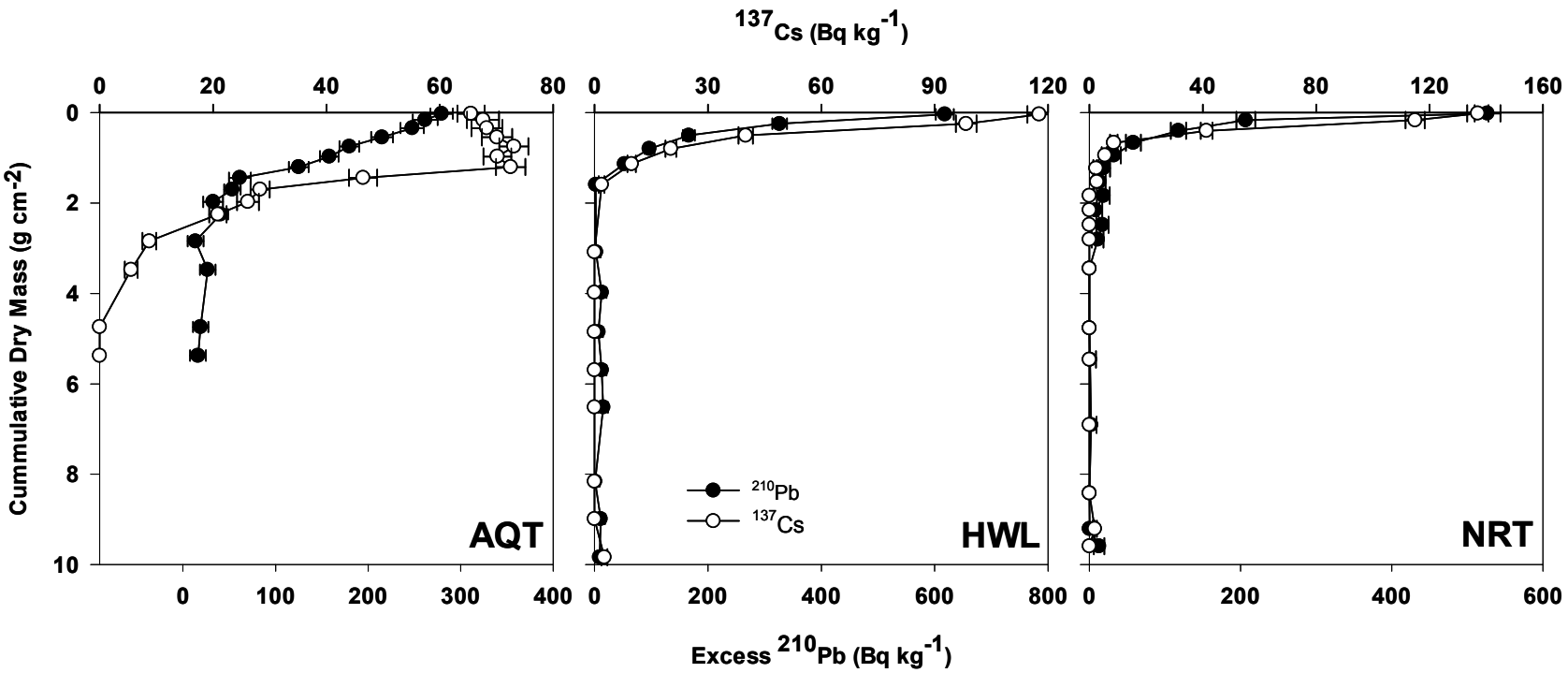

Figure 2.3: Excess ^{210}Pb ± SD (Bq kg^{-1}) and ^{137}Cs ± SD (Bq kg^{-1}) versus cumulative dry mass (g cm^{-2}) in sediment cores from Aquatuk (AQT), Hawley (HWL) and North Raft (NRT) lakes from the Hudson Bay Lowlands of Ontario, Canada.

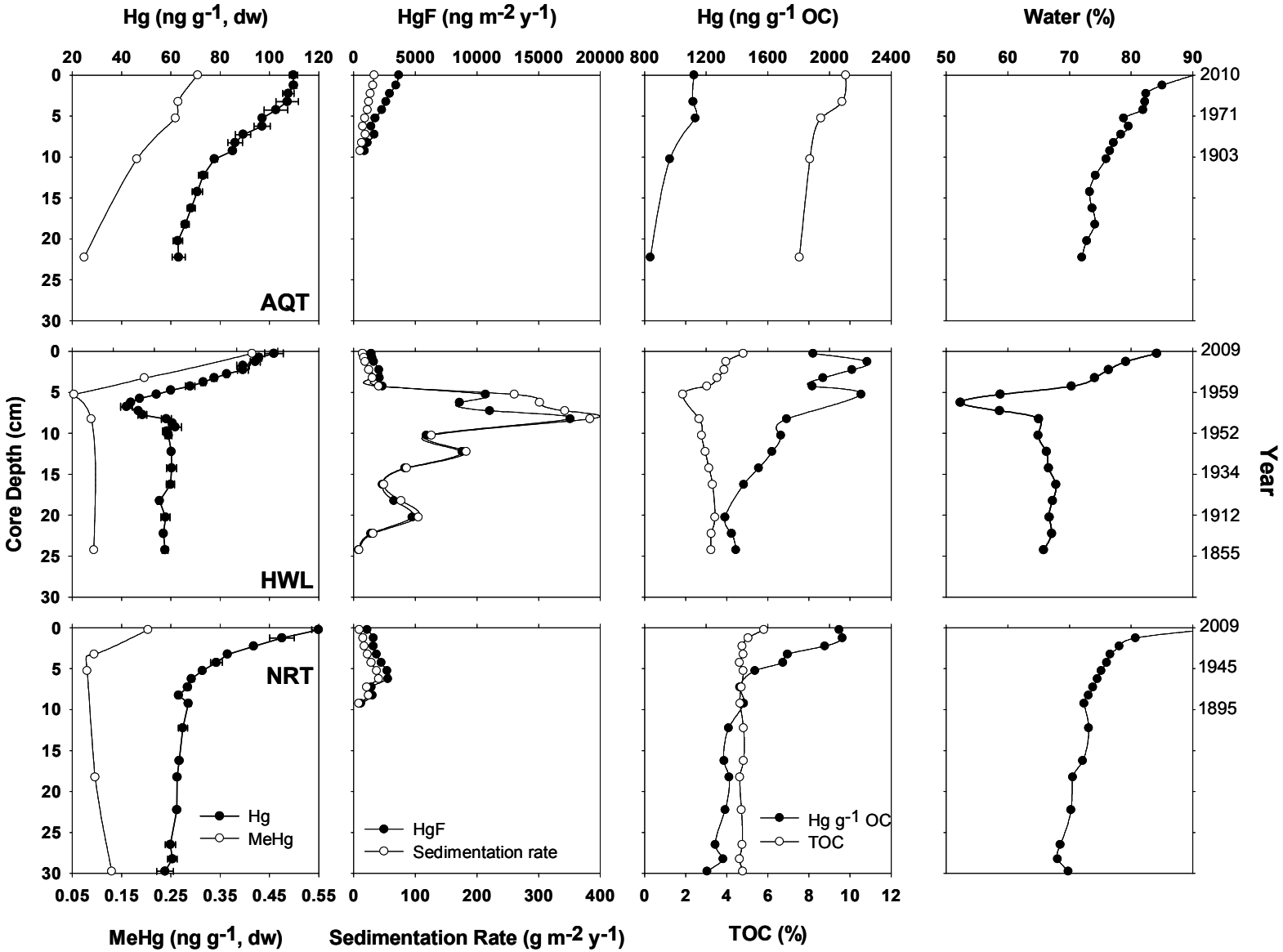
Hg (ng g-1, dw)
HgF (ng m-2 y-1)
Hg (ng g-1 OC)
Water (%)
Core Depth (cm)
Year
AQT
HWL
NRT
Hg
MeHg
HgF
Sedimentation rate
Hg g-1 OC
TOC
MeHg (ng g-1, dw)
Sedimentation Rate (g m-2 y-1)
TOC (%)

Figure 2.4: Mean mercury concentrations ± SD (Hg; ng g^{-1},dw), methylmercury concentrations (MeHg; ng g^{-1}, dw), mercury flux (HgF; ng m^{-2} y^{-1}), sedimentation rate (g m^{-2} y^{-1}), total organic carbon (TOC; %) and water content (%) according to the sediment core depth (cm) and calendar year determined by radiometric dating (constant rate of supply model) in Aquatuk (AQT), Hawley (HWL) and North Raft (NRT) Lakes from the Hudson Bay Lowlands of Ontario, Canada.

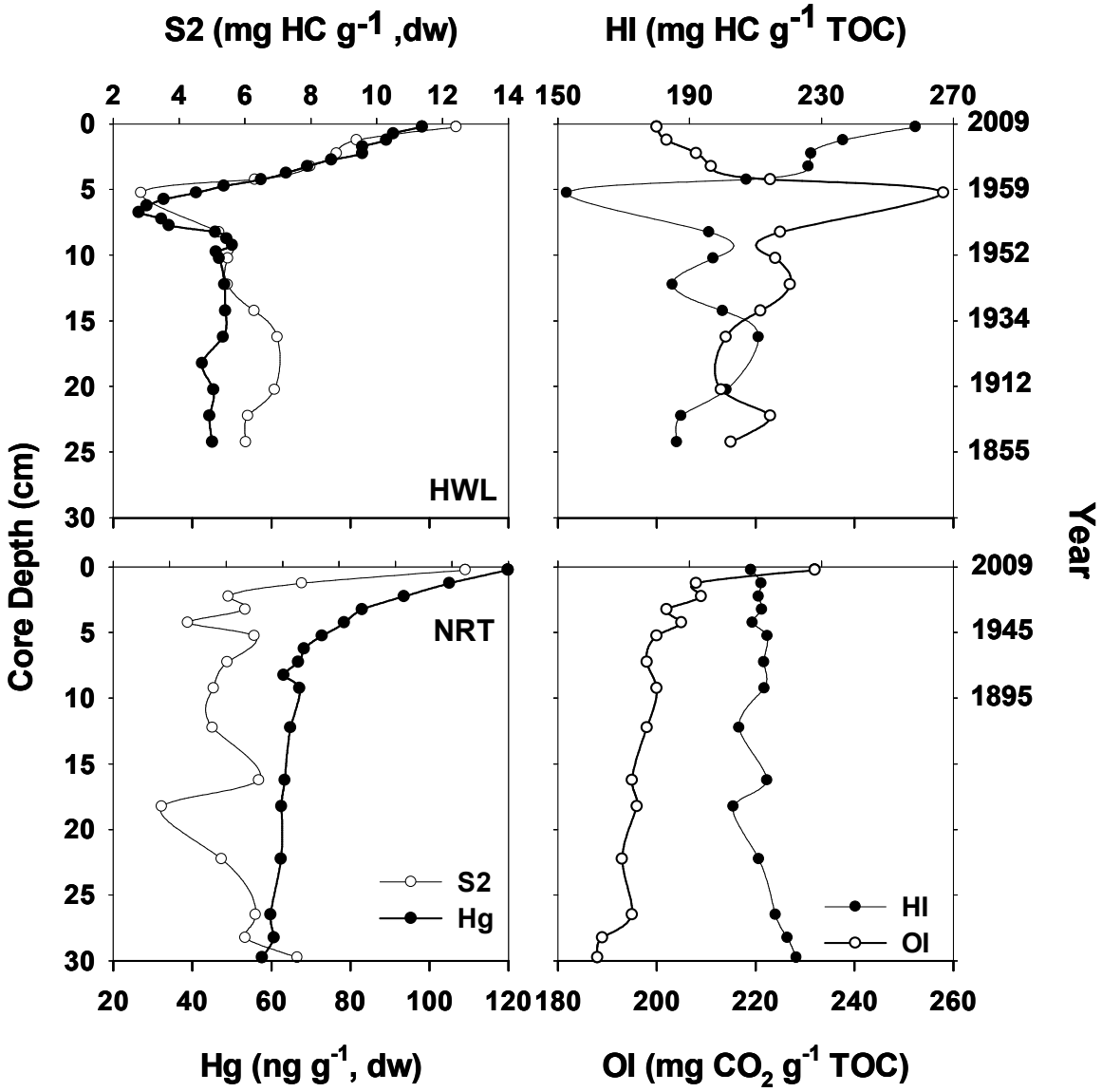

Figure 2.5: Algal-derived organic carbon (S2; mg HC g^{-1}, dw), mercury concentration (Hg; ng g^{-1}, dw) hydrogen index (mg HC g^{-1} TOC) and oxygen index (mg CO_2 g^{-1} TOC) according to depth and year of deposition in sediment cores from Hawley (HWL) and North Raft (NRT) Lakes. Dates were determined by radiometric dating according to the constant rate of supply model.

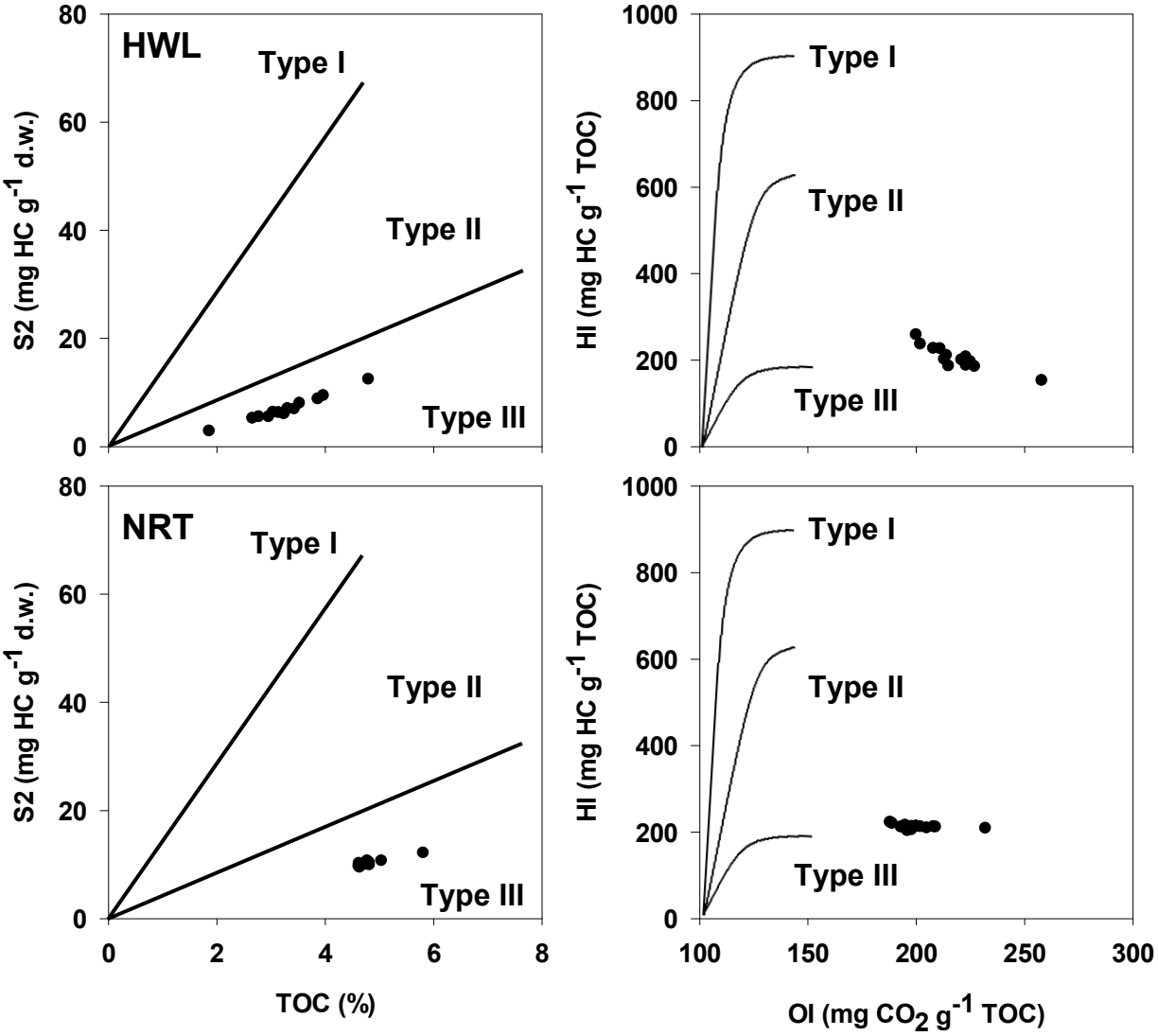

Figure 2.6: Van Krevelen diagrams of sediments from Hawley (HWL) and North Raft (NRT) Lakes. Kerogen type is characterized by plotting the relationship between S2 (algal-derived organic carbon; mg HC g^{-1}, dw) and total organic carbon (TOC; %) or hydrogen index (HI; mg HC g^{-1} TOC) and oxygen index (OI; mg CO_2 g^{-1} TOC). The solid lines define the boundaries of Type I, II, and III kerogens.

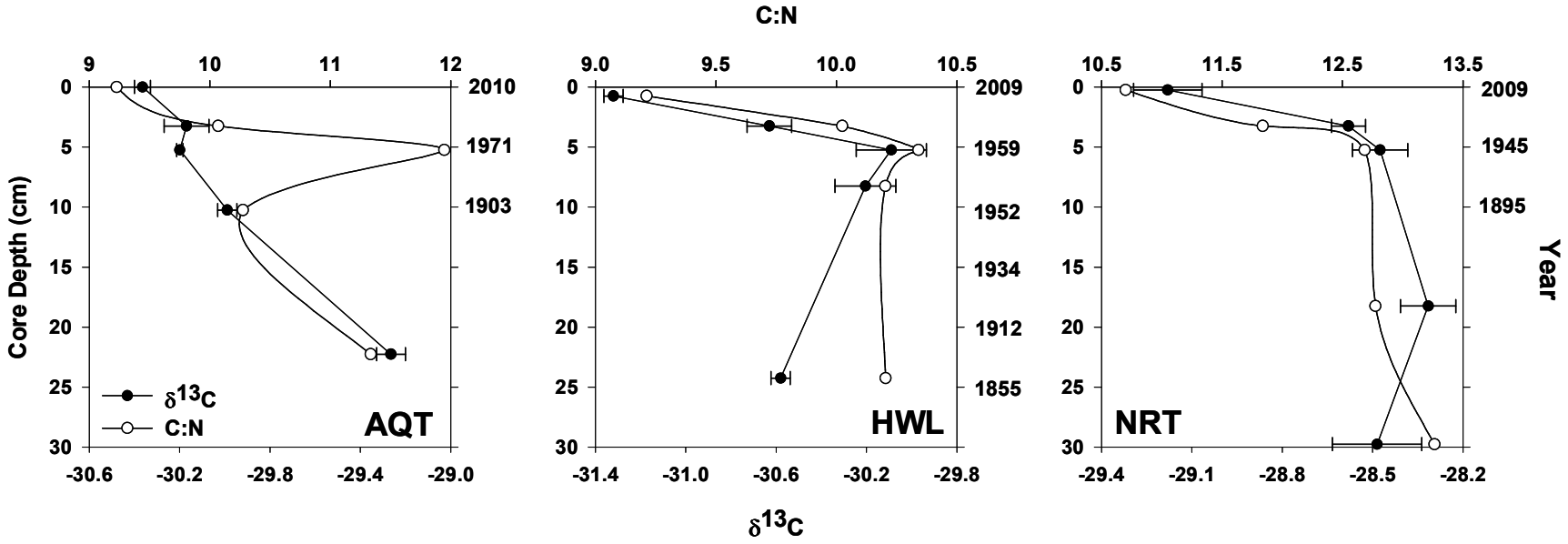

Figure 2.7: Carbon to nitrogen ratio (C:N) and $\partial^{13}C$ (average, n=3, ± SD) according to depth and year of deposition in sediment cores from Aquatuk (AQT), Hawley (HWL) and North Raft (NRT) lakes from the Hudson Bay lowlands. Dates were determined by radiometric dating according to the constant rate of supply model.

2.9 Supplemental Information

2.9.1 List of Figure

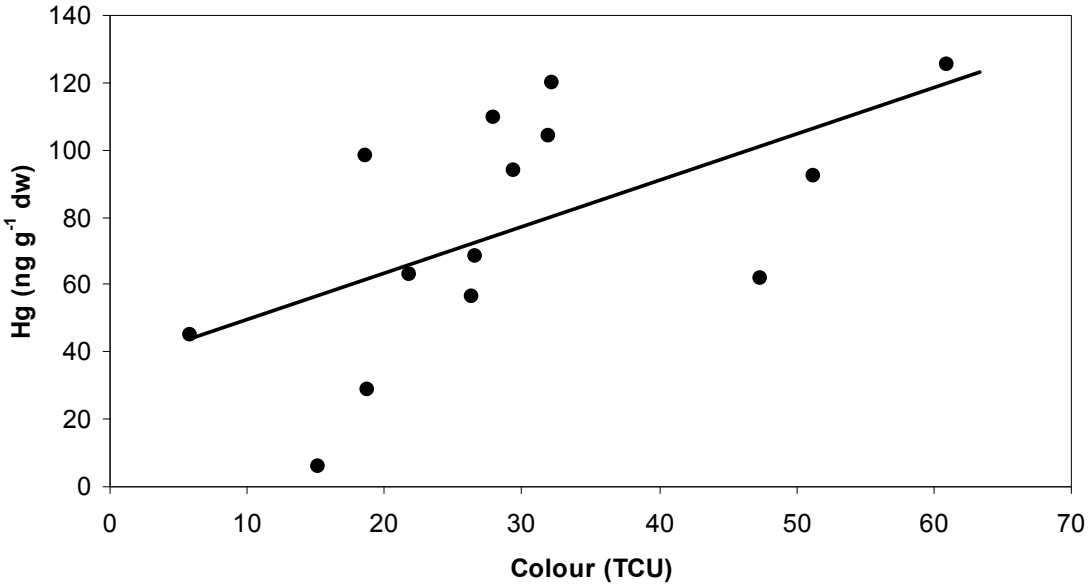

Figure S2.1: Correlation between mercury (ng g^{-1}, dw) in surface sediments and water colour (TCU) in 14 lakes from the Hudson Bay Lowlands of Ontario, Canada. $R^2 = 0.337$, $p = 0.0263$.

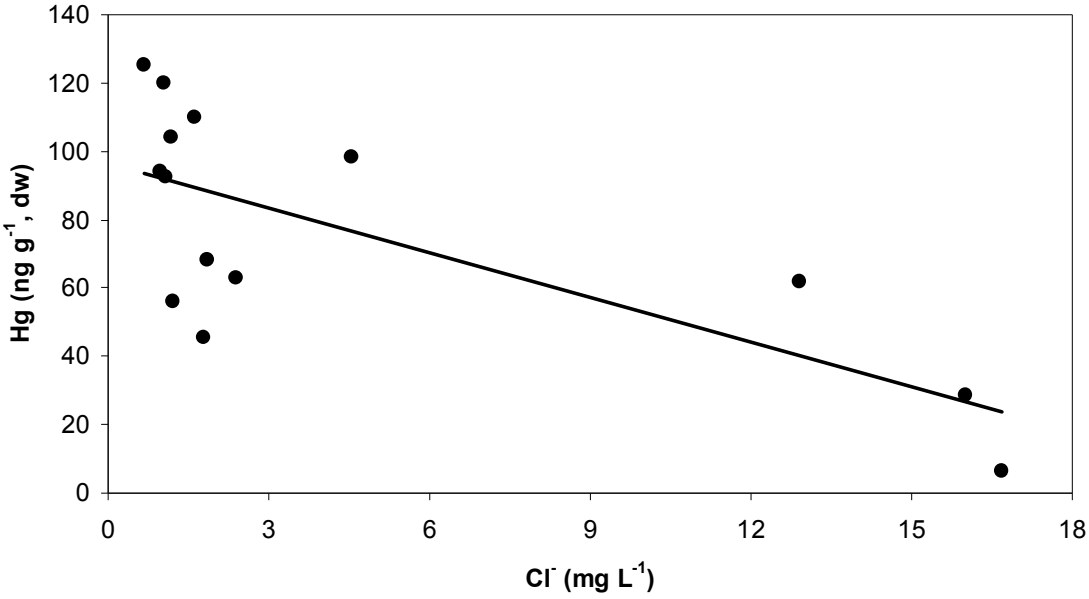

Figure S2.2: Correlation between mercury (ng g^{-1}, dw) in surface sediments and chloride (mg L^{-1}) in lakewater of 14 lakes from the Hudson Bay Lowlands of Ontario, Canada. $R^2 = 0.52$, $p = 0.005$.

Chapter 3.0: Abundance of Mercuric Reductase Genes (*merA*) in Lake Sediment Core Samples: Are Environmental Changes Responsible for an Enrichment of Microbial Hg Resistant Communities?

3.1 Abstract

Mercury (Hg) is a ubiquitous contaminant with a very complex biogeochemical cycle. Hg can become available to methylating bacteria which produce methylmercury (MeHg); a potent bioaccumulative neurotoxin. Processes that directly or indirectly affect the availability of Hg to methylating bacteria can therefore greatly alter its toxicity. Here, we use lake sediment archives to assess total Hg (THg) distribution in three freshwater lakes from the Hudson Bay Lowlands, Ontario, Canada. We also examined the distribution and quantified the mercuric reductase enzyme gene (*merA*) from lake sediment cores because this gene catalyzes the reduction of Hg(II) to Hg(0), making it less bioavailable to methylating bacteria.

[THg] was highest in the most recently deposited sediment, and decreased with depth. *MerA* genes were detected in all three lakes at almost all depths and for the first time, down to depths corresponding to sediments deposited prior to the industrial revolution. In contrast to the THg profile, *merA* gene copy numbers increased with depth, reaching a maximum in sediments deposited before 1960. The abundance of *merA* genes with depth did not match the profile of the control gene *glnA* which is involved in core nitrogen metabolism. Although great uncertainty remains on the origin and functionality of the *merA* genes detected at depth, this work suggests a yet unidentified set of conditions that may select for the preservation of these genes at depth.

3.2 Introduction

Mercury (Hg) is a ubiquitous contaminant that threatens human and wildlife health. It is emitted from natural sources such as volcanoes and forest fires, and anthropogenic sources such as coal and fossil fuel combustion, waste incineration, industrial activity, mining, etc. (Murdoch and Clair, 1986; Barkay *et al.*, 2003). The volatile form of mercury, Hg(0), accounts for >95% of the Hg in the atmosphere and has an atmospheric residence time of up to 2 years; allowing atmospheric transportation to areas far removed from point sources (Lindberg *et al.*, 2007; Gustin *et al.*, 2008). As a result, elevated levels of Hg are found in remote areas such as

the Arctic and subarctic ecosystems, where simplified food webs are especially susceptible to bioaccumulation of methylmercury (MeHg); the neurotoxic form of Hg (Poissant *et al.*, 2008). A recent study has shown that MeHg bioaccumulation in wildlife of the Canadian Arctic is still increasing, especially in marine mammals, which are the main dietary source of exposure to Inuit and Aboriginal populations (Fontaine *et al.*, 2008; Riget *et al.*, 2011). Changes in northern ecosystems due to climate warming have already been documented and are expected to alter the cycling of contaminants, including Hg, warranting the need to further study the Hg cycle in these fragile ecosystems (Macdonald *et al.*, 2005; Post *et al.*, 2009).

The principal source of Hg to Arctic and subarctic ecosystems is atmospheric deposition of inorganic mercury (Hg(II)) (Chemicals Branch, 2008). Bioaccumulation of MeHg depends on its *in situ* synthesis and ensuing uptake by primary producers and microbes. Hence microbes that can transform Hg play a subtle but critical role in the Hg cycle in ecosystems, ultimately controlling the fate of the deposited inorganic mercury. The *mer* operon is a cluster of genes that encodes bacterial mercury resistance (Hg^R) in certain bacteria; conferring the ability to reduce MeHg or Hg(II) into monoatomic elemental mercury vapor (Hg(0)) (Barkay *et al.*, 2003). The result is a net removal of Hg from the immediate environment, reducing its availability to methylating bacteria and its subsequent toxicity. The *mer* operon can be present on the bacterial chromosome or on broad host range plasmids and transposons which can be readily disseminated within the population (Rochelle *et al.*, 1989). Hg^R has been extensively studied in heavily Hg-contaminated environments but remains comparatively understudied in pristine, non-contaminated systems in which the only source of Hg is from atmospheric deposition (Schaefer *et al.*, 2004; Ramond *et al.*, 2009).

The *merA* gene is arguably the most important part of the *mer* operon; the Hg:NADP+ oxidoreductase (EC 1.16.1.1) is a cytoplasmic enzyme utilizes NADPH as a source of electrons to catalyze the conversion of Hg(II) to Hg(0) (Furukawa and Tonomura, 1972; Gopinath *et al.*, 1989). Although the *mer* operon can be very diverse among species, it must contain *merA* to be functional (Rosen, 1996).

Therefore the presence of *merA* can be used as a reliable proxy to assess the presence of a functional *mer* operon in a particular (meta)genome.

Several lakes in the Hudson Bay Lowlands (HBL) of Northern Ontario are displaying symptoms of ecological changes hypothesized to be the result of a changing climate; the most significant of which have been episodes of mass fish mortality (Gunn and Snucins, 2010). These lakes have recently become the subject of a multidisciplinary study to document changes occurring as a result of the warming climate. Here we use lake sediment cores to assess the history of mercury deposition to three remote lakes of the HBL in Northern Ontario. We also assess the potential for a biological influence to the Hg redox cycle by identifying and quantifying the bacterial mercury resistance gene; *merA*. Our goal was to test whether recent environmental changes combined with enhanced Hg deposition, have contributed to enrich the microbial community with mercury resistant bacteria.

3.3 Material and Methods

3.3.1 Sampling Site and Sample Collection

Sediment cores were collected from three lakes in the Hudson Bay Lowlands area in Northern Ontario, Canada. Hawley (HWL; 54º33'5.30"N, 84º37'58.80"W) and North Raft (NRT; 54º32'4.00"N, 84º45'21.60"W) Lakes were sampled in July 2009 and Aquatuk Lake (AQT; 54º21'11.80"N, 84º34'29.80"W) was sampled in August 2010. The lakes are freshwater, oligotrophic and located on the Precambrian bedrock of the Sutton Ridges (Gunn and Snucins, 2010). Sediment cores were taken using a MiniGlew KB gravity corer (Glew, 1991). The sediment cores were sectioned into 0.5 cm intervals over the first 10 cm (20 samples) and every 2 cm for the remaining fraction of the core. Upon collection, core samples were divided in two; half of the interval was put into a 50mL polypropylene centrifuge tube with 10mL of RNAlater® solution (Life Technologies, Inc.) and shaken to allow the solution to properly penetrate the sample, which was dedicated to molecular analyses. The other half of the interval was placed into a Whirl-Pak® bag and dedicated to Hg and radiometric analyses. All samples were kept at 4^{o}C and in the dark until frozen at -20^{o}C. All containers used for sampling were sterile and non-

powdered gloves were worn at all times during sampling and processing of the samples.

3.3.2 Mercury Analyses

Frozen sediments were transferred from Whirl-Pak® bags into 50mL sterile high density polypropylene Falcon® tubes. Samples were lyophilized for a period of 72 hours under a vacuum of 5 atm and homogenized. Total Hg in sediments was analyzed with Nippon Instruments Corporation's Mercury SP-3D Analyzer (CV-AAS) by thermal decomposition with gold trap amalgamation and cold vapour atomic absorption method (UOP Method 938-00, detection limit of 0.01ng Hg and range up to 1000ng Hg; Fox *et al.*, 2005). The instrument was calibrated with Mercury Reference Solution 1000ppm ±1% (Fisher CSM114-100) and MESS-3 (91±9 ng g^{-1}, National Research Council of Canada) was used as reference material. Blanks were performed as suggested by the manufacturer.

3.3.3 Radiometric dating

The sediment cores were radiometrically dated using gamma (γ) spectrometry and analyzed for the activity of ^{210}Pb, ^{137}Cs and ^{226}Ra in an Ortec germanium crystal well detector (DSPec, Ortec, model # GWL-120230) following the method by Appleby, (2001). Analysis of ^{210}Pb was performed on 14-18 selected depth intervals of the sediment cores to determine the sediment age, and the sediment accumulation rate. Samples were lyophilized, homogenized and hermetically sealed and left to reach secular equilibrium for a minimum of 21 days before being counted for 23 hours (82,800 seconds). The resulting spectrum files showed ^{210}Pb activity with a peak at 46.5 keV, and ^{137}Cs at 662 keV. ^{226}Ra activity was determined by γ-ray emissions of its daughter isotope ^{214}Pb, resulting in peaks at 295 and 352 keV. Long-term sedimentation rates were determined for each core using methods in Appleby and Oldfield, (1978). ^{137}Cs activity (from atmospheric fallout of nuclear weapons, peaking in 1963) was measured to verify ^{210}Pb dates.

3.3.4 Sample Preparation

Prior to subsampling for DNA or RNA extractions, sediment samples were thawed and centrifuged at 2000 × g for 10 min and the supernatant was discarded. For DNA extraction, a subsample of 0.5g was placed into a sterile 2mL Eppendorf tube. We used a sterile buffer modified from Zhou *et al.* (1996) to wash the sediment to remove contaminants such as humic substances and divalent cations that can be co-extracted with nucleic acids and inhibit subsequent downstream applications. The buffer consisted of 10mM EDTA, 50mM Tris-HCl and 50mM $Na_2HPO_4 \cdot 7H_2O$ at pH 8.0. We added 3 parts buffer for 1 part sediment, then samples were vortexed at maximum speed for 30 seconds, centrifuged at 700 × g for 3 min and the supernatant was discarded. For RNA extraction, a subsample of 5g was washed with 15mL of DEPC-made buffer in a sterile RNase-free 50mL Falcon® tube. Tubes were vortexed at maximum speed for 30 seconds, centrifuged at 5500 × g for 10 minutes and the supernatant was discarded. The washing procedure was repeated until the supernatant was clear (maximum of 5 washes). The washed sediment was immediately used for DNA or RNA extraction.

3.3.5 Bacterial DNA Extraction and Quantification

Bacterial DNA extraction from the washed sediment was performed using a PowerSoil DNA Isolation Kit (MoBio, Carlsbad, CA) according to the manufacturer's guidelines. DNA extraction was performed on sediment from 5 depth intervals of each core. The extraction was executed in a laminar flow hood with HEPA filter and all work surfaces and equipment were washed with 70% ethanol, 10% bleach and sterilized under UV light. The extracted DNA was quantified using an Invitrogen Quant-iT™ dsDNA High-Sensitivity Assay Kit (Invitrogen™, San Diego, CA) according to the manufacturer's protocol. DNA extracts were stored at -20ºC until further use.

3.3.6. RNA Extraction and cDNA Synthesis

All RNA work was performed in a laminar flow hood with HEPA filter. Work area and instruments were washed with 70% ethanol, 10% bleach, RNase *AWAY* (Molecular BioProducts, San Diego, CA) and sterilized under UV light. Bacterial

RNA extraction was performed using the RNA PowerSoil® Total RNA Isolation Kit (MoBio, Carlsbad, CA) according to the manufacturer's protocol (with the exception of Step 12: samples were incubated at room temperature instead of -20ºC). The pH of the phenol:chloroform:isoamyl alcohol solution used was 6.3. RNA was quantified by spectrophotometry using a NanoDrop ND-1000 spectrophotometer (NanoDrop Technologies). The RNA was treated with RQI RNase-Free DNase (Promega, Madison, WI) according to the manufacturer's protocol. A *glnA* PCR was performed on the RNA (as described below) to confirm the elimination of carry-over DNA before proceeding to cDNA synthesis. RNA was kept on ice during manipulations and stored at -80ºC.

Complementary DNA (cDNA) was synthesized using the iScript™ cDNA Synthesis Kit (BioRad Laboratories, Hercules, CA) with random hexamers as primers according to the manufacturer's instructions. We included a control reaction where the reverse transcriptase was omitted (-RT) to insure the absence of contaminating DNA. cDNA was used as template in PCR to detect *glnA* and *merA* transcripts. cDNA was stored at -20ºC.

3.3.7 Gene Amplification

In order to assess the quality of the extracted DNA, two commonly used house-keeping genes were amplified: 16S rRNA and *glnA*. The forward primer 27F (5'-AGAGTTTGATCMTGGCTCAG-3') and the reverse primer 907R (5'-CCGTCAATTCATTTGAG-3') were used for the amplification of a 880bp fragment of the 16S rRNA gene (Lane, 1991). The 25µL reaction mixture contained 1× GoTaq Buffer® (Promega, Madison, WI), 2.0 mM $MgCl_2$, 0.2 mM of each deoxynucleoside triphosphate (dNTP), 0.5 µM of each forward and reverse primer, 1% DMSO and 0.25 U Go*Taq*® DNA polymerase (Promega, Madison, WI). 1µL of genomic DNA was used as a template in all PCR reactions. Amplification conditions were as follows: 10 min at 94°C, followed by 35 cycles of 30 s at 94°C, 30 s at 55°C, and 60 s at 72°C, followed by a final extension of 5 min at 72°C. Each reaction included a positive control using DNA from *Escherichia coli* and a negative control in which the template was water. Amplicons were separated by agarose gel electrophoresis

(1.5% agarose, 5V/cm for 60 min, stained with EtBr) and compared to a 100bp exACTGene Low Range Plus DNA ladder (Fisher Scientific). The forward primer GS1β (5'-GATGCCGCCGATGTAGTA-3') and reverse primer GS2γ (5'-AAGACCGCGACCTTPATGCC-3') were used to amplify the prokaryotic *glnA* gene using the same cycling conditions as 16S rRNA with the annealing temperature modified to 60°C (Hurt *et al.*, 2001). The size of the amplicon is 154 bp.

The presence of the *merA* gene in DNA extracts could only be accurately detected using a nested PCR approach; attempts to directly amplify the 307-bp fragment from sediment DNA using the Nsf primer pair were unsuccessful. The first reaction of the nested approach amplified a 1246 bp fragment using the forward primer Nlf.F (5'-CCATCGGCGGCACYTGCGTYAA-3') and the reverse primer Nlf.R (5'-CGCYGCRAGCTTYAAYCYYTCRRCCATYGT-3') and the following reaction conditions: final volume of 10μL containing 1× GoTaq Buffer® (Promega, Madison, WI), 2.0 mM $MgCl_2$, 0.2 mM of each dNTP, 0.5 μM of each forward and reverse primer, 1% DMSO and 0.25 U Go*Taq*® DNA polymerase (Promega, Madison, WI). The amplification cycle was as follows: 10 min at 94°C followed by 25 cycles of 30 s at 94°C, 30 s at 62°C, 60 s at 72°C and a final extension of 5 min at 72°C. The amplicons were separated by agarose gel electrophoresis, as mentioned above, to confirm a successful and accurate amplification. The end product of the first PCR amplification was used as template for a second PCR, which amplified a 307 bp fragment internal to the 1246 bp template. PCR conditions for the nested reaction were the same as for the initial amplification, with the forward primer changed to Nsf F (5'-ATCCGCAAGTNGCVACBGTNGG-3'), the extension time changed to 30 s and the number of cycles increased to 35. The *merA* gene from the *Pseudomonas* transposon Tn501 served as the positive control. Two additional control reactions were added to include a nested positive (+N) and a nested negative (-N) control. Primers used in the nested PCR are degenerate to allow the capture of a greater diversity of sequences from these environmental samples.

MerA2 primers (MerA2 F: 5'-ACCTGCGTCAACGTCGGCTG-3', MerA2 R: 5'-GCGATCAGGCAGCGGTCGAA-3') are non-degenerate and were designed for use in the quantification assays described below. We applied them to amplify the *merA*

gene directly from the genomic DNA (without using a nested approach) for proof of principle. However, the amplicon was not as clear and specific as the ones achieved with the nested approach. The 10µL reactions included: 1µL 10× Platinum® *Taq* PCR Buffer, 2.0 mM $MgCl_2$, 0.2 mM of each dNTP, 0.5 µM of each forward and reverse primer, 1% DMSO and 0.25 U Platinum® *Taq* DNA polymerase (Invitrogen™, San Diego, CA). The amplification conditions were the following: 5 min at 95°C followed by 40 cycles of 30 s at 95°C, 15 s at 63°C and 30 s at 72°C with a final extension step of 5 min at 72°C. All of the oligonucleotides used as primers in this study were synthesized by Integrated DNA Technologies (Coraville, IA).

3.3.8 Cloning and Sequencing of merA Gene PCR Products

The PCR amplicon from the nested PCR on NRT 0-0.5cm DNA was cloned and sequenced to confirm the amplification of the desired *merA* gene. PCR products used for cloning were separated by gel electrophoresis (2% agarose, 5V/cm for 120 min.). The 307-bp amplicon was extracted and purified from the gel using QIAEX II Gel Extraction Kit (QIAGEN, Valencia, CA). The purified DNA amplicons were cloned into the vector pCR®4-TOPO®, using a TOPO-TA Cloning® Kit for Sequencing (Invitrogen™, San Diego, CA) according to the manufacturer's instructions. Plasmid DNA was isolated from 4 clones using a Wizard® *Plus* SV Minipreps DNA Purification System (Promega, Madison, WI) and screened for inserts of the correct size by PCR following the *merA* PCR protocol described above. DNA from the clones containing the 307-bp insert (100fmol) was sequenced using the primer M13F(-20) (5'-GTA AAA CGA CGG CCA G-3') and the Beckman Coulter CEQ™ 8000 Genetic Analysis System (Beckman Coulter, Fullerton, CA).

3.3.9 Gene Quantification

3.3.9.1 Production of Standards for qPCR

The plasmid pASK-IBA3C containing the complete *merA* gene (1686 bp) from *Pseudomonas* Transposon Tn501 (Brown *et al.*, 1983) was used to generate standards for the *merA* gene. The *glnA* gene was amplified from *Escherichia coli*, the band excised and purified using QIAEX II Gel Extraction Kit (QIAGEN, Valencia,

CA) and cloned into pGEM-T vector (Promega, Madison, WI) according to the manufacturers' protocol. The Wizard® *Plus* SV Minipreps DNA Purification System (Promega, Madison, WI) was used to extract the plasmids and the concentrations were quantified by spectrophotometry using a NanoDrop ND-1000 spectrophotometer (NanoDrop Technologies). The *merA* and *glnA* standards were verified by PCR and agarose gel electrophoresis following the respective protocols described above. Calculation of the plasmid copy number was performed according to the molar mass derived from the plasmid and amplicon sequences as follows;

1. Plasmid weight + insert weight = total weight (g mol^{-1})
2. Total weight (g mol^{-1}) ÷ Avogadro's number (6.02214199 × 10^{23} molecule mol^{-1}) = g $molecule^{-1}$
3. Concentration of plasmid (g μL^{-1}) ÷ g $molecule^{-1}$ = copy number (molecules μL^{-1})

Dilutions of plasmid DNA containing the cloned genes of *merA* and *glnA* were used to generate standard curves in quantities ranging from 1.73 × 10^2 to 1.73 × 10^7 copies for *merA* and 3.28 × 10^2 to 3.28 ×10^8 copies for *glnA.*

3.3.9.2 qPCR Assays for *merA* and *glnA* Absolute Quantification

qPCR assays for absolute quantification of *glnA* and *merA* genes were performed separately using SsoFast EvaGreen Supermix (Bio-Rad Laboratories, Hercules, CA) and the Eco™ Real-Time PCR System (Illumina Inc., San Diego, CA). Reaction preparations were performed in a laminar flow hood with HEPA filter and all work surfaces and equipment were washed with 70% ethanol, 10% bleach and sterilized under UV light. Each 20µL qPCR reaction contained 10µL SsoFast mix, 0.5µM each forward and reverse primer, 2µL DNA template (diluted 1/10 with sterile water) and 6µL water. Cycling conditions were the following: 98°C for 5 min then 35 cycles of 98°C for 15 s and 63°C for 30 s (*merA*) or 60°C for 30 s (*glnA*). Fluorescence was detected after each cycle. Each reaction efficiency (E) was calculated as E = 10(-1/slope); where the slope of the standard curve was determined by plotting the C_T versus log standard DNA dilution. Gene copy numbers were divided by genomic DNA concentrations to obtain copies ng^{-1} of DNA which

normalized the results to account for biases that may have occurred during the DNA extraction procedure.

3.3.9.3. Quality Control of qPCR Data

The specificity of the qPCR amplicons was assessed by a melt curve analysis. After the last cycle, amplicons were subjected to a programmed temperature increase from 55ºC to 98ºC. Fluorescence data was collected every 0.3ºC and the negative derivative of relative fluorescence units (RFU) was plotted versus temperature (-dRFU/dT) which calculates melting temperatures (T_m) based upon peak calls. The T_m of an amplicon is based on its nucleotide sequence; therefore the amplicons of a targeted gene should have a similar T_m as the standards. Information from the melt curve was combined with that of the agarose gels from traditional PCRs to identify and eliminate non-specific amplicons or primer dimer artifacts from the analyses.

3.4 Results and Discussion

3.4.1 Temporal Mercury Distribution and 210Pb Dating

Radiometric dating revealed that most excess ^{210}Pb and ^{137}Cs is concentrated in the top 2 cm of accumulated dry mass of the sediment cores, suggesting a very low sediment accumulation rate. As a result, background was achieved early in the NRT and AQT cores, limiting dating to the top 9 cm intervals. The constant rate of supply model (CRS) was used in the three cores to achieve dating with decadal resolution.

The Hg depth profiles of the sediment cores form AQT, HWL and NRT Lakes are consistent with those reported by others in the Arctic and subarctic (Kirk *et al.*, 2011). In all three lakes, Hg concentrations steadily increase towards the surface of the core, with the highest concentrations in the most recently deposited sediments (Fig. S3.1). We consider Hg concentrations in sediments deposited before 1900 to be historical/pre-industrial and the sediment at the surface of the core as recent. In AQT Lake, the average historical [Hg] is 68.8 ± 5 ng g^{-1} (dw) from 10.25 to 22.25cm depth and the recent [Hg] is 108.6 ± 1 ng g^{-1} (dw). When we compare the historical concentrations to the recent concentrations, we obtain an enrichment factor (EF) of

1.58. Historical concentration of Hg in HWL sediments from 22.25 to 24.25 cm is 44.8 ± 0.5 ng g^{-1} (dw) and the recent sediments have a concentration of 92.7 ± 5 ng g^{-1} (dw) yielding an EF of 2.07 and NRT Lake historical concentrations are 62.3 ± 3 ng g^{-1} (dw) between the depths of 9.25 to 29.75 cm and reach a maximum of 112.5 ± 11 ng g^{-1} (dw) in recent sediments for an EF of 1.80. The concentrations recorded on the surface sediments are comparable to those found in lakes from highly urbanized areas (i.e. Lake Winnipeg South: average of 125 ng g^{-1}, d.w. in sediments since 1950; Lockhart *et al.*, 1998).

3.4.2 DNA Extraction

Our wash buffer was efficient at removing extraction-inhibiting substances as tested on samples of goose excrements which are rich in organic matter and for which previous deoxyribonucleic acid (DNA) extractions failed. The sample was divided and submitted to three separate treatments; non-washed, washed with sterile water and washed with the buffer. Washing with the buffer greatly increased DNA yield; therefore we applied the wash protocol to all sediment DNA and RNA extractions (Fig. 3.1).

Mercury concentrations were used to select five depth intervals from the sediment cores for DNA extraction, including the top-most and bottom-most intervals. Selected intervals were as follows; AQT: 0-0.5cm, 3-3.5cm, 5-5.5cm, 10-10.5cm and 22-22.5cm; HWL: 0-0.5cm, 3-3.5cm, 5-5.5cm, 8-8.5cm and 24-24.5cm; NRT: 0-0.5cm, 3-3.5cm, 5-5.5cm, 18-18.5cm and 29.5-30cm. Genomic DNA was successfully extracted from all sediment samples (Fig. S3.2). DNA concentrations were highest in surface sediment and decreased progressively as depth/age of sediment increased (Table 3.2).

3.4.3 16S rRNA and glnA Gene Amplification

The 16S rRNA gene is commonly used in phylogenetic analyses and is known as a very useful molecular taxonomic marker. However, some organisms can possess multiple copies of the 16S rRNA gene, biasing quantification assays based solely on 16S genes (Case *et al.*, 2007). The glutamine synthetase (*glnA*) gene is

increasingly used in quantification assays as bacteria possess a single copy of this gene which codes for the enzyme that catalyses the biosynthesis of glutamine; an essential amino acid (Woods and Reid, 1993).

16SrRNA genes were amplified from HWL and NRT DNA to confirm the extraction of bacterial DNA and to assess its quality (Fig. 3.2). The first 16S rRNA PCR was performed on genomic DNA from NRT using non-diluted and diluted (1/10) DNA to determine if a dilution would increase PCR efficacy by also diluting possible PCR inhibitors. There was no difference between the diluted and non-diluted template therefore we proceeded to use non-diluted DNA for the remainder of the samples (Fig. 3.2 C). We then amplified the *glnA* gene from all depth intervals of AQT (Fig. 3.2 A). The successful amplification of these genes suggested that the DNA was of good quality and could be used for further PCR targeting functional genes.

3.4.4 merA Gene Amplification and Sequencing

Attempts to directly amplify the 307 bp fragment of the *merA* gene from genomic DNA using Nsf primers were unsuccessful, as observed in previous studies from Arctic biomass (Poulain *et al.*, 2007). However, the nested PCR approach proved to be very effective. The genomic DNA was used as template for an initial PCR using Nlf primers which generated a 1246 bp fragment (Table 3.1). The amplicons were not always visible on an agarose gel (Fig. S3.3). Regardless, 1µL of the resulting PCR product was used as template for a second PCR reaction using the Nsf primers. A 307 bp fragment was successfully amplified from all depth intervals from all lakes except NRT 18-18.5 cm and the band from NRT 29.5-30 cm is not as distinct as the bands from the other samples (Fig. 3.3).

In order to confirm that the amplified bands corresponded to the *merA* gene, the PCR product from NRT 0-0.5cm was cloned and sequenced. Clones contained a 307 bp insert and were all sequenced. The majority of the clones had >90% nucleotide coverage with *Enterobacter cloacae* DNA mosaic mercury resistance transposable element mer-operon (Y09025) which confirmed the amplification of the *merA* gene from the sediment samples.

Small amplicons (<300 bp) originating from non degenerate primers are better suited for qPCR analyses. However, using non degenerate primers may decrease the pool of sequences that can be accessed by PCR. Figure 3.4 shows the bands amplified with the MerA2 primer set. We clearly see a decrease in band intensity, especially in HWL; some non-specific amplification was also observed, suggesting that PCR conditions or primer design could be further improved.

3.4.5 cDNA Amplification

Total RNA was extracted from sediments from HWL 0.5-1 cm. as a pilot assay. cDNA was synthesized using random hexamer primers and used as template for a *glnA* PCR. Figure 3.5 shows the successful amplification of a faint band in the +RT treatment which is consistent with the 154 bp fragment of the positive control (+). Both negative control reactions are free of contamination. Several attempts at amplifying the *merA* gene from the same cDNA were unsuccessful (Fig. 3.6).

We attempted to synthesize *merA* gene specific cDNA (g.s.cDNA) by using the NIF reverse primer in lieu of random hexamers for the reverse transcription. A *merA* PCR on the resulting g.s.cDNA was successful, however, sequencing revealed it to be an erroneous artifact (Fig. S3.4).

3.4.6 Absolute Quantification (qPCR)

3.4.6.1 *glnA* Gene

The *glnA* gene was quantified in all three cores and used as a proxy for microbial community abundance as only one *glnA* gene copy is expected per bacterial genome (Kumada *et al.*, 1993). Gene copy numbers are listed in Table 3.3. R^2 values of the calibration curves for qPCR were above 0.98 and the efficiency varied from 92.6% for AQT and 122% for HWL and NRT. AQT had the highest overall *glnA* copy number followed by HWL then NRT. All of the sample melt curve profiles matched those of the standards therefore; along with the results of the traditional PCR on agarose gel, we are confident that the quantification data are accurate. The abundance of the *glnA* gene in AQT and HWL cores decreased with increasing depth and in NRT there is a slight increase in *glnA* genes up to 5cm

depth. Overall, microbial populations were most abundant in the surface sediment (at the water-sediment interface), where the sediment is oxic and organic matter is most abundant (see Chapter 2).

3.4.6.2 merA Gene

The R^2 values of the calibration curves were >0.99 and the efficiency of the AQT assay was 71.6% whereas for HWL and NRT it was 91.6% (Table 3.3). NRT had the highest merA copy numbers overall followed by AQT then HWL. The C_T values of the NRT 18-18.5cm and 29.5-30cm samples were high and outside the C_T value range of the standards. The melt curves of these two samples did not correspond to those of the standards (Fig. S3.5). In Figure 3.3C, we see that NRT 18-18.5cm and 29.5-20cm were the only two samples for which a distinct *merA* band could not be amplified through nested PCR. The DNA concentrations were also very low, and so we can confidently say that the values obtained for NRT 18-18.5cm and 29.5-30cm are artifacts. With these two omissions aside, we see a reoccurring trend in all three cores: *merA* gene copies increase with depth for the first 10-20 cm, corresponding to the last 150 years (Fig. 3.7). Furthermore, the sub-surface increase in *merA* genes is independent of the Hg profile and in some cases *merA* is more abundant than *glnA*.

There are several plausible explanations for the sub-surface increase in *merA* within the metagenome of these lake sediments. First, the enrichment of *merA*-containing bacteria could be evidence of a historical Hg stress that was once imposed on the bacterial community and what we register here is the 'fossilized' record of such a stress (Boere *et al.*, 2011). Another possibility is that the *merA* gene abundance is erroneously inflated by organisms that possess multiple copies since genes of the *mer* operon can be located on transposons and plasmids as well as the bacterial chromosome (Osborn *et al.*, 1997). However, as the overall population abundance does not increase with depth (as seen with the *glnA* gene profile), this would imply that bacteria containing multiple *merA* copies increase with depth, which is unlikely. Some bacteria have also been known to possess vestigial non-functional *mer* operons which could inflate the gene abundance without having any biological significance (Osborn *et al.*, 1997). We hypothesize that increasing Hg

concentrations in surface sediments may be applying a selective pressure to the microbial population, favouring bacteria possessing a functional *merA* gene, thus reducing the occurrence of merA gene artifacts and therefore the overall abundance of these genes. Information on the metatranscriptome of the *merA* gene in these sediments would be instrumental in determining the cause of this sub-surface *merA* gene increase; however, several attempts to quantify *merA* transcripts were unsuccessful despite the successful amplification of the *glnA* gene. This suggests that either the microbial population is not expressing the *merA* gene or that transcript levels are below our current detection limit.

3.5 Conclusions

Sediment cores from three freshwater lakes form the Hudson Bay Lowlands were analyzed for Hg and the mercury resistance gene encoding for the mercuric reductase enzyme (*merA*) was quantified in the metagenome of *in situ* microbial populations of the sediment. Despite their remote location, Hg concentrations have increased steadily in the lake sediments, up to 119.9 ± 3 ng g^{-1}, since the onset of the industrial revolution with the highest concentrations being found in the most recently deposited sediments.

This work is the first to report *merA* gene copy numbers in lake sediment cores, down to depths corresponding to sediments deposited prior to the industrial revolution. Great uncertainty remains on the origin and functionality of the *merA* genes detected at depth. We propose that the pattern of *merA* copy number distribution could be i) the result of historical conditions that may have favoured *merA* containing bacteria and left a legacy signal, ii) an overestimation due to individuals containing multiple copies per genome, or iii) that bacteria in deeper sediments have a vestigial non-functional form of the gene whereas the increasing Hg concentrations are selecting for functional genes in populations of the surface sediments. This work contributed to develop novel extraction and quantification methods to assess the abundance of functional genes of the mercury cycle within deep sediment cores. It opened new research avenues aiming at testing whether these genes are indeed functional. Such work is relevant to model Hg geochemistry

in sediments as the mercuric reductase gene catalyzes the transformation of Hg(II) to Hg(0), its volatile and more mobile form. It is difficult to elucidate the reason for the decrease in *merA* abundance in the surface sediments without any information on the metatranscriptome. Further studies should focus on mRNA to determine if the microbial population is actively transforming Hg in these lake sediments. A *merA* clone library from a pre- and post-industrialization depth interval would also be instrumental in revealing the changes in *merA*-containing microbial populations.

3.6 References

Appleby, P.G. 2001. Chronostratigraphic techniques in recent sediments. In: Tracking environmental changes in lake sediments: Physical and chemical techniques, W. M. Last and J. P. Smol, (Eds.). Kluwer Academic Publishers, Dordrect.

Appleby, P.G. and F. Oldfield. 1978. The calculation of lead-210 dates assuming a constant rate of supply of unsupported 210pb to the sediment. Catena, 5(1): 1-8.

Barkay, T., S.M. Miller and A.O. Summers. 2003. Bacterial mercury resistance from atoms to ecosystems. Fems Microbiology Reviews, 27(2-3): 355-384.

Boere, A.C., W.I.C. Rijpstra, G.J. de Lange, E. Malinverno, J.S.S. Damste and M.J.L. Coolen. 2011. Exploring preserved fossil dinoflagellate and haptophyte DNA signatures to infer ecological and environmental changes during deposition of sapropel s1 in the eastern mediterranean. Paleoceanography, 26.

Brown, N.L., S.J. Ford, R.D. Pridmore and D.C. Fritzinger. 1983. Nucleotide sequence of a gene from the *pseudomonas* transposon-tn501 encoding mercuric reductase. Biochemistry, 22(17): 4089-4095.

Case, R.J., Y. Boucher, I. Dahllof, C. Holmstrom, W.F. Doolittle and S. Kjelleberg. 2007. Use of 16s rrna and rpob genes as molecular markers for microbial ecology studies. Appl Environ Microb, 73(1): 278-288.

Chemicals Branch, U.N.E.P. 2008. The global atmospheric mercury assessment: Sources, emissions and transport. Editor. Geneva.

Fontaine, J., E. Dewailly, J.L. Benedetti, D. Pereg, P. Ayotte and S. Dery. 2008. Re-evaluation of blood mercury, lead and cadmium concentrations in the inuit population of nunavik (quebec): A cross-sectional study. Environmental Health, 7: 1-13.

Fox, B.S., Mason, K.J., McElroy, F.C., 2005. Determination of total mercury in crude oil by combustion cold vapor atomic absorption spectrometry (CVAAS), in: Nadkarni, R.A.K. (Ed.), Elemental Analysis of Fuels and Lubricants: Recent Advances and Future Prospects, pp. 196-206.

Furukawa, K. and K. Tonomura. 1972. Metallic mercury-releasing enzyme in mercury-resistant *pseudomonas*. Agricultural and Biological Chemistry, 36(2): 217-&.

Glew, J. 1991. Miniature gravity corer for recovering short sediment cores. J. Paleolimn., 5(3): 285.

Gopinath, E., Kaaret, T.W. and Bruice, T.C. 1989. Mechanism of mercury (II) reductase and influence of ligation on the reduction of mercury (II) by a water soluble 1,5-dihydroflavin. Proceedings of the National Academy of Science, 86: 3041-3044.

Gunn, J. and E. Snucins. 2010. Brook charr mortalities during extreme temperature events in sutton river, hudson bay lowlands, canada. Hydrobiologia, 650(1): 79-84.

Gustin, M.S., S.E. Lindberg and P.J. Weisberg. 2008. An update on the natural sources and sinks of atmospheric mercury. Applied Geochemistry, 23: 482-493.

Hurt, R.A., X.Y. Qiu, L.Y. Wu, Y. Roh, A.V. Palumbo, J.M. Tiedje and J.H. Zhou. 2001. Simultaneous recovery of rna and DNA from soils and sediments. Appl Environ Microb, 67(10): 4495-4503.

Kirk, J.L., D.C.M. Muir, D. Antoniades, M.S.V. Douglas, M.S. Evans, T.A. Jackson, H. Kling, S. Lamoureux, D.S.S. Lim, R. Pienitz, J.P. Smol, K. Stewart, X. Wang and F. Yang. 2011. Climate change and mercury accumulation in canadian high and subarctic lakes. Environmental Science & Technology, 45(3): 964-970.

Kumada, Y., D.R. Benson, D. Hillemann, T.J. Hosted, D.A. Rochefort, C.J. Thompson, W. Wohlleben and Y. Tateno. 1993. Evolution of the glutamine synthetase gene, one of the oldest existing and functioning genes. Proceedings of the National Academy of Sciences of the United States of America, 90(7): 3009-3013.

Lane, D.J. 1991. 16S/23S rRNA sequencing. New York, USA: John Wiley & Sons.

Lindberg, S., R. Bullock, R. Ebinghaus, D. Engstrom, X. Feng, W. Fitzgerald, N. Pirrone and C. Seigneur. 2007. A synthesis of progress and uncertainties in attributing the sources of mercury in deposition. Ambio., 36: 19-32.

Lockhart, W.L., P. Wilkinson, B.N. Billeck, R.A. Danell, R.V. Hunt, G.J. Brunskill, J. Delaronde and V. St Louis. 1998. Fluxes of mercury to lake sediments in central and northern canada inferred from dated sediment cores. Biogeochemistry, 40(2-3): 163-173.

Macdonald, R.W., T. Harner and J. Fyfe. 2005. Recent climate change in the Arctic and its impact on contaminant pathways and interpretation of temporal trend data. Science of the Total Environment, 342(1-3): 5-86.

Murdoch, A. and T.A. Clair. 1986. Transport of arsenic and mercury from gold mining activities through an aquatic system. Science of the Total Environment, 57: 205-216.

Osborn, A.M., K.D. Bruce, P. Strike and D.A. Ritchie. 1997. Distribution, diversity and evolution of the bacterial mercury resistance (mer) operon. Fems Microbiology Reviews, 19(4): 239-262.

Poissant, L., H.H. Zhang, J. Canario and P. Constant. 2008. Critical review of mercury fates and contamination in the Arctic tundra ecosystem. Science of the Total Environment, 400(1-3): 173-211.

Post, E., M.C. Forchhammer, M.S. Bret-Harte, T.V. Callaghan, T.R. Christensen, B. Elberling, A.D. Fox, O. Gilg, D.S. Hik, T.T. Hoye, R.A. Ims, E. Jeppesen, D.R. Klein, J. Madsen, A.D. McGuire, S. Rysgaard, D.E. Schindler, I. Stirling, M.P. Tamstorf, N.J.C. Tyler, R. van der Wal, J. Welker, P.A. Wookey, N.M. Schmidt and P. Aastrup. 2009. Ecological dynamics across the Arctic associated with recent climate change. Science, 325(5946): 1355-1358.

Poulain, A.J., S.M. Ni Chadhain, P.A. Ariya, M. Amyot, E. Garcia, P.G.C. Campbell, G.J. Zylstra and T. Barkay. 2007. Potential for mercury reduction by microbes in the high Arctic. Appl Environ Microb, 73(7): 2230-2238.

Ramond, J.B., T. Berthe, R. Duran and F. Petit. 2009. Comparative effects of mercury contamination and wastewater effluent input on gram-negative mera gene abundance in mudflats of an anthropized estuary (seine, france): A microcosm approach. Research in Microbiology, 160(1): 10-18.

Riget, F., B. Braune, A. Bignert, S. Wilson, J. Aars, E. Born, M. Dam, R. Dietz, M. Evans, T. Evans, M. Gamberg, N. Gantner, N. Green, H. Gunnlaugsdottir, K. Kannan, R. Letcher, D. Muir, P. Roach, C. Sonne, G. Stern and O. Wiig. 2011. Temporal trends of hg in Arctic biota, an update. Science of the Total Environment, 409(18): 3520-3526.

Rochelle, P.A., J.C. Fry and M.J. Day. 1989. Factors affecting conjugal transfer of plasmids encoding mercury resistance from pure cultures and mixed natural

suspensions of epilithic bacteria. Journal of General Microbiology, 135: 409-424.

Rosen, B.P. 1996. Bacterial resistance to heavy metals and metalloids. Journal of Biological Inorganic Chemistry, 1(4): 273-277.

Schaefer, J.K., J. Yagi, J.R. Reinfelder, T. Cardona, K.M. Ellickson, S. Tel-Or and T. Barkay. 2004. Role of the bacterial organomercury lyase (merb) in controlling methylmercury accumulation in mercury-contaminated natural waters. Environmental Science & Technology, 38(16): 4304-4311.

Woods, D.R. and S.J. Reid. 1993. Recent developments on the regulation and structure of glutamine-synthetase enzymes from selected bacterial groups. FEMS Microbiology Reviews, 11(4): 273-284.

Zhou, J.Z., M.A. Bruns and J.M. Tiedje. 1996. DNA recovery from soils of diverse composition. Appl Environ Microb, 62(2): 316-322.

3.7 List of Tables

Table 3.1: The sequence of oligonucleotides used as primers and polymerase chain reaction (PCR) cycling conditions used to amplify the bacterial 16S rRNA gene, the mercuric reductase gene (*merA*) and the glutamine synthetase (*glnA*) gene.

Target gene	Primer name	Oligonucleotide sequence (5' → 3')	Amplicon size (bp)	PCR cycle
16S rRNA	27F	AGAGTTTGATCMTGGCTCAG	880	94ºC-10 min, (94ºC-30 s, 55 ºC-30 s, 72 ºC-60 s) × 35, 72 ºC-5 min
	907R	CCGTCAATTCATTTGAG		
	Nlf F	CCATCGGCGGCACYTGCGTYAA	1246	94ºC-10 min, (94ºC-30 s, 62 ºC-30 s, 72 ºC-60 s) × 25, 72 ºC-5 min
	Nlf R	CGCYGCRAGCTTYAAYCYYTCRRCCATYGT		
merA	Nsf F	ATCCGCAAGTNGCVACBGTNGG	307	94ºC-10 min, (94ºC-30 s, 62 ºC-30 s, 72 ºC-30 s) × 35, 72 ºC-5 min
	Nsf R	CGCYGCRAGCTTYAAYCYYTCRRCCATYGT		
	MerA2F	ACCTGCGTCAACGTCGGCTG	300	95ºC-10 min, (95ºC-30 s, 63 ºC-15 s, 72 ºC-30 s) × 35, 72 ºC-5 min
	MerA2R	GCGATCAGGCAGCGGTCGAA		
glnA	GS1β	GATGCCGCCGATGTAGTA	156	95ºC-5 min, (95ºC-30 s, 60 ºC-30 s, 72 ºC-60 s) × 30, 72 ºC-5 min
	GS2γ	AAGACCGCGACCTTPATGCC		

Table 3.2: Concentrations (ng μL^{-1}) of genomic DNA extracted from various depth intervals (cm) of sediment cores from three lakes from the Hudson Bay Lowlands of Ontario, Canada.

Lake	Depth Interval (cm)	DNA (ng μL^{-1})
Aquatuk	0-0.5cm	32.7
	3-3.5cm	27.4
	5-5.5cm	30.2
	10-10.5cm	10.6
	22-22.5cm	4.41
Hawley	0-0.5cm	18.2
	3-3.5cm	8.79
	5-5.5cm	3.60
	8-8.5cm	4.17
	24-24.5cm	2.54
North Raft	0-0.5cm	27.1
	3-3.5cm	6.99
	5-5.5cm	2.24
	18-18.5cm	0.516
	29.5-30cm	0.589

Table 3.3: Quantitative polymerase chain reaction (qPCR) results for the quantification of the glutamine synthetase (*glnA*) gene and the mercuric reductase (*merA*) gene (copies ng^{-1} DNA) in sediments from Aquatuk, Hawley and North Raft Lakes from the Hudson Bay Lowlands of Ontario, Canada.

		glnA				*merA*			
Lake	Interval (cm)	R^2	E* (%)	C_T value (SD)	Copies (SD)	R^2	E* (%)	C_T value (SD)	Copies (SD)
Aquatuk	0-0.5	0.98	92.6	12.0 (0.2)	95792 (20000)	0.99	71.6	19.8 (0.3)	2743 (400)
	3-3.5			14.3 (0.2)	24122 (3000)			19.8 (0.4)	3213 (600)
	5-5.5			14.1 (0.06)	24519 (1000)			19.8 (0.2)	2897 (300)
	10-10.5			14.8 (0.08)	45855 (3000)			18.9 (0.2)	13472 (1000)
	22-22.5			17.3 (0.05)	21296 (700)			19.1 (0.03)	28629 (400)
Hawley	0-0.5	0.98	122	13.3 (1)	16912 (3000)	0.99	91.6	19.6 (0.03)	2366 (50)
	3-3.5			15.8 (0.06)	2584 (100)			19.7 (0.008)	4722 (30)
	5-5.5			17.0 (0.1)	2553 (200)			19.9 (0.03)	9827 (200)
	8-8.5			16.7 (0.02)	2698 (40)			19.8 (0.1)	9486 (70)
	24-24.5			17.9 (0.07)	1763 (100)			20.7 (0.3)	8601 (2000)
North Raft	0-0.5	0.98	122	14.3 (0.3)	2966 (800)	0.99	91.6	18.2 (0.1)	3967 (400)
	3-3.5			15.3 (0.1)	5086 (400)			18.4 (0.03)	14043 (200)
	5-5.5			16.2 (0.06)	7773 (400)			19.1 (0.04)	27239 (800)
	18-18.5			23.5 (0.7)	107 (60)			24.3 (0.07)	3970 (200)▲
	29.5-30			22.3 (0.2)	225 (40)			23.1 (0.1)	7221 (500) ▲

* Reaction efficiency
▲ Artifact

3.8 List of Figures

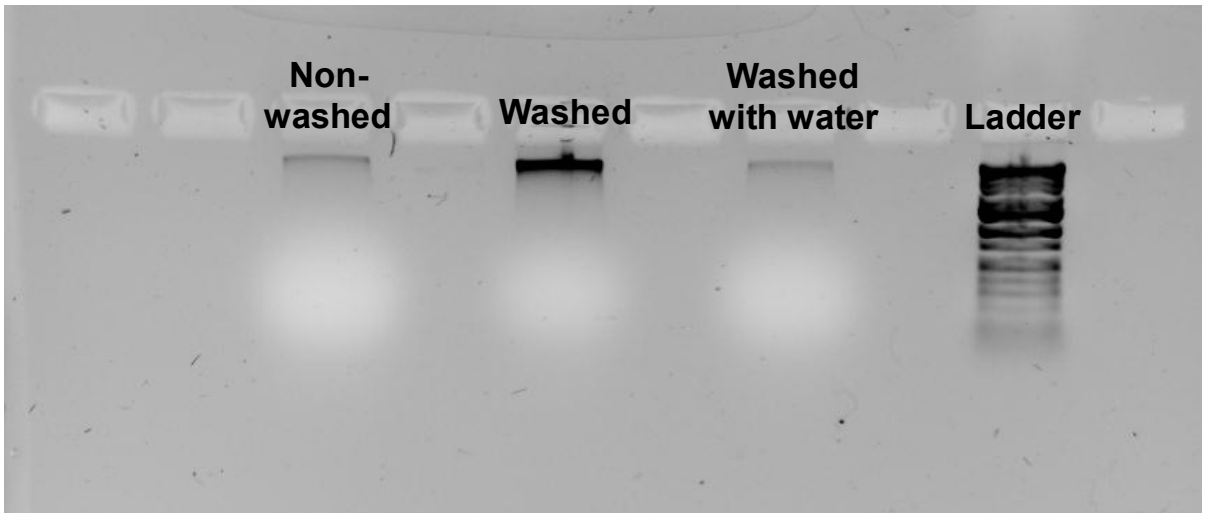

Figure 3.1: Optimization of genomic DNA extraction from goose excrements that were non-washed, washed with buffer and washed with water. The gel is 2% agarose, stained with EtBr and was migrated at 5V/cm for 60 minutes Ladder: 1kb Full Scale DNA Ladder (Fisher Scientific).

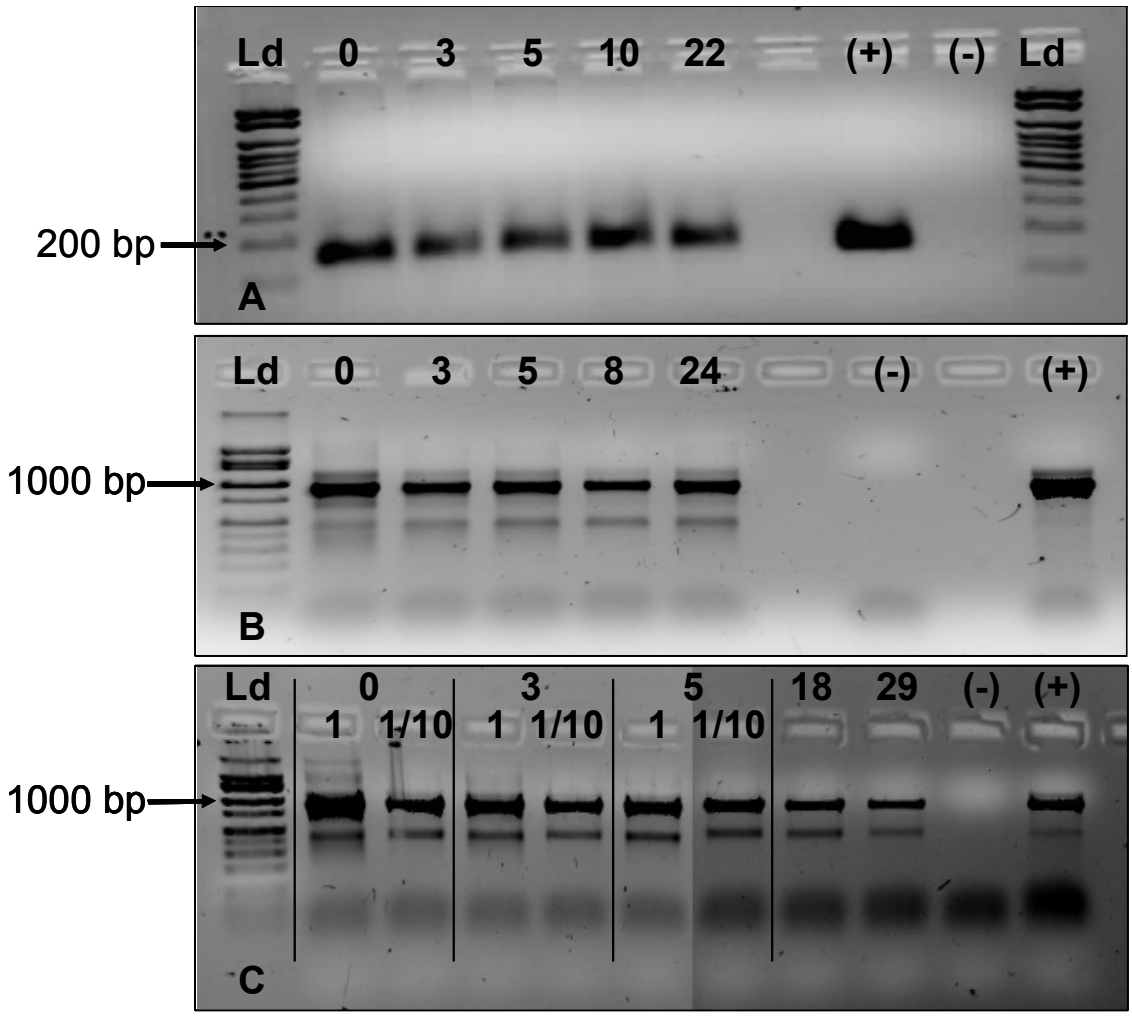

Figure 3.2: A) Results of a PCR targeting the glutamine synthetase (*glnA*) gene in genomic DNA from Aquatuk Lake sediments. Expected amplicon size is 154 bp. Ld: exACTGene Low Range DNA Ladder (Fisher Scientific). B) 16S rRNA gene PCR on genomic DNA from Hawley Lake sediments. Expected amplicon size is 880 bp. Ld: 100bp Low Scale DNA Ladder (Fisher Scientific) C) 16S rRNA gene PCR on genomic DNA from North Raft Lake sediments. The template DNA from 0, 3 and 5 cm intervals was non-diluted (1) or diluted 10x with sterile water (1/10) to assess the impact of dilution on the PCR efficacy. Ld: 100bp Low Scale DNA Ladder (Fisher Scientific). All gels were 2% agarose, stained with EtBr and migrated at 5V/cm for 60 minutes, (+): positive control (*E. coli* DNA as template), (-): negative control (water as template).

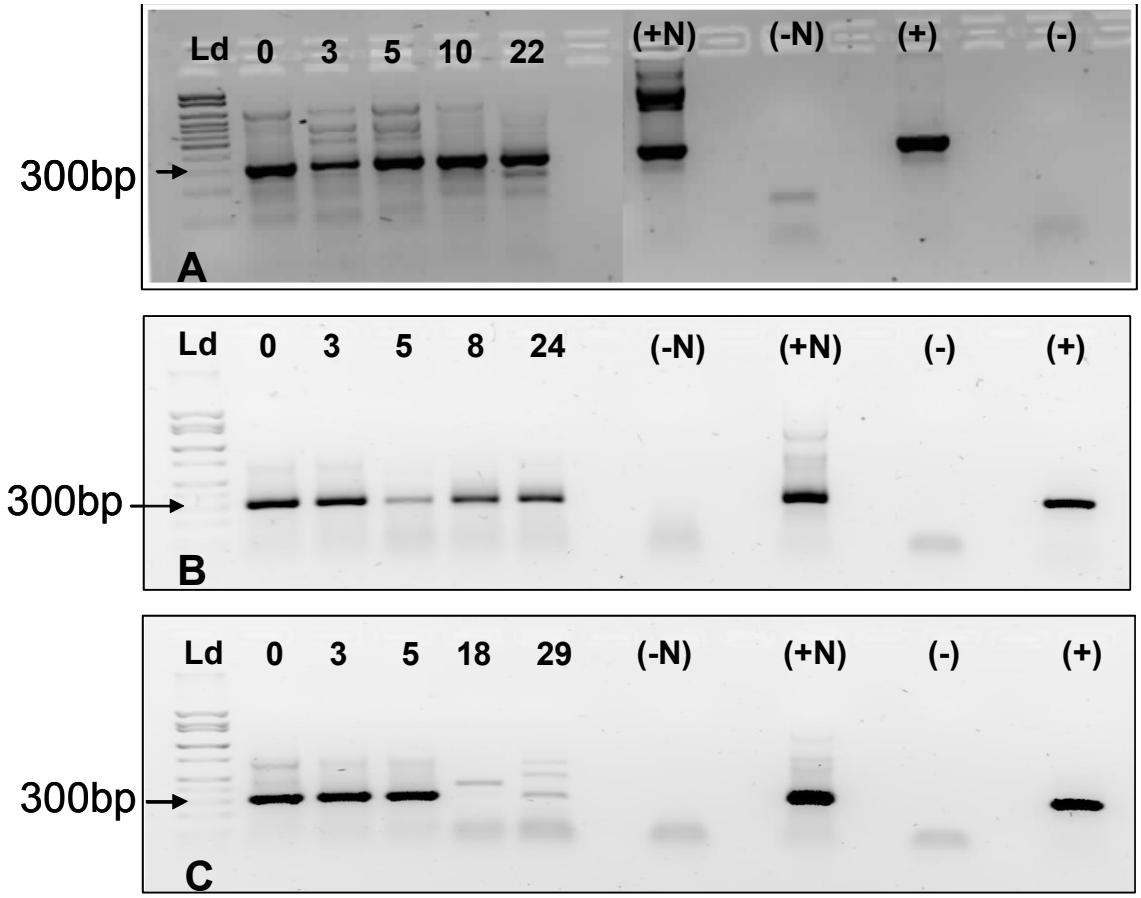

Figure 3.3: Results of a nested PCR targeting the mercuric reductase (*merA*) gene in genomic DNA extracted from selected depths of A) Aquatuk, B) Hawley and C) North Raft Lake sediment cores. Expected amplicon size is 307 bp. Ladder: exACTGene low Range Plus DNA ladder (Fisher Scientific). All gels were 2% agarose, stained with EtBr and migrated at 5V/cm for 60 minutes, (+): positive control (*Pseudomonas* transposon Tn501 DNA as template), (-): negative control (water as template), (+N): nested positive control, (-N): nested negative control.

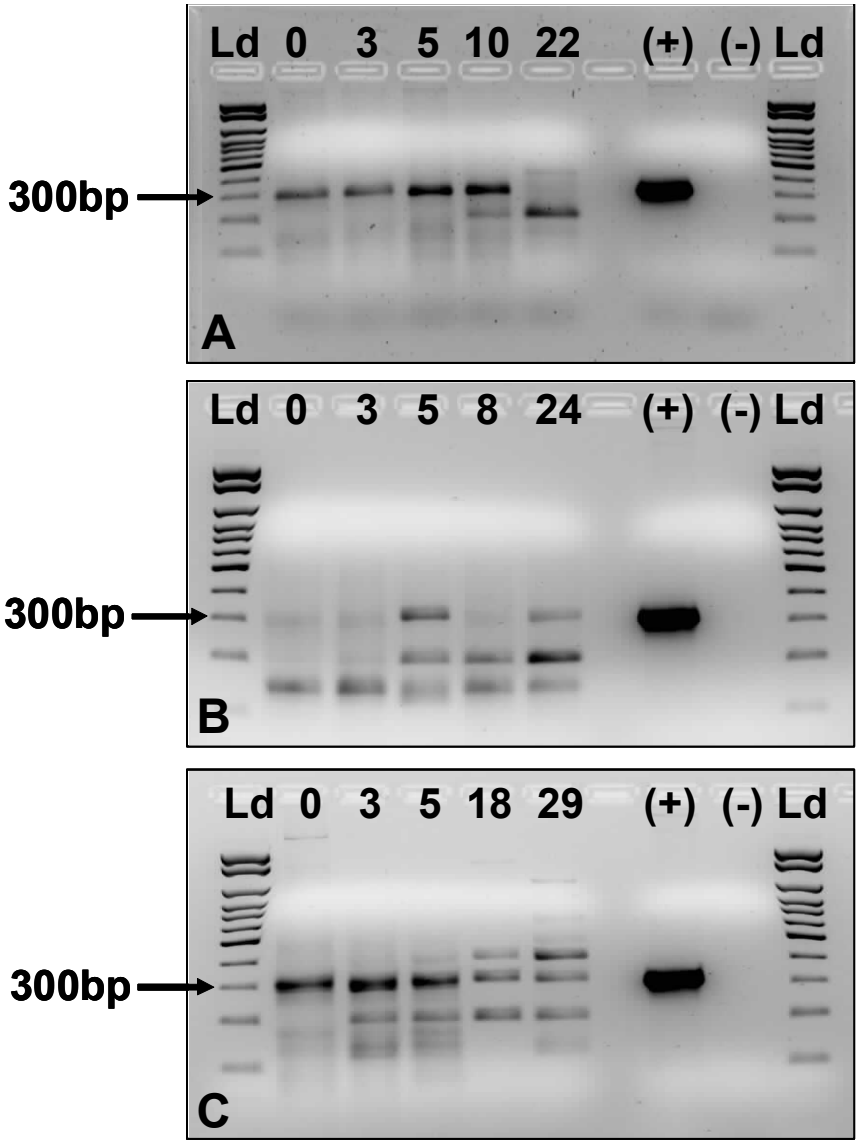

Figure 3.4: Results of a PCR targeting the mercuric reductase (*merA*) gene with the oligonucleotide primers used in the qPCR assay (MerA2) in genomic DNA extracted from selected depths of A) Aquatuk, B) Hawley and C) North Raft Lake sediment cores. Expected amplicon size is 300 bp. Ladder: exACTGene low Range Plus DNA ladder (Fisher Scientific). All gels were 2% agarose, stained with EtBr and migrated at 5V/cm for 60 minutes.

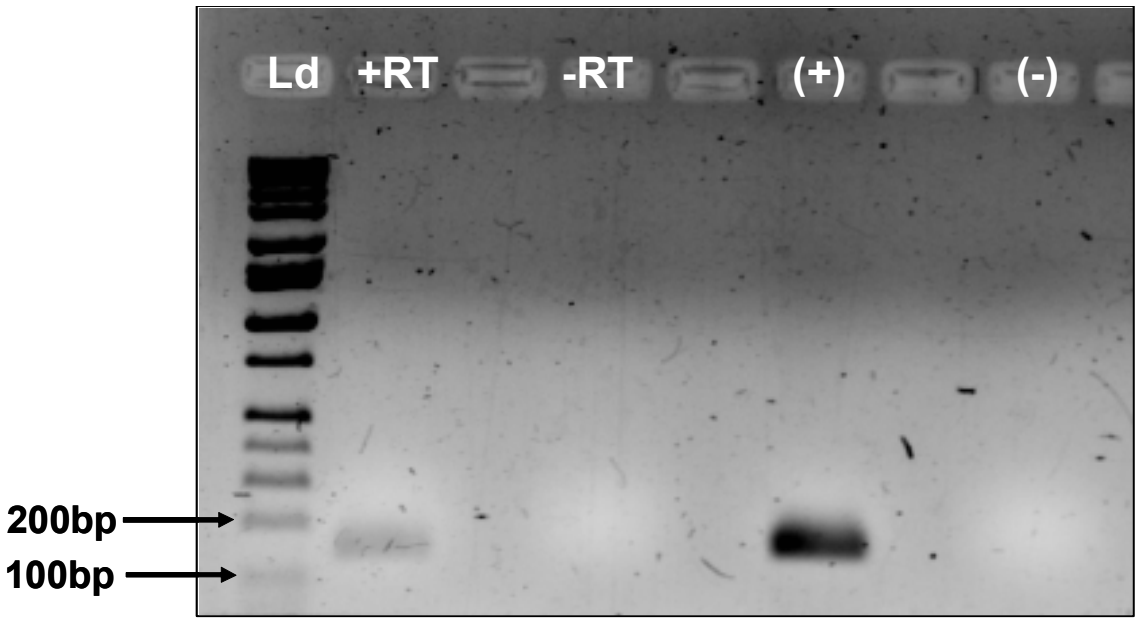

Figure 3.5: Results of a PCR targeting the glutamine synthetase (*glnA*) gene in cDNA synthesized from RNA extracted from Hawley Lake surface sediment. Expected amplicon size is 156 bp. Ld: 1 kb Full Scale DNA Ladder (Fisher Scientific), -RT: no reverse transcriptase control, (+): PCR positive control (*E. coli* DNA as template), (-): PCR negative control (water as template). The gel was 2% agarose, stained with EtBr and was migrated at 5V/cm for 60 minutes

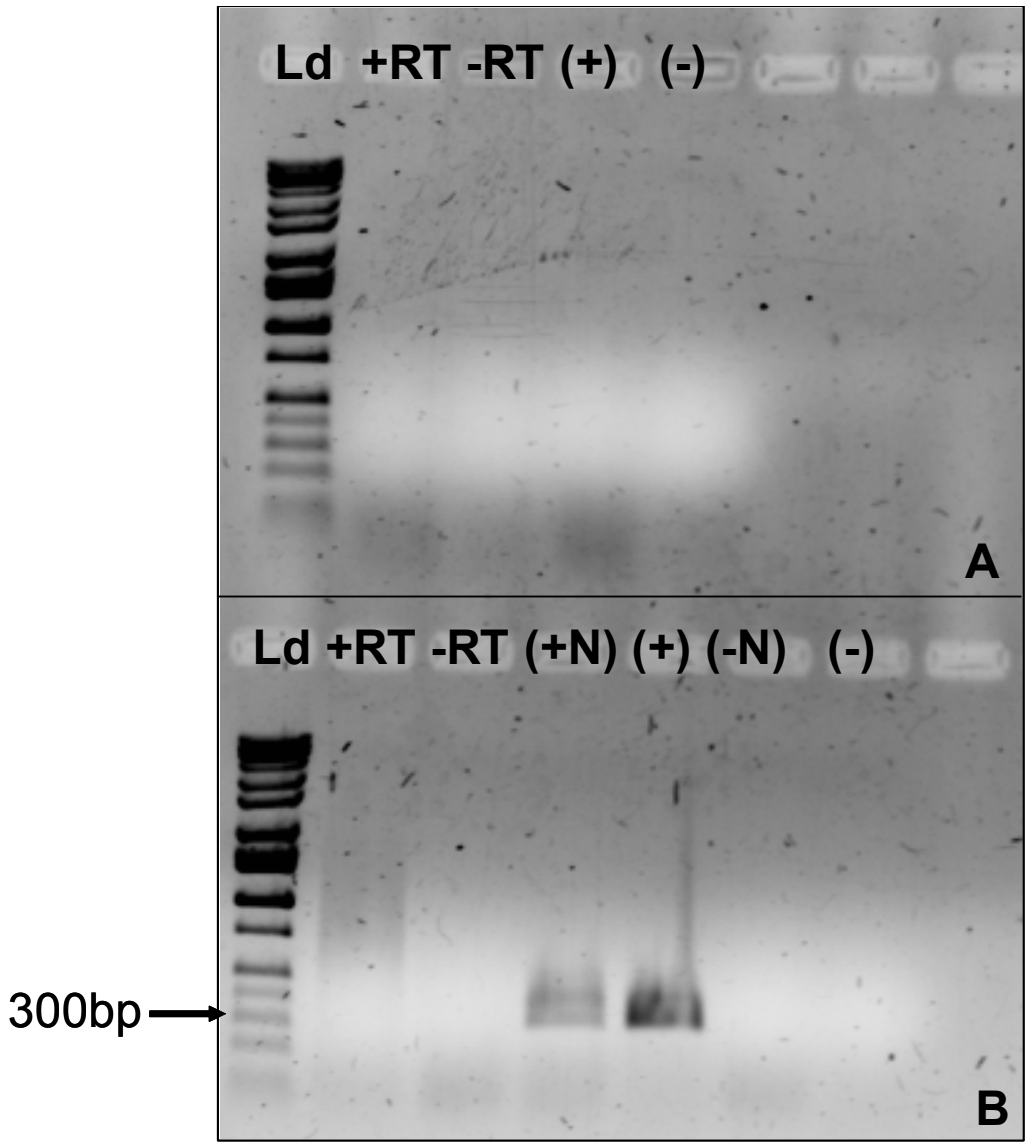

Figure 3.6 – Results of a nested PCR targeting the mercuric reductase (*merA*) gene in cDNA synthesized from RNA extracted from Hawley Lake surface sediments. A) PCR with Nlf primers. Expected amplicon size is 1246 bp. B) PCR with Nsf primers using Nlf amplicon as template. Expected amplicon size is 307 bp. Ld: 1 kb Full Scale DNA ladder (Fisher Scientific), -RT: no reverse transcriptase control, (+N): PCR nested positive control, (+): PCR positive control (*Pseudomonas* transposon Tn501 DNA as template), (-N): PCR nested negative control, (-): PCR negative control (water as template). The gel was 2% agarose, stained with EtBr and migrated at 5V/cm for 60 minutes.

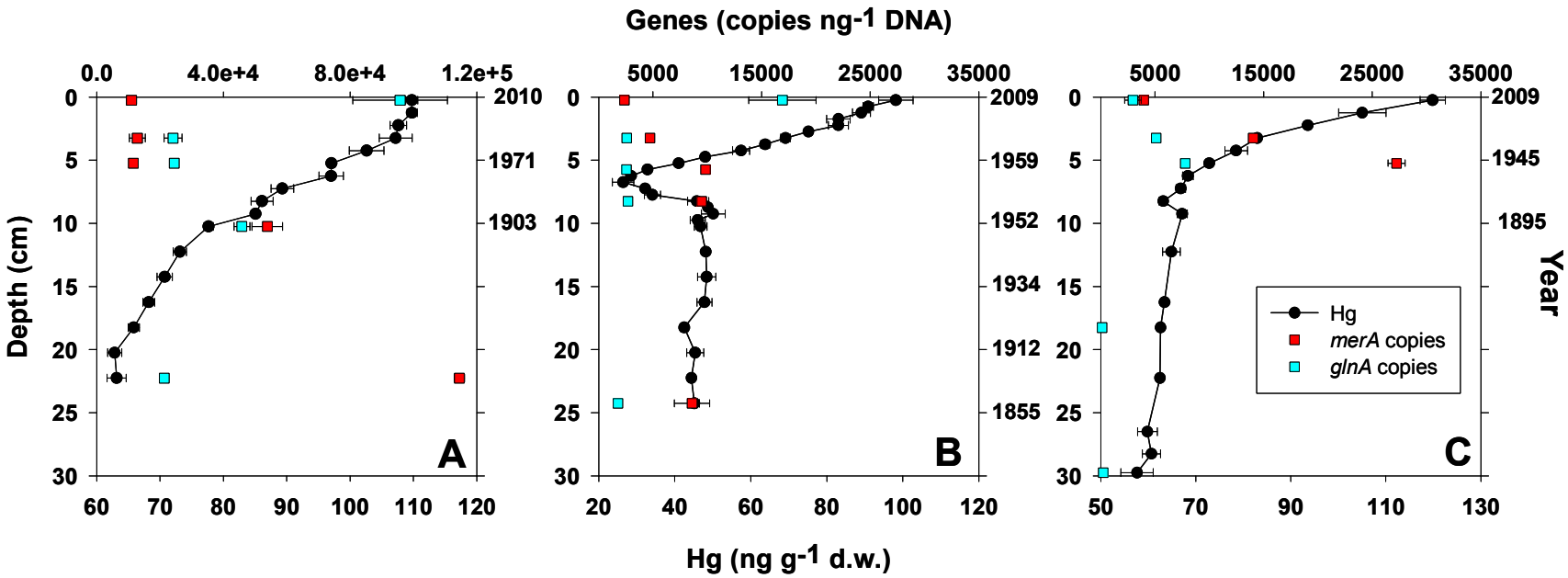

Figure 3.7: Total mercury (ng g^{-1}, dry weight), mercuric reductase (*merA*) gene copy number (copies ng^{-1} of DNA) and glutamine synthetase (*glnA*) gene copy number (copies ng^{-1} of DNA) in sediment from A) Aquatuk, B) Hawley and C) North Raft Lakes from the Hudson Bay Lowlands of Ontario, Canada. Calendar years were attributed to the sediment by ^{210}Pb dating according to the Constant Rate of Supply model. n = 3 ± SD

3.9 Supplemental Information

3.9.1 List of Figures

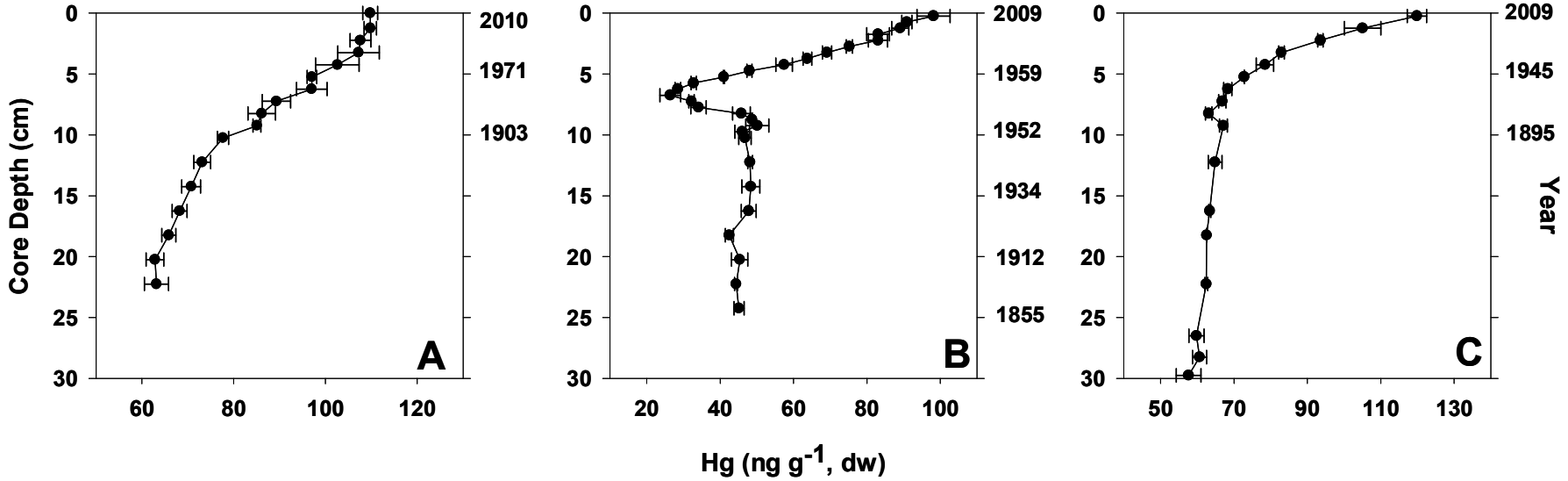

Figure S3.1: Mean mercury ± SD (ng g^{-1}, dry weight) and ^{210}Pb dates (Constant Rate of Supply model) in sediment cores from A) Aquatuk, B) Hawley and C) North Raft Lakes from the Hudson Bay Lowlands of Ontario, Canada.

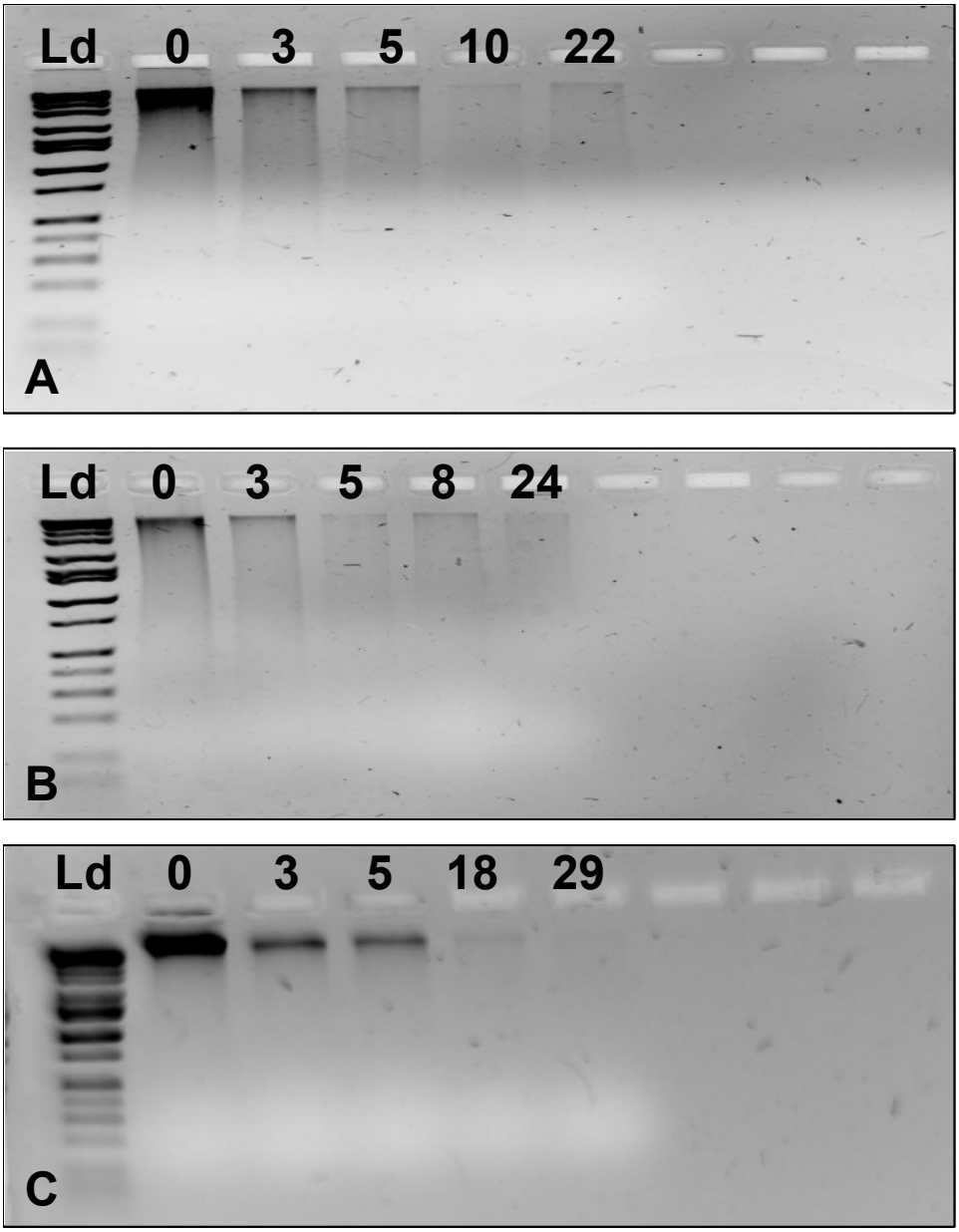

Figure S3.2: Genomic DNA extracted from various depths of sediment cores from Aquatuk (A), Hawley (B) and North Raft (C) Lakes from the Hudson Bay Lowlands of Ontario, Canada. All gels were 2% agarose, stained with EtBr and migrated at 5V/cm for 60 minutes

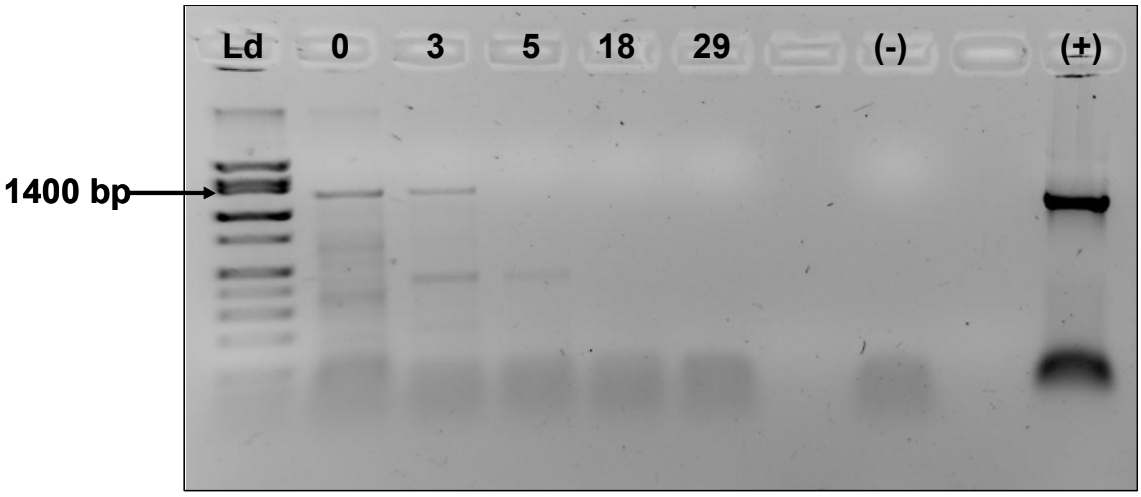

Figure S3.3: Results of a PCR targeting the mercuric reductase (*merA*) gene using Nlf oligonucleotide primers in DNA from North Raft Lake sediments. (+): positive control (*Pseudomonas* transposon Tn501 DNA as template), (-): negative control (water as template). The expected amplicon size is 1246 bp. Ld: 100bp Low Scale DNA Ladder (Fisher Scientific). The gel was 2% agarose, stained with EtBr and migrated at 5V/cm for 60 minutes

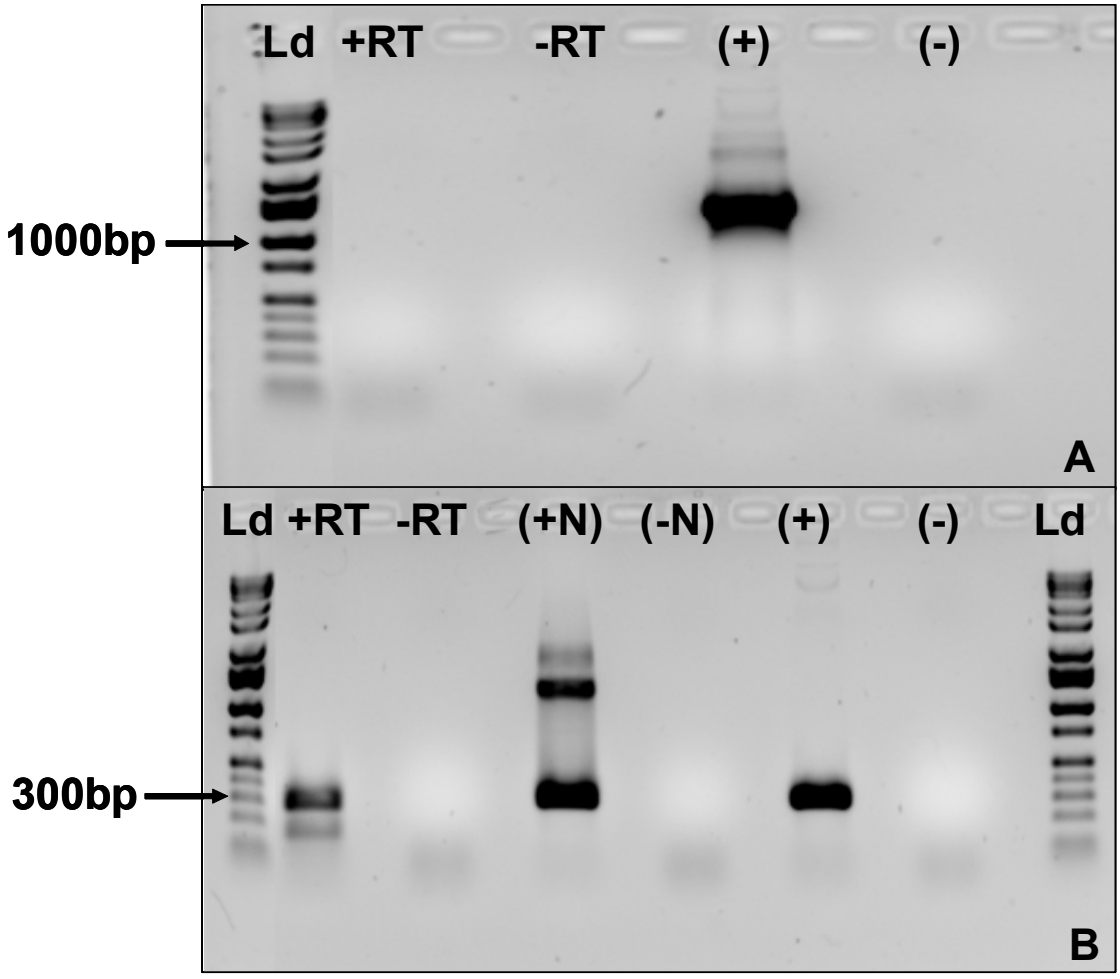

Figure S3.4: – Results of a nested PCR targeting the mercuric reductase (*merA*) gene in gene specific cDNA synthesized from RNA extracted from Hawley Lake surface sediments. A) Results of the PCR with Nlf primers. Expected amplicon size is 1246 bp. B) Results of the PCR with Nsf primers using Nlf amplicon as template. Expected amplicon size is 307 bp. Ld: 1 kb Full Scale DNA ladder (Fisher Scientific), -RT: no reverse transcriptase control, (+N): nested positive control, (+): PCR positive control (Pseudomonas transposon Tn501 DNA as template), (-N): nested negative control, (-): PCR negative control (water used as template). Both gels were 2% agarose, stained with EtBr and migrated at 5V/cm for 60 minutes

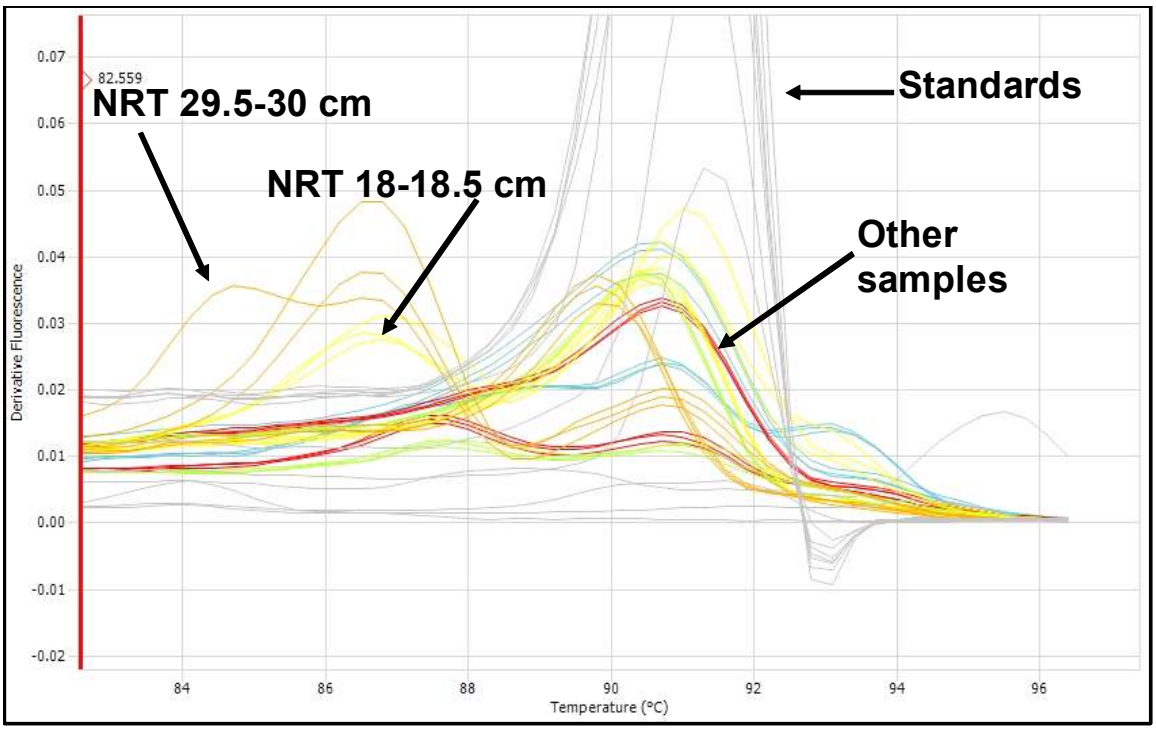

Figure S3.5: The melt curve from the quantitative PCR targeting the mercuric reductase (*merA*) gene in DNA from North Raft Lake.

4.0 Biogenic production of elemental mercury (Hg^0) in lake sediments from Northern Ontario

4.1 Abstract

The mercury (Hg) redox cycle in sediments, especially Hg(0) production, can potentially control the availability of Hg(II) to methylating bacteria, greatly reducing its toxicity. However, Hg(0) production in sediments remains poorly characterized. Here, we assess the effect of nutrients, pH and ionic strength on the rate of Hg(0) production from lake sediments in microcosms. We show, with a combination of analytical and molecular techniques, that Hg(0) production from the sediment is of a biogenic nature. We also show that ionic strength has the greatest influence on Hg(0) production, with increased Hg(0) production as ionic strength increases. Additions of phosphate did not enhance Hg(0) production but addition of carbon substrate stimulated Hg(0) production. These results illustrate the unrecognized effect of ionic strength on Hg(0) production, likely originating from Hg(II) reduction by bacteria. These data are also relevant for Hg modeling and mass-balance studies, which have, until now, underestimated the potential contribution of microbial populations to the Hg redox cycle in lake sediments.

4.2 Introduction

Mercury is a ubiquitous contaminant that has a very complex biogeochemical cycle. The elemental volatile form, Hg(0), has an atmospheric residence time of up to two years, allowing a global distribution (Lindberg *et al.*, 2007). As a result, areas far removed from industrial activity have received significant inputs of Hg since the onset of the industrial revolution, including Arctic and subarctic ecosystems (Kirk *et al.*, 2011). Mercury methylation occurs in the water column and sediments of boreal lakes (Miskimmin *et al.*, 1992; Desrosiers *et al.*, 2006). Hence, processes that control the availability of the substrate for methylation, also indirectly control Hg methylation. We are interested in redox processes that control the availability of reduced and oxidized forms of Hg which can include both biotic and abiotic processes in sediments (Poulain *et al.*, 2004). Abiotic processes include reactions with humic substances (Nagase *et al.*, 1982). Bacteria can reduce Hg on purpose or accidentally; a dedicated pathway for Hg reduction is that of the *mer* operon

however other studies have shown that bacteria can reduce Hg via non-specific pathways (Wiatrowski *et al.*, 2006).

The rate of production and the fate of biogenically produced Hg(0) remains elusive, especially in aquatic environments. As a result, many Hg models and mass-balance studies do not include a component of biologically produced Hg(0); a potentially critical omission (Diamond, 1999; Macleod *et al.*, 2005). Here, we performed a series of incubations to quantify the production of Hg(0) under oxic conditions in sediments form Aquatuk lake; a pristine lake in the Hudson Bay Lowlands of Ontario. Our goal was: i) to characterize and quantify Hg(0) production from sediments and ii) to identify key environmental variables that influence its production.

4.3 Material and Methods

4.3.1 Sampling Site and Sample Collection

Sediments were collected from Aquatuk (AQT) Lake in the Hudson Bay Lowlands (HBL) area in Northern Ontario, Canada (54º21'11.80"N, 84º34'29.80"W) on August 8th 2010 and August 20th 2011. AQT is a freshwater, oligotrophic lake located on the Precambrian bedrock of the Sutton Ridges (Gunn and Snucins, 2010). Sediment samples were taken using a Birge-Ekman grab sampler and stored in 1L Nalgene® wide mouth square bottles (Blomqvist, 1990). Depth at sampling location was 11.7m, the water column was not thermally stratified; water temperature at the water-sediment interface was 16.3ºC and dissolved oxygen was 7.05 mg L^{-1}. All sediment samples were kept at 4^{o}C and protected from light. All containers used for sampling were sterile and non-powdered gloves were worn at all times during sampling and processing of the samples. Dissolved oxygen and temperature in lakewater was measured using a YSI 55 dissolved oxygen probe and meter (YSI Inc., Yellow Springs, OH) and water chemistry was collected using a composite sampling technique.

4.3.2 Total Mercury Analyses

Total Hg in wet sediments was analyzed with Nippon Instruments Corporation's Mercury SP-3D Analyzer (CV-AAS) by thermal decomposition with gold trap amalgamation and cold vapour atomic absorption method (UOP Method 938-00, detection limit of 0.01ng Hg and range up to 1000ng Hg; Fox *et al.*, 2005). The instrument was calibrated with Mercury Reference Solution 1000ppm ±1% (Fisher CSM114-100) and MESS-3 (91±9 ng g^{-1}, National Research Council of Canada) was used as reference material. Blanks were performed as suggested by the manufacturer.

4.3.3 Microcosm Design and Hg(0) Measurements

Microcosms were constructed by fitting a 1L glass Erlenmeyer with the glass head of a gas washing bottle (Fig. 4.1, panel A). A Tekran® Model 1100 Zero Air Generator (Tekran Instruments Corporation, Toronto, ON) was used to pump Hg-free air directly into the sediment slurry in the microcosm through Teflon tubing. The output line was connected to a Tekran® Model 2537B (Tekran Instruments Corporation, Toronto, ON). Hg(0) produced by the microcosm was pre-concentrated onto a pure gold collector cartridge, then thermally desorbed in argon gas and detected via cold vapor atomic fluorescence spectroscopy (CVAFS). Sampling volume was 7.5 L and Hg(0) measurements were performed every 5 minutes. The detection limit was <0.1 ng m^{-3}.

4.3.4. Treatments and Reagents

All incubations were performed at room temperature, under oxic conditions to reflect the oxic water-sediment interface of Aquatuk Lake. The incubations were performed over a period of 20 days. Microcosms were protected from light to avoid the confounding effects of photoreduction. All glassware which came in contact with the sediment slurry was soaked in 5% nitric acid for 24 hours and rinsed thoroughly with sterile milliQ water to eliminate trace amounts of Hg and autoclaved at 134ºC/28 psi for 60 minutes. Sediment slurries consisted of ±40 g of fresh (i.e. never frozen) wet sediment in a 600 mL volume and were placed on a magnetic stirrer and

constantly stirred by a stir bar. The volume was kept constant by periodic additions of sterile milliQ water.

Several methods were used to sterilize the sediments. After optimization, control treatments were sterilized by incubating the sediment slurry with 0.5% formaldehyde for 24 hours. Formaldehyde incubations did not alter the pH of the slurry. Table 4.1 shows the various treatments performed in this study. The reagents used were: phosphate buffered saline solution (PBS) which contained 137mM sodium chloride (NaCl), 2.7mM potassium chloride (KCl), 8.1 mM disodium hydrogen phosphate (Na_2HPO_4) and 1.76mM monopotassium phosphate (KH_2PO_4); a 10mM 3-(N-morpholino)propanesulfonic acid (MOPS) buffer; acetate (CH_3COONa); butyrate ($CH_3CH_2CH_2COONa$); citrate ($C_6H_7NaO_7$); lactate ($C_3H_5NaO_3$); monopotassium phosphate (KH_2PO_4); sodium chloride (NaCl); potassium chloride (KCl); magnesium chloride ($MgCl_2$); sodium sulfate (Na_2SO_4) and magnesium sulfate ($MgSO_4$). Mercury concentrations of all solutions and water used in this study were measured and were below detection limit.

4.3.5 Calculations

4.3.5.1 Elemental Mercury Emissions

The Tekran 2537B recorded elemental Hg concentrations in ng m^{-3} for every 7.5 L of air sampled. We divided this value by 1000 to obtain ng L^{-1} and then multiplied by 7.5 to obtain ng of Hg(0). This was repeated every 5 minutes over the 20 day incubation period and combined to have a cumulative amount of Hg(0) produced (ng).

4.3.5.2 Elemental Mercury Production Rates

Hg(0) production over time typically followed an exponential increase. Elemental mercury production rates were determined during the exponential section of the curve. We used a best-fit model based on exponential growth to normalize the data and calculated the slope of the cumulative Hg(0) (ng) produced at day 10 and day 20 and divided it by the amount of sediment used to prepare the slurry (g) to obtain a production rate of ng day^{-1} g^{-1} of sediment (Table 4.3, Fig. S4.3 – S4.6).

4.3.5.3 Ionic Strength

The ionic strength (I) of the treatments was calculated using the equation in Solomon (2001):

$$I = \frac{1}{2} \sum c_i z_i^2$$

Where c_i is the ionic concentration in mol L^{-1} and z_i is the number of charges on the ion. The I of Aquatuk lake water was calculated using the formula above and the concentrations of Al, Ca, Cl, Fe, Mg, Mn, Na, SiO_3, Sr and SO_4.

4.3.5.4 Elemental Mercury Flux

Atmospheric deposition rates of Hg were obtained from the National Atmospheric Deposition Program and used to calculate a yearly rate of wet deposition in the HBL region of Northern Ontario. The surface area of Aquatuk Lake was estimated using Google Earth software to estimate the amount of Hg deposited on Aquatuk Lake each year. The water content of the first cm of sediment was used to estimate sediment density based on the method by Håkanson and Jansson (1983). Rates of Hg(0) production were used to calculate potential Hg(0) flux from the sediment to the water column.

4.3.6 DNA Extraction

After 20 days of incubation, the slurry was transferred into sterile 50mL polypropylene tubes and frozen at -20ºC. Prior to subsampling for DNA extractions, sediment slurry samples were thawed and centrifuged at 2000 × g for 10 min and the supernatant was discarded. A subsample of 0.5g was placed into a sterile 2mL Eppendorf tube. We used a sterile buffer modified from Zhou *et al.* (1996) to wash the sediment to remove contaminants such as humic substances and divalent cations that can be co-extracted with nucleic acids and inhibit subsequent downstream applications (see Chapter 3). The buffer consisted of 10mM EDTA, 50mM Tris-HCl and 50mM $Na_2HPO_4 \cdot 7H_2O$ at pH 8.0. We added 3 parts buffer for 1 part sediment, then samples were vortexed at maximum speed for 30 seconds, centrifuged at 2000 × g for 3 min and the supernatant was discarded.

Bacterial DNA extraction from the washed sediment was performed using a PowerSoil DNA Isolation Kit (MoBio, Carlsbad, CA) according to the manufacturer's guidelines. The extraction was executed in a laminar flow hood with HEPA filter and

all work surfaces and equipment were washed with 70% ethanol, 10% bleach and sterilized under UV light. The extracted DNA was quantified using an Invitrogen Quant-iT™ dsDNA High-Sensitivity Assay Kit (Invitrogen™, San Diego, CA) according to the manufacturer's protocol. DNA extracts were stored at -20ºC until further use.

4.3.7 Gene Amplification

We used polymerase chain reaction (PCR) to amplify the glutamine synthetase gene (*glnA*) that we used as a proxy of bacterial abundance. The forward primer GS1β (5'-GATGCCGCCGATGTAGTA-3') and reverse primer GS2γ (5'-AAGACCGCGACCTTPATGCC-3') were used to amplify a 154bp fragment of the prokaryotic *glnA* gene (Hurt *et al.*, 2001). The 10µL reaction mixtures contained 1× EconoTaq Plus Green Mix (Lucigen Corp., Middleton, WI), 2.5 mM $MgCl_2$, 0.5 µM of each forward and reverse primer and 1µL of template DNA. Amplification conditions were as follows: 10 min at 95°C, followed by 35 cycles of 30 s at 95°C, 30 s at 60°C, and 30 s at 72°C, followed by a final extension of 5 min at 72°C. Each reaction included a positive control using DNA from *Escherichia coli* and a negative control in which the template was water. Amplicons were separated by agarose gel electrophoresis (2% agarose, 5V/cm for 60 min, stained with EtBr) and compared to a 100bp exACTGene Low Range Plus DNA ladder (Fisher Scientific).

4.3.8 Gene Quantification

4.3.8.1 Production of Standards for qPCR

The *glnA* gene was amplified from *Escherichia coli*, the band excised and purified using QIAEX II Gel Extraction Kit (QIAGEN, Valencia, CA) and cloned into pGEM-T (Promega, Madison, WI) according to the manufacturers' protocol. The Wizard® *Plus* SV Minipreps DNA Purification System (Promega, Madison, WI) was used to extract the plasmids and the concentrations were quantified by spectrophotometry using a NanoDrop ND-1000 spectrophotometer (NanoDrop Technologies). The *glnA* standards were verified by PCR and agarose gel electrophoresis following the protocol described above. Calculation of the plasmid

copy number was performed according to the molar mass derived from the plasmid and amplicon sequences as follows;

1. Plasmid weight + insert weight = total weight (g mol^{-1})
2. Total weight (g mol^{-1}) ÷ Avogadro's number (6.02214199 × 10^{23} molecule mol^{-1}) = g $molecule^{-1}$
3. Concentration of plasmid (g μL^{-1}) ÷ g $molecule^{-1}$ = copy number (molecules μL^{-1})

Dilutions of plasmid DNA containing the cloned genes of *glnA* were used to generate standard curves in quantities ranging from 3.22 × 10^2 to 3.22 ×10^8 copies.

4.3.8.2 qPCR Assays for *glnA* Absolute Quantification

qPCR assays for absolute quantification of *glnA* genes were performed with SsoFast EvaGreen Supermix (Bio-Rad Laboratories, Hercules, CA) and the Eco™ Real-Time PCR System (Illumina Inc., San Diego, CA). Reaction preparations were performed in a laminar flow hood with HEPA filter and all work surfaces and equipment were washed with 70% ethanol, 10% bleach and sterilized under UV light. Each 10µL qPCR reaction contained 5µL SsoFast mix, 0.5µM each forward and reverse primer, 1µL DNA template and 3µL water. Cycling conditions were the following: 98°C for 5 min then 35 cycles of 98°C for 15 sec and 60°C for 30 sec. Fluorescence was detected after each cycle. Reaction efficiency (E) was calculated as E = 10(-1/slope); where the slope of the standard curve was determined by plotting the C_T versus the log of the standard DNA dilutions. The R^2 of the standard curve was above 0.9. Gene copy numbers were divided by genomic DNA concentrations to obtain copies ng^{-1} of DNA which normalizes the results to account for biases that may have occurred during the DNA extraction procedure.

4.3.8.3. Quality Control of qPCR Data

The specificity of the qPCR amplicons was assessed by a melt curve analysis and control of the amplicon on an agarose gel electrophoresis. After the last cycle, amplicons were subjected to a programmed temperature increase from 55ºC to 98ºC. Fluorescence data was collected every 0.3ºC and the negative derivative of relative fluorescence units (RFU) was plotted versus temperature (-dRFU/dT) which calculates melting temperatures (T_m) based upon peak calls. The T_m of an amplicon

is based on its nucleotide sequence; therefore the amplicons of a targeted gene should have a similar T_m as the standards. Information from the melt curve was combined with that of the agarose gels from traditional PCRs to identify and eliminate non-specific amplicons or primer dimer artifacts from the analyses.

4.4 Results and Discussion

4.4.1. Mercury and Water Chemistry in Aquatuk Lake

Tables 4.1 and 4.2 contain key characteristics of Aquatuk lakewater chemistry. The total mercury concentration of the sediments used in the microcosm experiments was 19.6 ± 1 ng g^{-1} (wet weight) and total mercury concentration in water was 0.87 ± 0.2 ng L^{-1}.

4.4.2 Biogenic Production of Elemental Mercury

Initial attempts to sterilize the sediment slurry consisted of autoclaving at 134ºC/28 psi for 60 minutes. However, autoclaving can severely alter the physicochemical properties of the slurry and increase the availability of certain nutrients such as phosphate and dissolved organic carbon (Anderson and Magdoff, 2005; Berns *et al.*, 2008). Additionally, autoclaving is not always effective at killing bacterial spores. In some cases the heat and pressure can stimulate spore growth which is enhanced by the nutrients released during the autoclaving procedure (Tuominen *et al.*, 1994). We found this to be the case in our study; the autoclaved sediment became very frothy and thick and when bubbled it coated the walls of the microcosm and blocked the air outlet (Fig. S4.1). While a typical graph of Hg(0) production over time resembles that of an exponential growth curve similar to that of bacteria, our treatment Autoclaved + PBS + C exhibited an extended lag phase prior to the exponential production of Hg(0) (Fig. S4.2). Numerous Hg resistant bacteria form spores and so we hypothesize that bacterial spores survived the autoclaving process and thrived due to the availability of phosphate and carbon (Wang *et al.*, 1989). The Autoclaved + Water treatment produced far less Hg(0) than the Autoclaved + PBS + C treatment since there were no nutrient amendments to sustain spore growth. However, the Hg(0) production rate of the Autoclaved + Water

treatment is similar to that of the live Water treatment, hence we considered autoclaving an ineffective way of sterilizing sediment.

4.4.2.1 Rate of Elemental Mercury Production

Tuominen *et al.* (1994) reported that the most effective way to sterilize sediment without altering its physicochemical properties or its pH is by incubating the sediment slurry with 0.1% to 0.5% formaldehyde. Concurringly, we performed a 0.5% formaldehyde-treated control for each medium used in this study and recorded very low rates of Hg(0) production or none at all (Water + 0.5% formaldehyde: 0 ng day^{-1} g^{-1}; MOPS + 0.5% formaldehyde: 0 ng day^{-1} g^{-1}; PBS + 0.5% formaldehyde: 1.1×10^{-5} ng day^{-1} g^{-1}). The live treatment of each corresponding buffer had higher rates of Hg(0) production which supports our hypothesis that Hg(0) emissions were biogenic (Water: 2.1×10^{-4} ng day^{-1} g^{-1}; MOPS: 2.9×10^{-3} ng day^{-1} g^{-1} ; PBS: 1.5×10^{-3} ng day^{-1} g^{-1}) (Table 4.4, Fig. 4.2).

4.4.2.2 *glnA* Gene Absolute Quantification

A traditional PCR was performed on the sediment to amplify the *glnA* gene; a house-keeping gene used as a proxy of bacterial abundance. Figure 4.3 shows the amplified 154bp bands on a 2% agarose gel stained with EtBr. The autoclaved treatment (D) shows lower band intensity, as expected. Formaldehyde damages DNA and inhibits its repair rendering the cell unable to survive, however, it also prevents its hydrolysis (Grafstrom *et al.*, 1983; Puchtler and Meloan, 1985). This is likely the reason we observe a relatively intense band for the *glnA* gene in the formaldehyde treated sediment despite having a very low Hg(0) production rate (Figure 4.3, lane E). A clean discrete band characteristic of a small amplicon was observed in all treatments suggesting that the primers and PCR conditions are suitable in a qPCR approach.

A quantitative PCR assay was performed for absolute quantification of the *glnA* gene in the sediment as a proxy for bacteria abundance. The efficiency of the standard curve was 89.6 and the R^2 was 0.998. Figure 4.4 shows the *glnA* gene (copies ng^{-1} of DNA) normalized for the amount of DNA that was extracted and the Hg(0) production rates (ng day^{-1} g^{-1}). The gene copy number in the pre-incubation sediment serves as a control. We see that in both control treatments (Autoclaved +

water and Formaldehyde + PBS) the *glnA* gene abundance decreases, confirming the reduction of bacterial abundance by both sterilization methods. The reduction in bacteria is also reflected in the reduced rates of Hg(0) production, as we previously showed that Hg(0) production was mostly of bacterial origin. The two live treatments clearly show an increase in *glnA* gene abundance compared to the control, suggesting a thriving bacteria population. The PBS and PBS + C treatments also display a higher rate of Hg(0) production when compared to the sterilized treatments suggesting that addition of carbon sources stimulated bacterial growth. By combining a sensitive monitoring approach with advanced molecular technique, we can assert that the production of Hg(0) from these microcosms is biogenic.

4.4.3 Nutrient Amendments

Live treatments were supplemented with phosphate and carbon to assess the role of nutrients amendments on Hg(0) production rates. PBS buffer was initially used to maintain a pH of 7.4 in all treatments; however, it also contains high levels of P (9.86 mM) and salts (137 mM NaCl and 2.7 mM KCl). As an alternative to PBS, we used MOPS buffer to maintain a constant pH without the addition of P and salts. Initial treatments of PBS and MOPS had very similar Hg(0) production rates (Fig. 4.2). We proceeded to add a source of carbon to both buffers and recorded a much higher production rate in the PBS + C treatment (PBS + C: 5.0×10^{-3} ng day^{-1} g^{-1} and MOPS + C: 1.2×10^{-3} ng day^{-1} g^{-1}) (Fig. 4.5).

We hypothesized that phosphorus could be a limiting nutrient of the microbial community in our microcosm since other studies have identified phosphate as a limiting nutrient in aquatic environments (Jeon *et al.*, 2001; Graneli *et al.*, 2004). To test for a P limitation in Hg(0) production, we designed a series of treatments with increasing concentrations of P added as KH_2PO_4 using buffered MOPS or unbuffered sediments (milliQ). Hg(0) production rate with MOPS + 100µM P and MOPS + 1mM P treatments were 9.3×10^{-4} ng day^{-1} g^{-1} and 9.8×10^{-4} ng day^{-1} g^{-1}, respectively. Both treatments yielded very similar Hg(0) production rates. We further increased phosphorus concentration to 10mM P in unbuffered sediments (using milliQ water). Hg(0) production rate was 1.5×10^{-4} ng day^{-1} g^{-1} which is lower than the

1mM and 100μM P treatments. We concluded that phosphorus is unlikely to limit Hg(0) production in Aquatuk sediments.

The PBS buffer treatment with carbon yielded a higher Hg(0) production rate than MOPS with carbon suggesting that salts in the PBS buffer may be required for Hg(0) production. Furthermore, the addition of C to the PBS buffer increased the production of Hg(0) when compared to PBS alone (Table 4.4). However, the addition of C to the MOPS treatment decreased Hg(0) production rates when compared to the MOPS only treatment therefore carbon is unlikely to be the sole variable influencing biogenic Hg(0) production (MOPS + C: 1.2×10^{-3} ng day^{-1} $g^{-1}$and MOPS: 2.9×10^{-3} ng day^{-1} g^{-1}) (Fig. 4.5).

4.4.4 pH

To assess the influence of pH on Hg(0) production, we compared buffered and non-buffered treatments. We compared Hg(0) production in sediments in PBS buffer and in a treatment similar to PBS in term of components concentrations that was non-buffered, adding P (as KH_2PO_4) + NaCl + KCl. The pH of the buffered treatment was 7.23. The pH of the non-buffered treatment was 5.66. Hg(0) production rate of the non-buffered treatment (pH=5.66) was 1.5×10^{-3} ng day^{-1} g^{-1} which was identical to the buffered treatment which had a pH of 7.23 and a production rate of 1.5×10^{-3} ng day^{-1} g^{-1}. The $[H^+]$ concentration is 38 times greater at pH=5.66 than at pH=7.24. We conclude that pH did not appear to have a significant influence on biological Hg(0) production rates (Fig. 4.6).

4.4.5 Ionic Strength

The phosphate buffered saline solution (PBS) also contains high concentrations of sodium chloride (137mM NaCl) and potassium chloride (2.7mM KCl). We tested the effects of these salts on the Hg(0) production rates using sediments resuspended in milliQ containing variable salt concentrations. The first treatment consisted of water + 137mM NaCl + 2.7mM KCl and yielded one of the highest Hg(0) production rate thus far: 2.7×10^{-3} ng day^{-1} g^{-1}. We decreased the salt concentration 10 and 100 fold and recorded a corresponding decrease in Hg(0)

production; water + 13.7mM NaCl + 0.27mM KCl: 7.4×10^{-4} ng day^{-1} g^{-1}, water + 1.37mM NaCl + 0.027mM KCl: 1.5×10^{-4} ng day^{-1} g^{-1} (Fig. 4.7). This led us to suspect that NaCl might be an important contributor to microbial Hg(0) production in sediment. Na^+ has been shown to increase Hg(II) uptake in pure cultures of *Escherichia coli* containing the Tn21 *mer* operon (Selifonova and Barkay, 1994). Selifonova and Barkay (1994) proposed that sodium-coupled transport of mercuric ions can be one of the mechanisms for mercury uptake and that the Na^+ gradient may energize the transport of Hg(II).

We assessed the effect of Na^+ and Cl^- separately, while maintaining the ionic strength (I) constant at 140 mmol L^{-1}. We used magnesium chloride to asses the influence of Cl^- without Na^+. The treatment consisted of water + 45.6mM $MgCl_2$ and had a production rate of 1.5×10^{-3} ng day^{-1} g^{-1}. To asses the effect of Na^+, we used 45.6 mM sodium sulfate (Na_2SO_4) with water and recorded a Hg(0) production rate of 4.5×10^{-3} ng day^{-1} g^{-1}. Although the Na_2SO_4 treatment had a higher Hg(0) production rate, the $MgCl_2$ had a comparable rate of Hg(0) production. We propose that ionic strength, instead of the Na^+ ion alone, may be the key factor influencing microbial Hg(0) production in lake sediments.

4.4.6 Potential Elemental Mercury Fluxes

The atmospheric deposition rate of Hg in the HBL of Northern Ontario is approximately 5.8 µg m^{-2} y^{-1} (NADP, 2010). The Hg(0) production rate of the Na_2SO_4 treatment, which had an ionic strength of 140mM and yielded the highest Hg(0) production rate, was 1.64 ng y^{-1} g^{-1}. The sediment had a water content of 90% therefore a density of 1.5 g cm^{-3} (Håkanson and Jansson, 1983). The rate of Hg(0) production was converted to a flux of 24.6 µg m^{-2} y^{-1}. Rates were obtained at room temperature which is considered optimal for bacterial growth and metabolic processes. Based on the work of Price and Sowers (2004), when the temperature is reduced to 15ºC, comparable to the water temperature at the sediment-water interface of Aquatuk Lake (16.3 ºC), metabolic activity is reduced by 90% which corresponds to a Hg(0) production rate of 2.46 µg m^{-2} y^{-1}, representing 42% of the annual Hg deposition rate. When the temperature is reduced further to 4ºC,

metabolic activity is reduced by 99% and the Hg(0) production rate becomes 0.25 μg m^{-2} y^{-1}; 4% of the annual deposition rate.

The Hg(0) production rate of the microcosm which contained only water was 1.17 μg m^{-2} y^{-1}. Corrected for a temperature of 15 ºC, this represents 0.117 μg m^{-2} y^{-1} , 2% of the annual deposition, and when corrected at 4ºC the rate is reduced to 0.0117 μg m^{-2} y^{-1}; 0.2% of the Hg deposited annually. These Hg(0) emission rates from lake sediments are only based on the first cm, under oxic conditions, and presume that the Hg(0) produced is freely emitted into the water column. We believe that this novel information is relevant to the understanding of biogenic influences to the Hg redox cycle in pristine lake sediments.

4.4.7 Implications

The use of salts as deicing agents on roadways has led to the contamination of land and water resources across temperate and northern regions (Rosenberry *et al.*, 1999 and references therein). Judd *et al.* (2005) reported that, in addition to salt, snow melt runoff also contains a significant amount of nutrients which can alter the structure and function of the lake ecosystem. The results of this study suggest that increases in ionic content due to roadway runoff in the spring could potentially increase microbial Hg(0) production in lakes of temperate regions, thus altering the Hg cycle. Development in Northern regions is increasing rapidly as the changing climate is offering prospects for the exploitation of untapped natural resources. Our study suggests that the development of roads and increased circulation, and the ensuing use of de-icing agents, could create significant changes in these fragile northern ecosystems.

4.5 Conclusions

This study reports that ionic strength has the greatest influence on rates of biogenic Hg(0) production. This is, to the best of our knowledge, the first time that biological Hg(0) production rates are reported in microcosms using non-contaminated lake sediments. Additionally, we did not spike the sediment with Hg and maintained oxic conditions which increases environmental relevance. This is

also the first work to report on factors influencing the rate of Hg(0) production by microbes *in situ*. Knowledge of the factors influencing microbial Hg(0) production in lake sediments is essential to the understanding of the Hg biogeochemical cycle. *In situ* Hg(0) production rates are vital to Hg modeling studies, however they remain elusive and are often overlooked. Most Hg modeling studies acknowledge the evasion of Hg(0) from the sediment compartment without specifically attributing it to be of biogenic origin (Diamond, 1999; Ethier *et al.*, 2008; Macleod *et al.*, 2005). This study shows that the amount of Hg(0) produced from sediment is small ranging from 0.008% to 0.27% of the total mercury, which corresponds to 0.068 to 2.15 ng of Hg in our microcosms. Over a year, assuming that the surface of the sediment is 7 000 000 m^2, the estimated flux form the sediment to the water column in the most conservative treatment corresponds to 0.0117 µg m^{-2} y^{-1}, or 0.2% of the annual deposition from atmospheric origin. We believe that, with previous knowledge of the chemical and physical characteristics of the system in question, models can be improved by incorporating these Hg(0) production rates. Further studies are needed to characterize the influence of other critical parameters such as temperature and oxygen levels on Hg(0) production rates to achieve increased accuracy when modeling an omnipresent and dangerous chemical such as Hg.

4.6 References

Anderson, B.H. and F.R. Magdoff. 2005. Autoclaving soil samples affects algal-available phosphorus. J. Environ. Qual., 34(6): 1958-1963.

Berns, A.E., H. Philipp, H.D. Narres, P. Burauel, H. Vereecken and W. Tappe. 2008. Effect of gamma-sterilization and autoclaving on soil organic matter structure as studied by solid state NMR, UV and fluorescence spectroscopy. Eur. J. Soil Sci., 59(3): 540-550.

Blomqvist, S. 1990. Sampling performance of Ekman grabs - insitu observations and design improvements. Hydrobiologia, 206(3): 245-254.

Desrosiers, M., D. Planas and A. Mucci. 2006. Mercury methylation in the epilithon of Boreal shield aquatic ecosystems. Environmental Science & Technology, 40(5): 1540-1546.

Diamond, M.L. 1999. Development of a fugacity/aquivalence model of mercury dynamics in lakes. Water Air and Soil Pollution, 111(1-4): 337-357.

Ethier, A.L.M., D. Mackay, L.K. Toose-Reid, N.J. O'Driscoll, A.M. Scheuttammer and D.R.S. Lean. 2008. The development and application of a mass balance model for mercury (total, elemental and methyl) using data from a remote lake (Big Dam West, Nova Scotia, Canada) and the multi-species multiplier method. Applied Geochemistry, 23(3): 467-481.

Fox, B.S., Mason, K.J., McElroy, F.C., 2005. Determination of total mercury in crude oil by combustion cold vapor atomic absorption spectrometry (CVAAS), in: Nadkarni, R.A.K. (Ed.), Elemental Analysis of Fuels and Lubricants: Recent Advances and Future Prospects, pp. 196-206.

Grafstrom, R.C., A.J. Fornace, H. Autrup, J.F. Lechner and C.C. Harris. 1983. Formaldehyde damage to DNA and inhibiting of DNA-repair in human bronchial cells. Science, 220(4593): 216-218.

Graneli, W., S. Bertilsson and A. Philibert. 2004. Phosphorus limitation of bacterial growth in high Arctic lakes and ponds. Aquatic Sciences, 66(4): 430-439.

Gunn, J. and E. Snucins. 2010. Brook charr mortalities during extreme temperature events in sutton river, Hudson Bay Lowlands, Canada. Hydrobiologia, 650(1): 79-84.

Håkanson, L. and M. Jansson. 1983. Principles of lake sedimentology. Cladwell: The Blackburn Press. 316.

Hurt, R.A., X.Y. Qiu, L.Y. Wu, Y. Roh, A.V. Palumbo, J.M. Tiedje and J.H. Zhou. 2001. Simultaneous recovery of RNA and DNA from soils and sediments. Appl Environ Microb, 67(10): 4495-4503.

Jeon, C.O., D.S. Lee and J.M. Park. 2001. Enhanced biological phosphorus removal in an anaerobic-aerobic sequencing batch reactor: Characteristics of carbon metabolism. Water Environment Research, 73(3): 295-300.

Judd, K.E., H.E. Adams, N.S. Bosch, J.M. Kostrzewski, C.E. Scott, B.M. Schultz, D.H. Wang and G.W. Kling. 2005. A case history: Effects of mixing regime on nutrient dynamics and community structure in Third Sister Lake, Michigan during late winter and early spring 2003. Lake and Reservoir Management, 21(3): 316-329.

Kirk, J.L., D.C.M. Muir, D. Antoniades, M.S.V. Douglas, M.S. Evans, T.A. Jackson, H. Kling, S. Lamoureux, D.S.S. Lim, R. Pienitz, J.P. Smol, K. Stewart, X. Wang and F. Yang. 2011. Climate change and mercury accumulation in Canadian high and subarctic lakes. Environmental Science & Technology, 45(3): 964-970.

Lindberg, S., R. Bullock, R. Ebinghaus, D. Engstrom, X. Feng, W. Fitzgerald, N. Pirrone and C. Seigneur. 2007. A synthesis of progress and uncertainties in attributing the sources of mercury in deposition. Ambio., 36: 19-32.

Macleod, M., T.E. McKone and D. Mackay. 2005. Mass balance for mercury in the San Francisco Bay area. Environmental Science & Technology, 39(17): 6721-6729.

Miskimmin, B.M., J.W.M. Rudd and C.A. Kelly. 1992. Influence of dissolved organic carbon, pH, and microbial respiration rates on mercury methylation and demethylation in lake water. Canadian Journal of Fisheries and Aquatic Sciences, 49(1): 17-22.

Nagase, H., Y. Ose, T. Sato and T. Ishikawa. 1982. Methylation of mercury by humic substances in an aquatic environment. Science of the Total Environment, 25(2): 133-142.

National Atmospheric Deposition Program (NRSP-3). 2007. NADP Program Office, Illinois State Water Survey, 2204 Griffith Dr., Champaign, IL 61820.

Poulain, A.J., M. Amyot, D. Findlay, S. Telor, T. Barkay and H. Hintelmann. 2004. Biological and photochemical production of dissolved gaseous mercury in a Boreal lake. Limnol Oceanogr, 49(6): 2265-2275.

Price, P.B. and T. Sowers. 2004. Temperature dependence of metabolic rates for microbial growth, maintenance, and survival. Proceedings of the National Academy of Sciences of the United States of America, 101(13): 4631-4636.

Puchtler, H. and S.N. Meloan. 1985. On the chemistry of formaldehyde fixation and its effects on immunohistochemical reactions. Histochemistry, 82(3): 201-204.

Rosenberry, D.O., P.A. Bukaveckas, D.C. Buso, G.E. Likens, A.M. Shapiro and T.C. Winter. 1999. Movement of road salt to a small New Hampshire lake. Water Air and Soil Pollution, 109(1-4): 179-206.

Selifonova, O.V. and T. Barkay. 1994. Role of Na^{+} in transport of Hg^{2+} and induction of the Tn21 *mer* operon. Appl Environ Microb, 60(10): 3503-3507.

Solomon, T. 2001. The definition and unit of ionic strength. Journal of Chemical Education, 78(12): 1691-1692.

Tuominen, L., T. Kairesalo and H. Hartikainen. 1994. Comparison of methods for inhibiting bacterial activity in sediment. Appl Environ Microb, 60(9): 3454-3457.

Wang, Y., M. Moore, H.S. Levinson, S. Silver, C. Walsh and I. Mahler. 1989. Nucleotide sequence of a chromosomal mercury resistance determinant from a Bacillus sp. with broad-spectrum mercury resistance. Journal of Bacteriology, 171(1): 83-92.

Wiatrowski, H.A., P.M. Ward and T. Barkay. 2006. Novel reduction of mercury(II) by mercury-sensitive dissimilatory metal reducing bacteria. Environmental Science & Technology, 40(21): 6690-6696.

Zhou, J.Z., M.A. Bruns and J.M. Tiedje. 1996. DNA recovery from soils of diverse composition. Appl Environ Microb, 62(2): 316-322.

4.7 List of Tables

Table 4.1: Aquatuk Lake water chemistry.

	Alkalinity (mg L^{-1} $CaCO_3$)	Colour (TCU*)	Conductivity (µS cm^{-1})	DIC▲ (mg L^{-1})	DOC¤ (mg L^{-1})	pH	TP‡ (µg L^{-1})	Chlorophyll *a* (µg L^{-1})
Water	105	28	206	27	7.4	8.4	16	20

*TCU: true color units
▲DIC: dissolved inorganic carbon
¤DOC: dissolved organic carbon
‡TP: total phosphorous

Table 4.2: Ion concentrations in Aquatuk lakewater.

	Al ($\mu g\ L^{-1}$)	Ca ($mg\ L^{-1}$)	Cl ($mg\ L^{-1}$)	Fe ($\mu g\ L^{-1}$)	Mg ($mg\ L^{-1}$)	Mn ($\mu g\ L^{-1}$)	Na ($mg\ L^{-1}$)	SiO_3 ($mg\ L^{-1}$)	Sr ($\mu g\ L^{-1}$)	SO_4 ($mg\ L^{-1}$)
Water	3.5	35	1.6	20	5.6	27	2.5	1.5	49	0.45

Table 4.3: Data used to calculate Hg(0) production rates (ng Hg^0 day^{-1} g^{-1}). Raw data was transformed using a best-fit model based on exponential growth.

Treatment	Reagents	Equation (f = a*exp(b*x))			Hg(0) (ng)		Sediment (g)[§]
		a	b	R^2	Day 10	Day 20	
Control	Autoclaved, water	0.018	0.088	0.96	0.043	0.11	41.2
Control	Autoclaved, PBS, 1mM acetate, 1µM butyrate, 1mM citrate, 1mM lactate	0.057	0.28	0.96	0.96	16 †	45.7
Control	0.5% formaldehyde, water	0.0014	2.9×10^{-26}	1.0	0.0014	0.0014	40.8
Control	0.5% formaldehyde, MOPS	0.0024	3.7×10^{-18}	1.0	0.0024	0.0024	42.1
Control	0.5% formaldehyde, PBS	0.0004	0.14	0.88	0.0016	0.0063	44.3
Live, buffered, P, ions	PBS	0.013	0.20	0.95	0.095	0.7	40.6
Live, buffered, P, C, ions	PBS, 1mM acetate, 1µM butyrate, 1mM citrate, 1mM lactate	0.050	0.19	0.98	0.35	2.4	40.9
Live, buffered	MOPS	0.022	0.20	0.98	0.18	1.3 †	40.4
Live, buffered, C	MOPS, 1mM acetate, 1µM butyrate, 1mM citrate, 1mM lactate	0.0035	0.25	0.99	0.043	0.52	41.1
Live, buffered, P	MOPS, 100µM P	0.0075	0.20	0.99	0.058	0.44	41.6

Live, buffered, P	MOPS, 1mM P	0.0001	0.42	0.99	0.0072	0.42 †	41.6
Live, unbuffered, P	Water, 10mM P	0.0001	0.32	0.98	0.0026	0.065	40.7
Live, unbuffered	Water	0.0002	0.31	0.99	0.0041	0.093	41.6
Live, unbuffered, P, NaCl, KCl	Water, 10mM P, 137mM NaCl, 2.7mM KCl	0.013	0.20	0.97	0.096	0.69	40.6
Live, unbuffered, NaCl, KCl	Water, 137mM NaCl, 2.7mM KCl	0.032	0.19	0.99	0.21	1.3	41.6
Live, unbuffered, NaCl, KCl	Water, 13.7mM NaCl, 0.27mM KCl	0.003	0.24	0.97	0.032	0.34	41.2
Live, unbuffered, NaCl, KCl	Water, 1.37mM NaCl, 0.027mM KCl	1.5×10^{-8}	0.76	0.95	3.1×10^{-5}	0.065	43.3
Live, unbuffered, $MgCl_2$	Water, 45.6mM $MgCl_2$	0.0096	0.21	0.98	0.083	0.67	40.8
Live, unbuffered, Na_2SO_4	Water, 46.5mM Na_2SO_4	0.0053	0.29	0.96	0.10	1.9	40.9

†Extrapolated
§In microcosms

Table 4.4: Various treatments and rates of Hg(0) production (ng day^{-1} g^{-1}) from bioreactors containing sediment from Aquatuk Lake.

Treatment	Reagents	pH	Rate of Hg(0) production (ng day^{-1} g^{-1})	THg reduced to Hg(0) (%)
Control	Autoclaved, water	6.70	1.5×10^{-4}	0.012
Control	Autoclaved, PBS, 1mM acetate, 1μM butyrate, 1mM citrate, 1mM lactate	7.22	3.3×10^{-2}	1.8
Control	0.5% formaldehyde, water	7.16	0	0.00017
Control	0.5% formaldehyde, MOPS	7.31	0	0.00030
Control	0.5% formaldehyde, PBS	7.06	1.1×10^{-5}	0.00075
Live, buffered, P, ions	PBS	7.23	1.5×10^{-3}	0.086
Live, buffered, P, C, ions	PBS, 1mM acetate, 1μM butyrate, 1mM citrate, 1mM lactate	7.18	5.0×10^{-3}	0.27
Live, buffered	MOPS	7.39	2.9×10^{-3}	0.17
Live, buffered, C	MOPS, 1mM acetate, 1μM butyrate, 1mM citrate, 1mM lactate	7.64	1.2×10^{-3}	0.064
Live, buffered, P	MOPS, 100μM P	7.14	9.3×10^{-4}	0.052
Live, buffered, P	MOPS, 1mM P	7.35	9.8×10^{-4}	0.051

Live, unbuffered, P	Water, 10mM P	5.63	1.5×10^{-4}	0.0088
Live, unbuffered	Water	6.48	2.1×10^{-4}	0.011
Live, unbuffered, P, NaCl, KCl	Water, 10mM P, 137mM NaCl, 2.7mM KCl	5.66	1.5×10^{-3}	0.084
Live, unbuffered, NaCl, KCl	Water, 137mM NaCl, 2.7mM KCl	6.33	2.7×10^{-3}	0.17
Live, unbuffered, NaCl, KCl	Water, 13.7mM NaCl, 0.27mM KCl	6.53	7.4×10^{-4}	0.047
Live, unbuffered, NaCl, KCl	Water, 1.37mM NaCl, 0.027mM KCl	6.52	1.5×10^{-4}	0.008
Live, unbuffered, $MgCl_2$	Water, 45.6mM $MgCl_2$	6.12	1.5×10^{-3}	0.077
Live, unbuffered, Na_2SO_4	Water, 46.5mM Na_2SO_4	6.63	4.5×10^{-3}	0.21

Table 4.5: Ionic strength (mM) of lakewater from various lakes from the Hudson Bay Lowlands of Ontario, Canada.

	Lake															
	BLB	CSE	HWL	JLN	KSO	NRT	NWG	OPE	OPU	RFT	SAM	SPC	SRT	STN	WCU	WGN
I (mM)	1.9	2.1	2.5	2.4	0.85	1.9	0.93	0.93	1.4	1.6	1.7	1.6	2.2	2.1	1.2	1.6

BLB = Billbear; CSE = Cassie; HWL = Hawley; JLN = Julison; KSO = Kinushseo; NRT = North Raft; NWG = North Washagami; OPE = Opinnagau East; OPU = Opinnagau; RFT = Raft; SAM = Sam; SPC = Spruce; SRT = Stuart; STN = Sutton, WCU = Warchesku; WGN = Wolfgang.

4.8 List of Figures

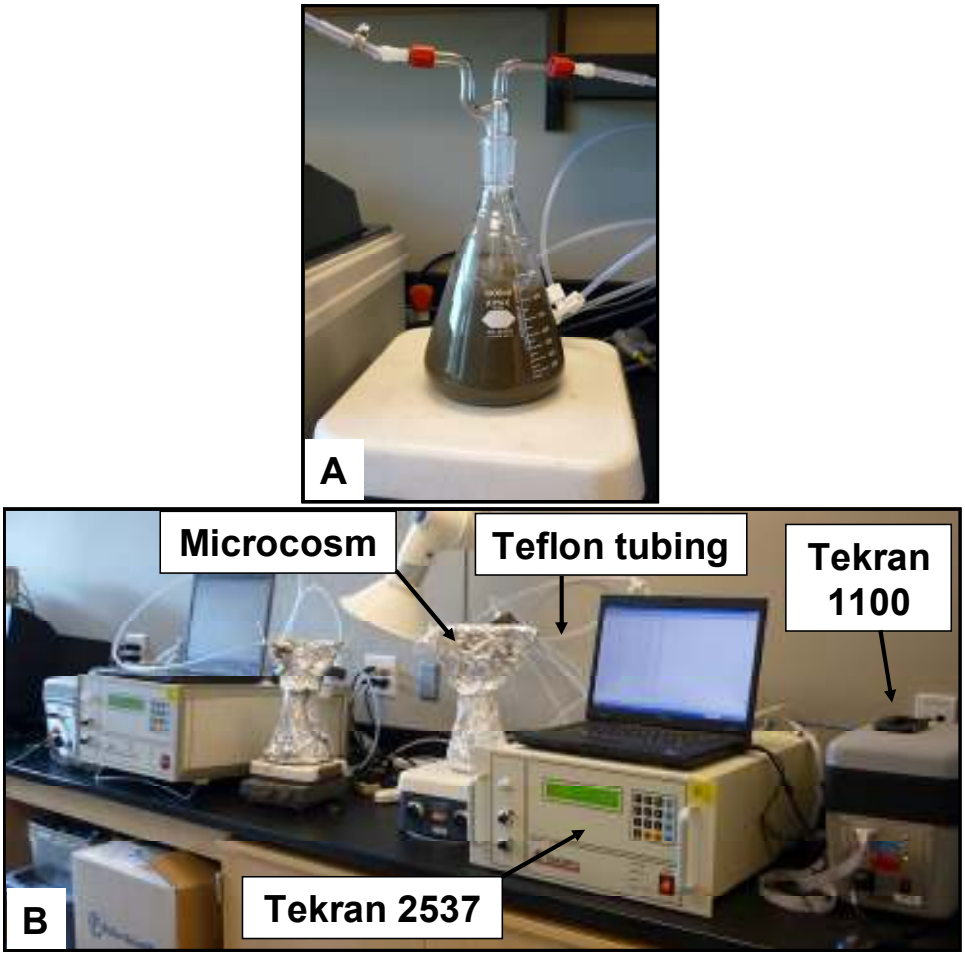

Figure 4.1: Experimental microcosms. A) 1L Erlenmeyer fitted with the head of a gas washing bottle and connected with Teflon tubing. B) Tekran 2537B and 1100 connected to the microcosm.

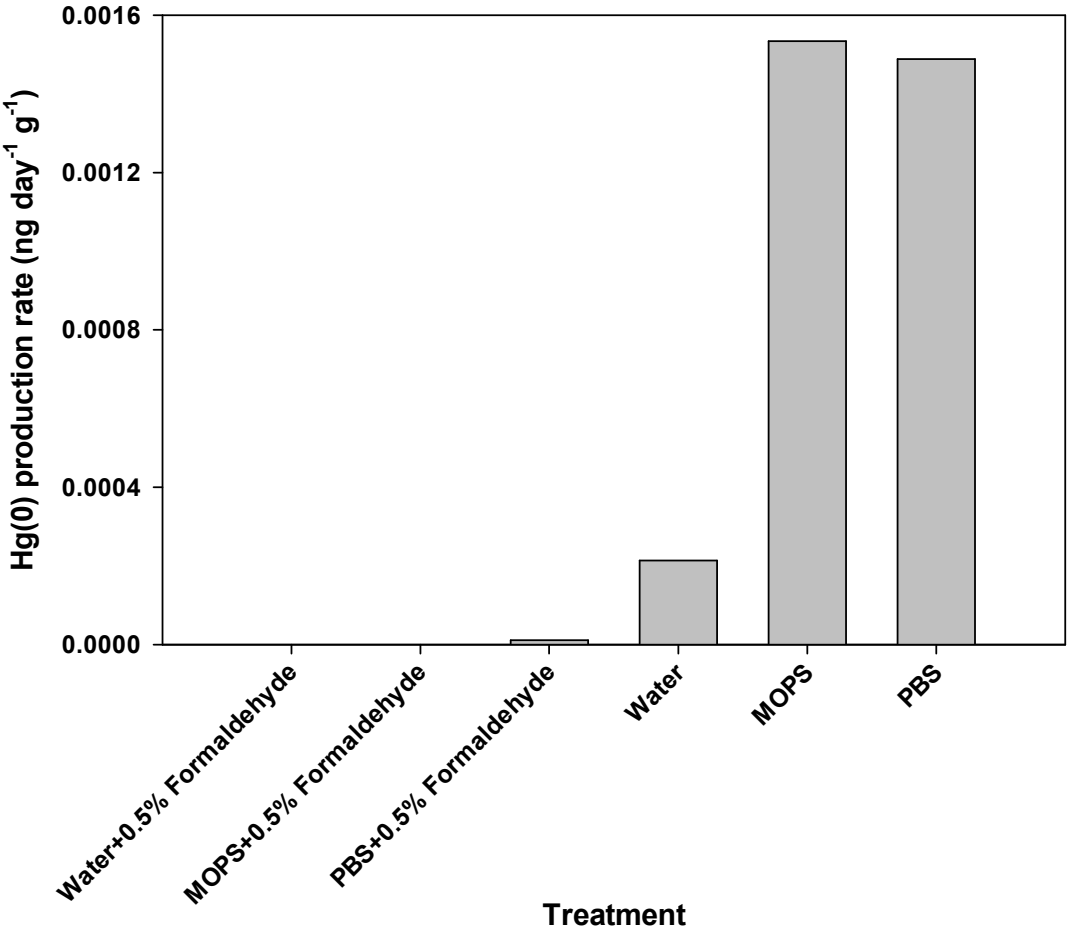

Figure 4.2: Hg(0) production rates (ng day^{-1} g^{-1}) from Aquatuk Lake sediment microcosms subjected to live and sterilized treatments. PBS; phosphate buffered saline solution:137mM NaCl, 2.7mM KCl, 8.1 mM Na_2HPO_4 and 1.76mM KH_2PO_4, MOPS: 10mM $C_7H_{15}NO_4S$.

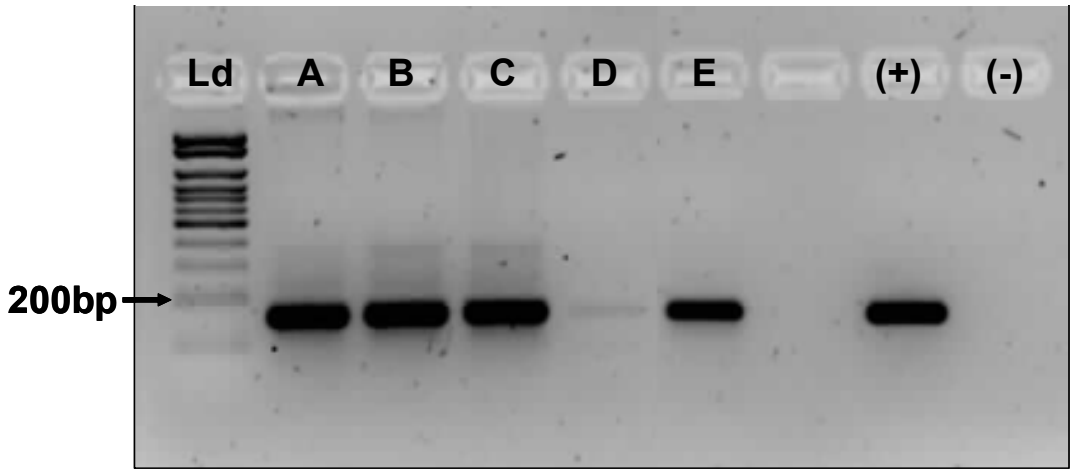

Figure 4.3: Results of a PCR targeting the glutamine synthetase (*glnA*) gene in DNA extracted from sediment microcosms after a 20 day incubation period. A: PBS + Carbon, B: PBS, C: Fresh Sediment (pre-incubation), D: Autoclaved + water, E: Formaldehyde + PBS. Expected amplicon size is 154 bp. Ld: exACTGene Low Range Plus DNA ladder (Fisher Scientific). The gel was 2% agarose, stained with EtBr and migrated at 5V/cm for 60 minutes. PBS; phosphate buffered saline solution:137mM NaCl, 2.7mM KCl, 8.1 mM Na_2HPO_4 and 1.76mM KH_2PO_4. Formaldehyde; 24 hour incubation with 0.5% formaldehyde. C; 1mM acetate, 1µM butyrate, 1mM citrate and 1mM lactate.

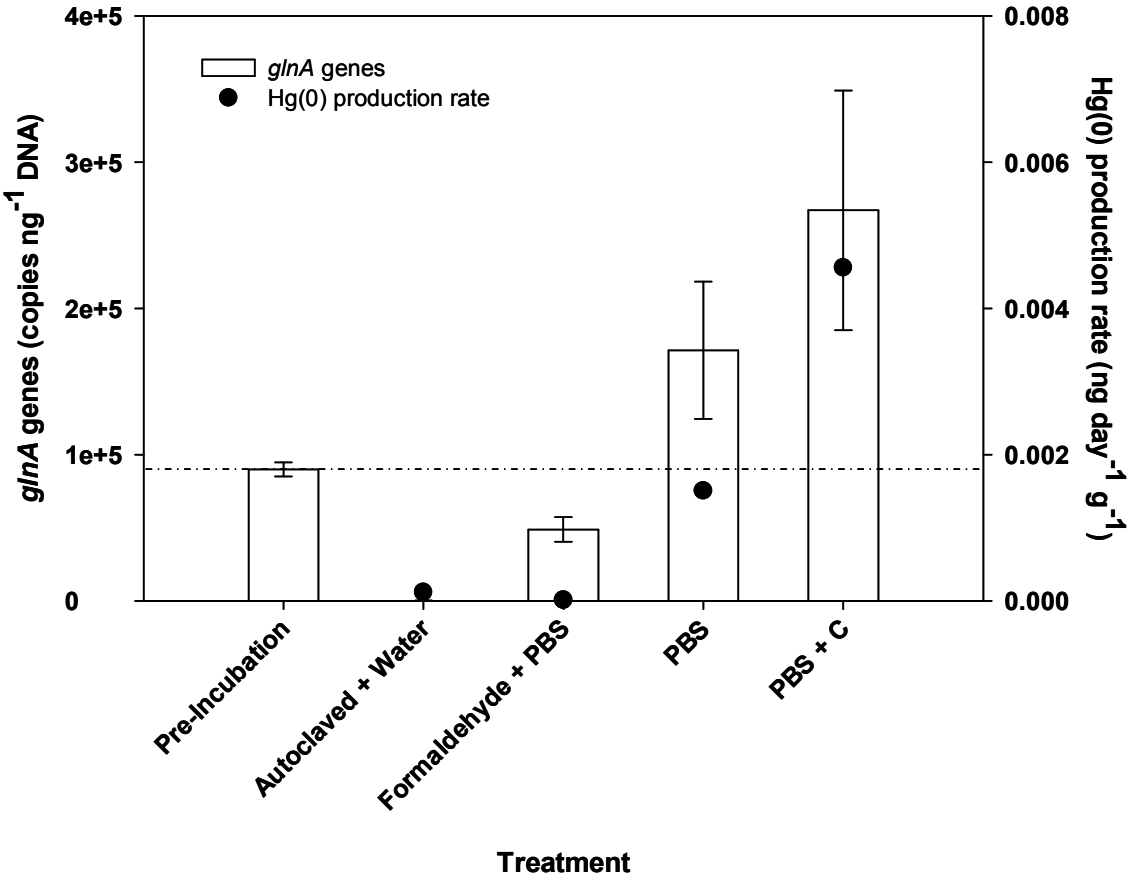

Figure 4.4: Mean glutamine synthetase (*glnA*) gene (copies ng^{-1} of DNA) ± SD and Hg(0) production rates (ng day^{-1} g^{-1}) in various sediment microcosms after 20 days of incubation. The dashed line represents the baseline *glnA* gene copies in the sediment at day 0. PBS; phosphate buffered saline solution:137mM NaCl, 2.7mM KCl, 8.1 mM Na_2HPO_4 and 1.76mM KH_2PO_4. Formaldehyde; 24 hour incubation with 0.5% formaldehyde. C; 1mM acetate, 1µM butyrate, 1mM citrate and 1mM lactate.

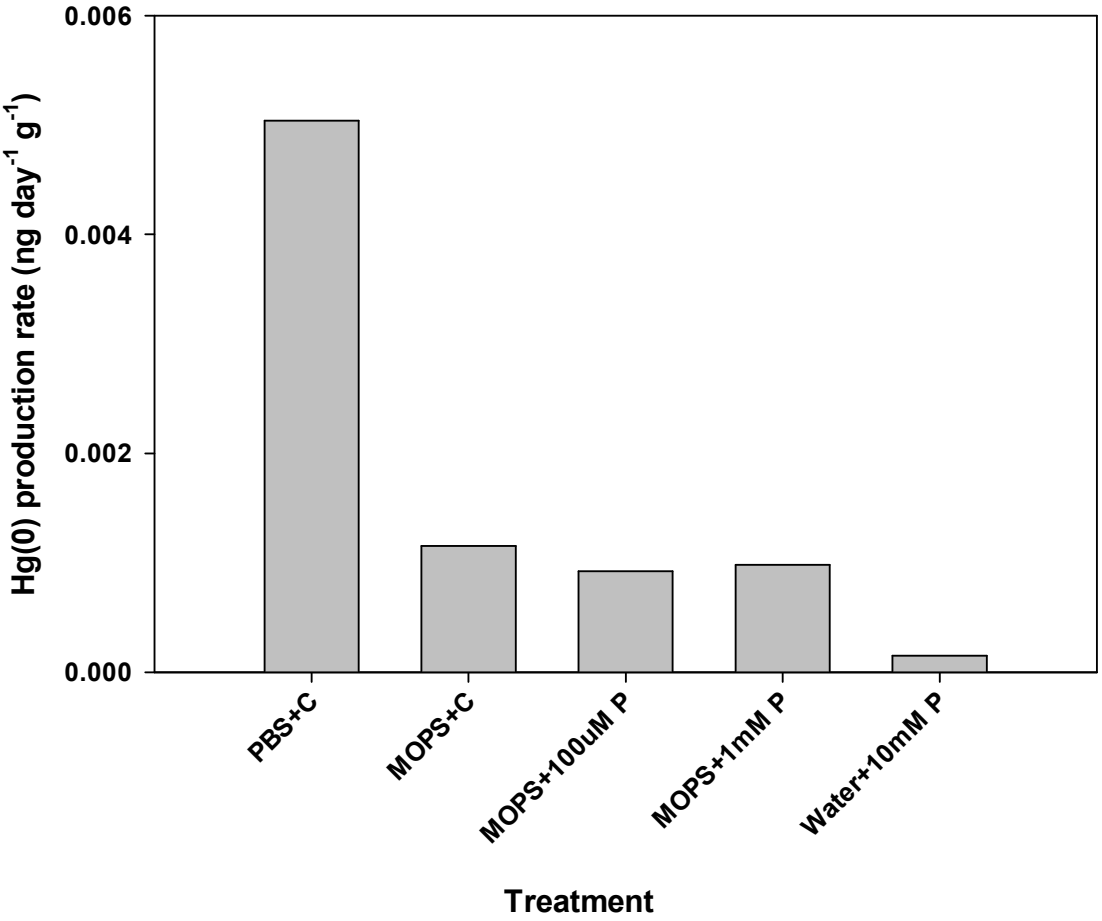

Figure 4.5: Hg(0) production rates (ng day^{-1} g^{-1}) from lake sediment microcosms subjected to various nutrient amendments for a period of 20 days. PBS; phosphate buffered saline solution:137mM NaCl, 2.7mM KCl, 8.1 mM Na_2HPO_4 and 1.76mM KH_2PO_4, C; 1mM acetate, 1µM butyrate, 1mM citrate and 1mM lactate. MOPS: 10mM $C_7H_{15}NO_4S$, P: KH_2PO_4,

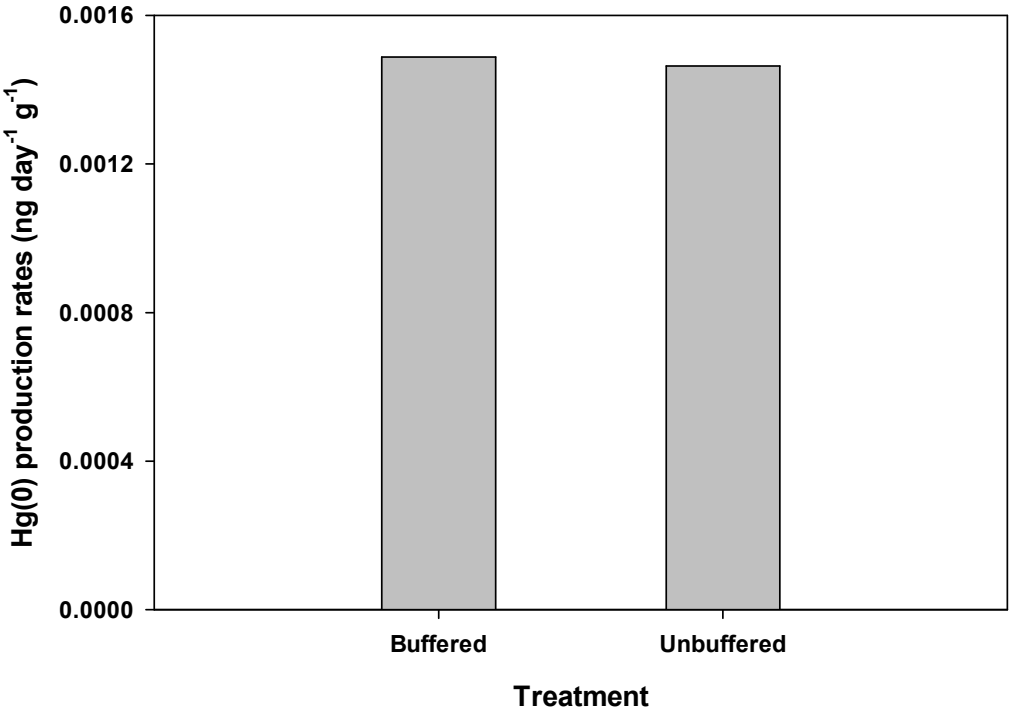

Figure 4.6: Hg(0) production rates (ng day^{-1} g^{-1}) from lake sediment microcosms subjected to a pH buffered and un-buffered treatment for a period of 20 days. Both treatments contained 137mM NaCl, 2.7mM KCl, 8.1 mM Na_2HPO_4 and 1.76mM KH_2PO_4 however the buffered treatment had a pH of 7.4 and the unbuffered treatment had a pH of 5.66.

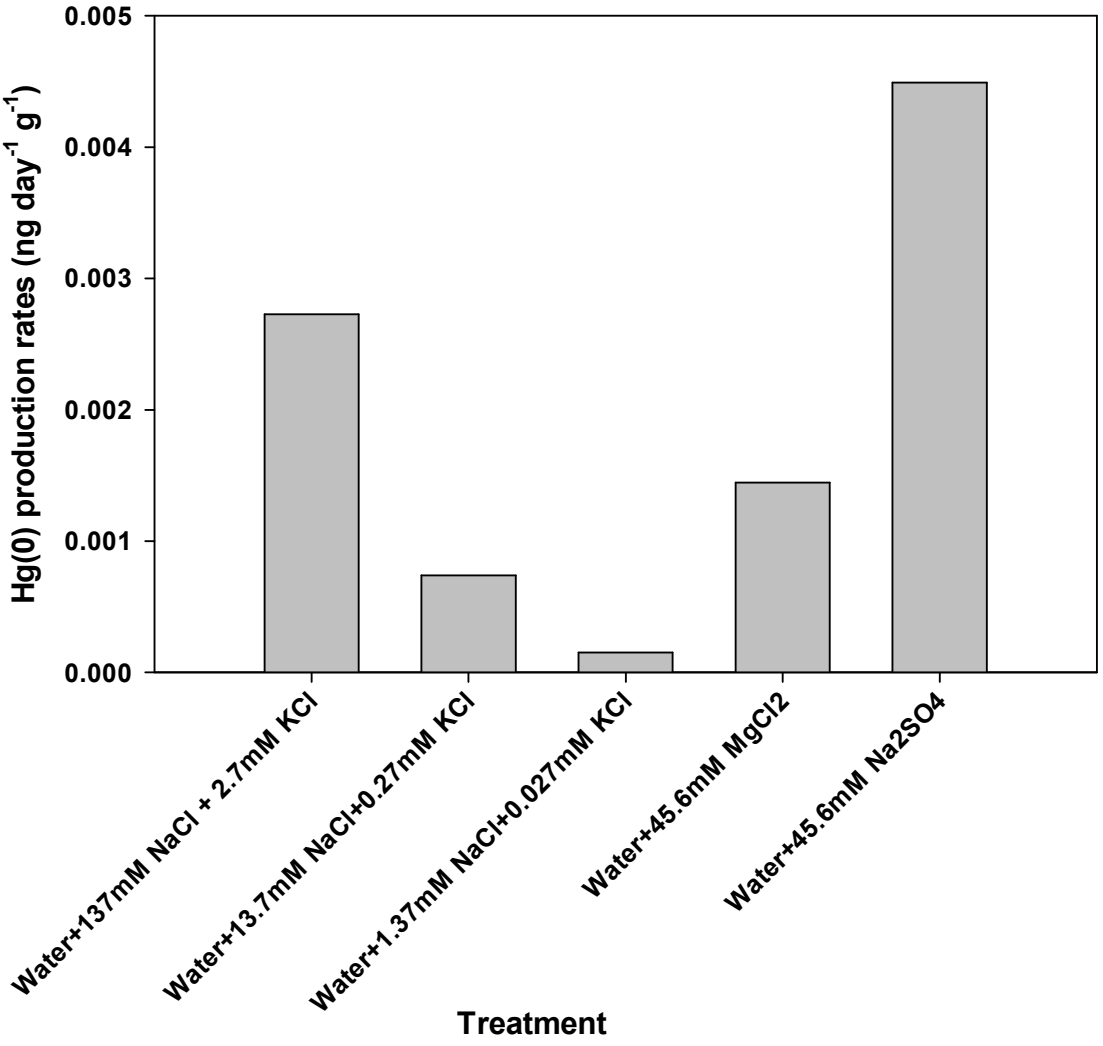

Figure 4.7: Hg(0) production rates (ng day^{-1} g^{-1}) from lake sediment microcosms subjected to various ionic strengths for a period of 20 days.

4.9 Supplemental Information

4.9.1 List of Figures

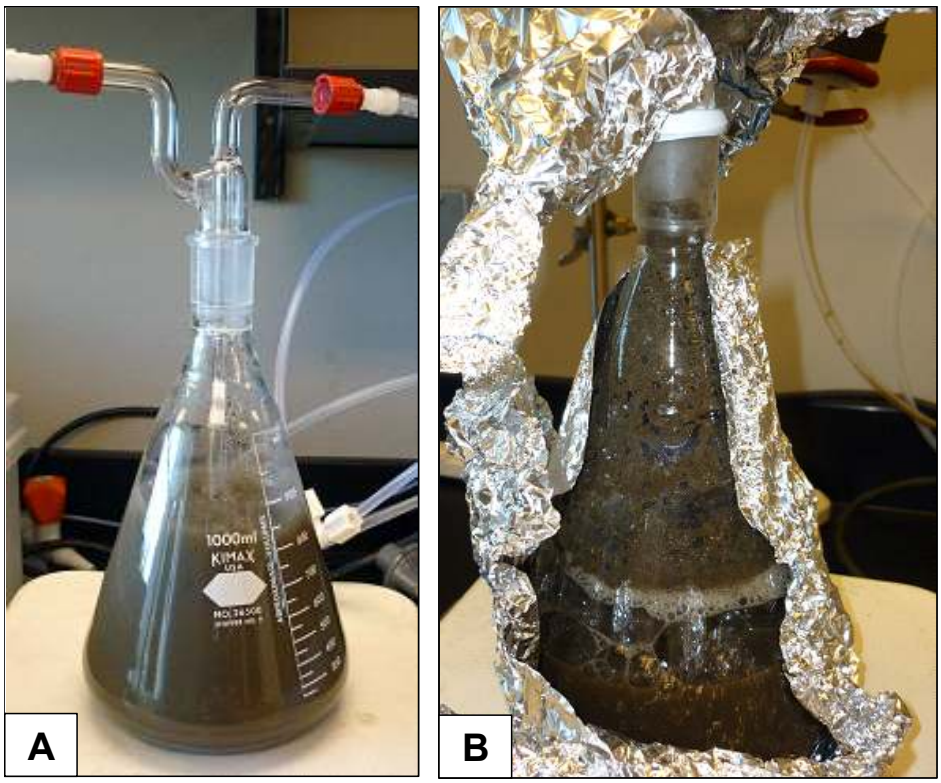

Figure S4.1: A) Non-autoclaved and B) autoclaved sediment slurries used in microcosm experiments.

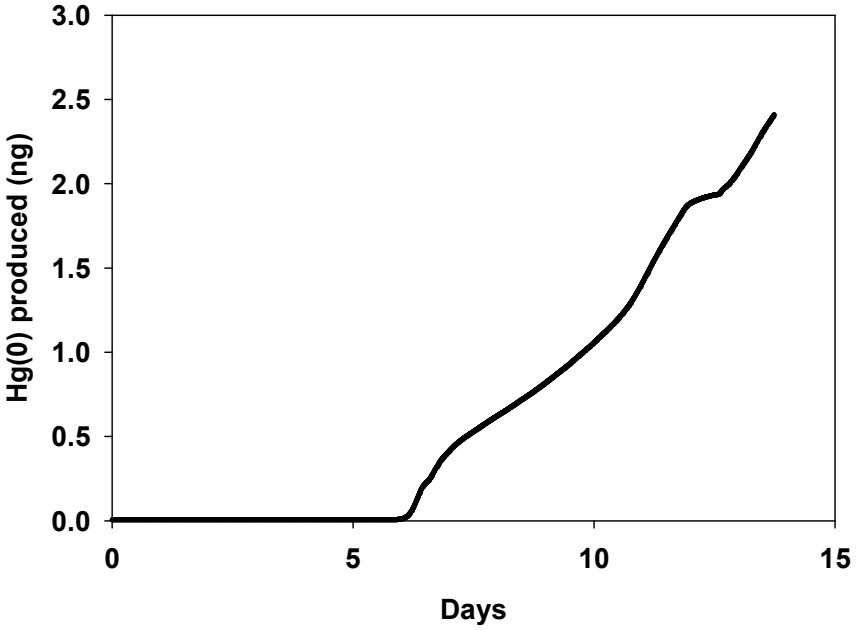

Figure S4.2: Cumulative elemental mercury (Hg(0)) emitted (ng) over 14 days of incubation of the Autoclaved + PBS + C sediment microcosm.

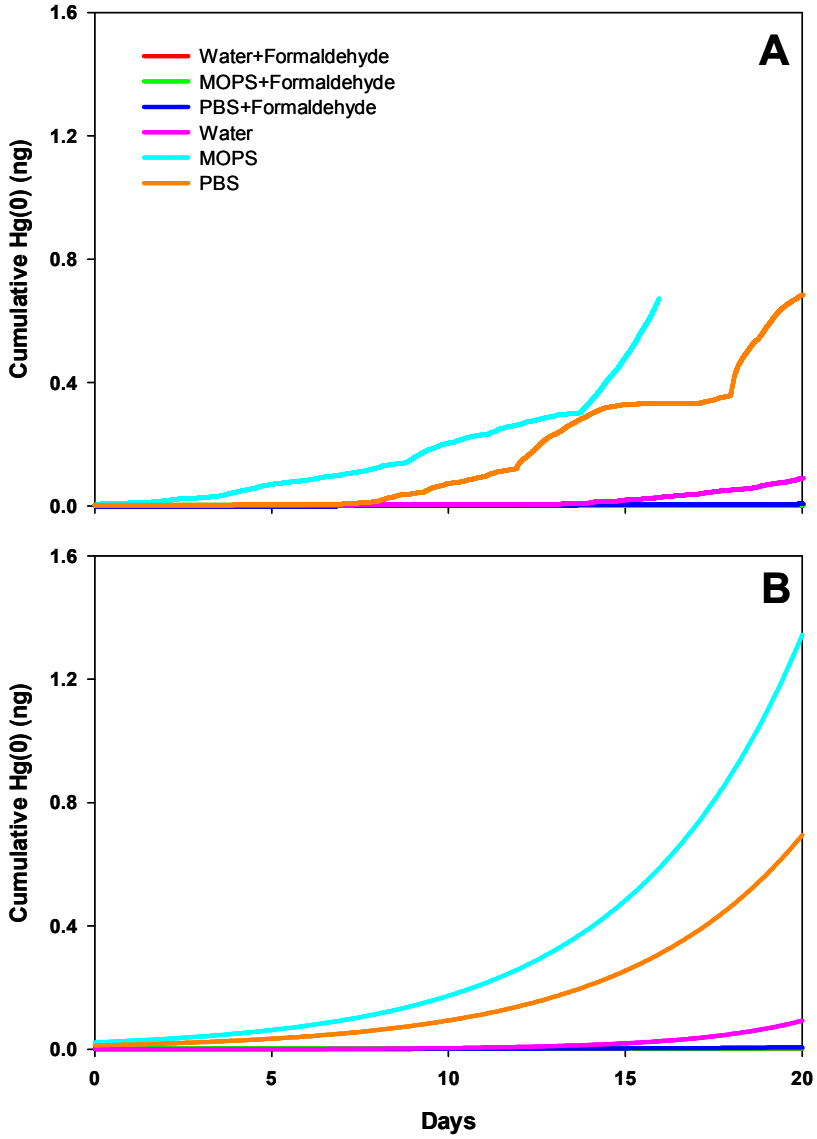

Figure S4.3: Cumulative Hg(0) (ng) emitted from lake sediment microcosms subjected to various live and sterilized treatments over a 20 day incubation period. A) Raw data. B) Data transformed by a best-fit model based on exponential growth. PBS; phosphate buffered saline solution:137mM NaCl, 2.7mM KCl, 8.1 mM Na_2HPO_4 and 1.76mM KH_2PO_4, MOPS: 10mM $C_7H_{15}NO_4S$.

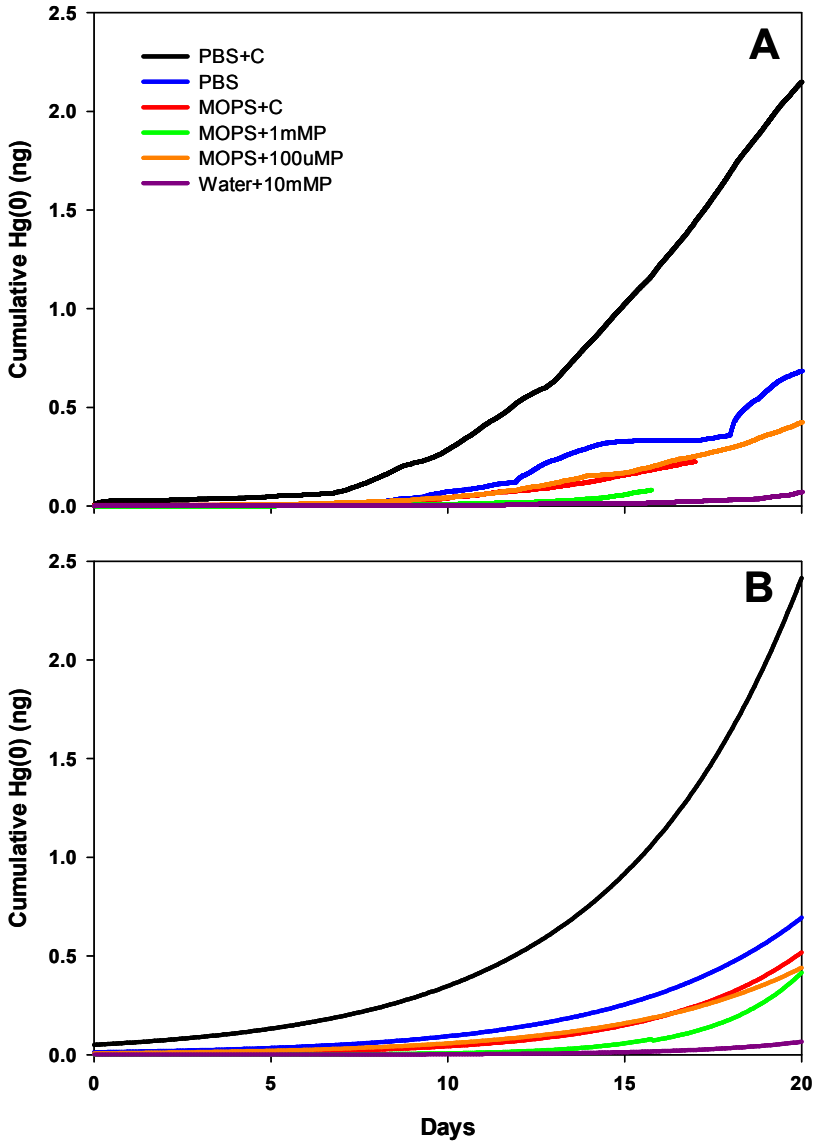

Figure S4.4: Cumulative Hg(0) (ng) emitted from lake sediment microcosms subjected to various nutrient amendments over a 20 day incubation period. A) Raw data. B) Data transformed by a best-fit model based on exponential growth. PBS; phosphate buffered saline solution:137mM NaCl, 2.7mM KCl, 8.1 mM Na_2HPO_4 and 1.76mM KH_2PO_4, MOPS: 10mM $C_7H_{15}NO_4S$, P: KH_2PO_4.

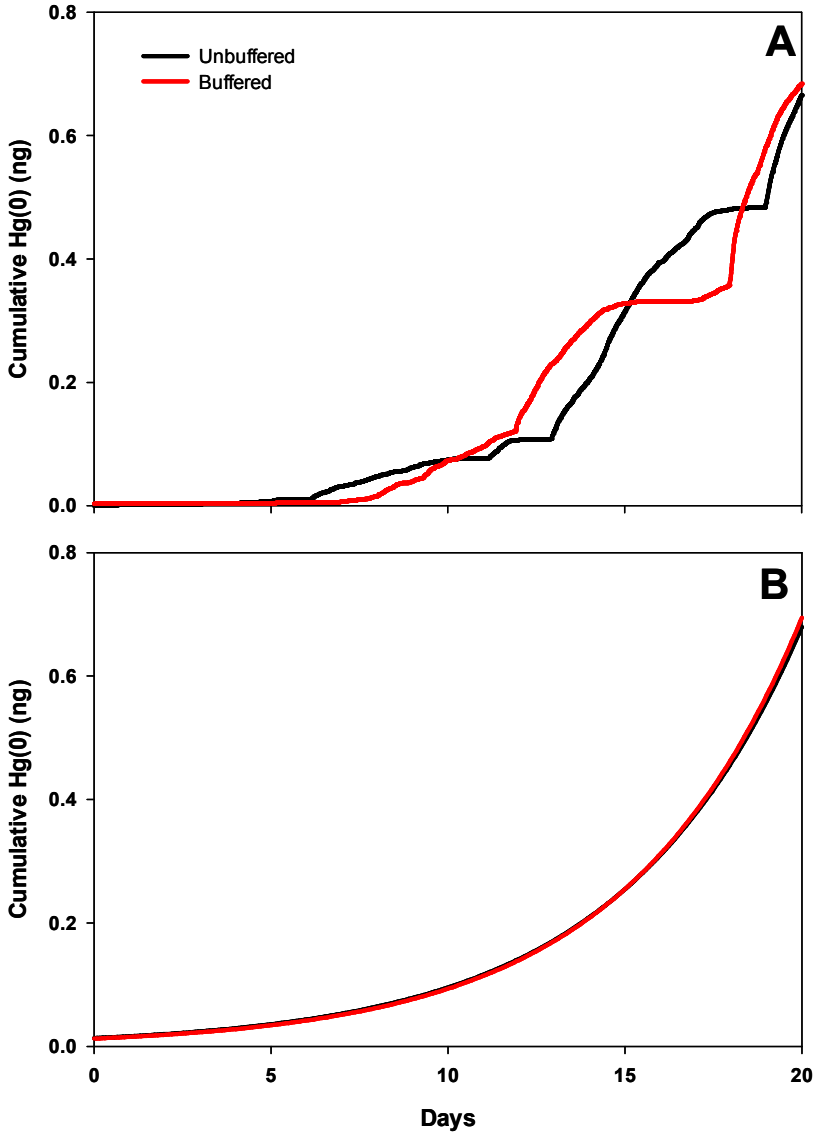

Figure S4.5: Cumulative Hg(0) (ng) emitted from lake sediment microcosms subjected to a pH buffered and un-buffered treatment over a 20 day incubation period. A) Raw data. B) Data transformed by a best-fit model based on exponential growth. Both treatments contained 137mM NaCl, 2.7mM KCl, 8.1 mM Na_2HPO_4 and 1.76mM KH_2PO_4 however the buffered treatment had a pH of 7.4 and the unbuffered treatment had a pH of 5.66.

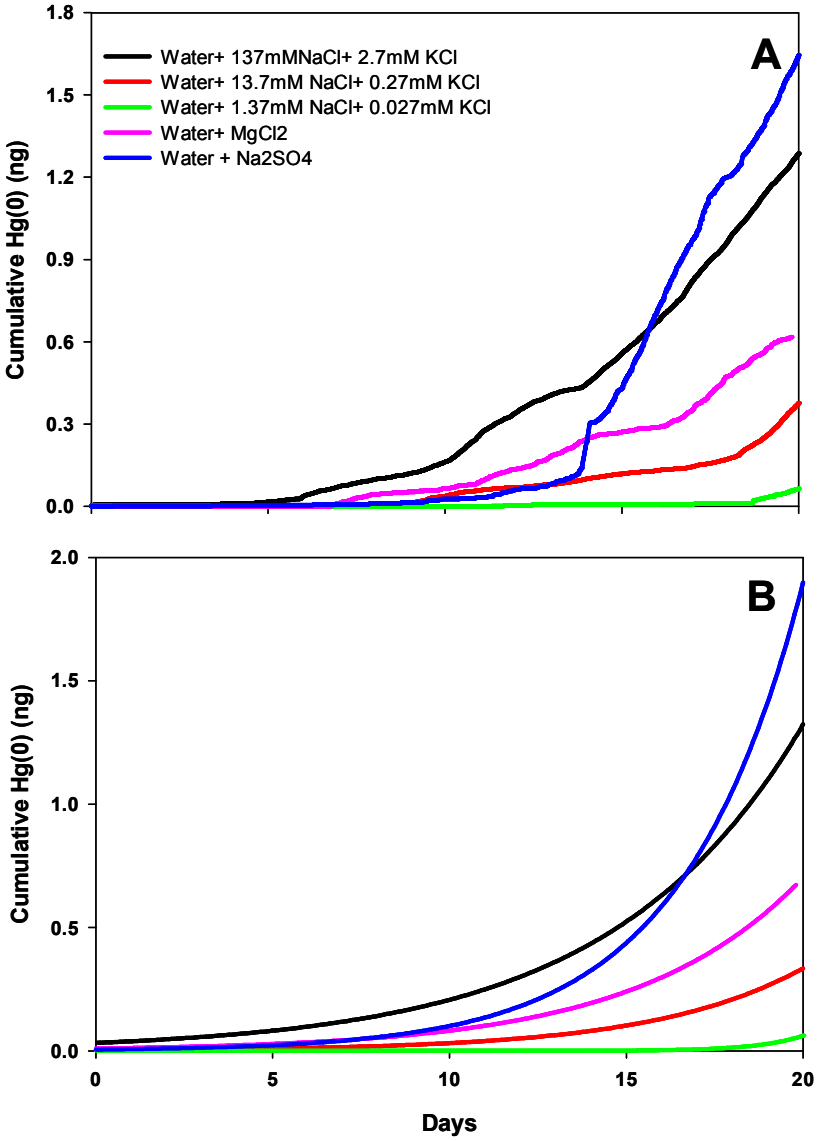

Figure S4.6: Cumulative Hg(0) (ng) emitted from lake sediment microcosms subjected to various ionic strengths over a 20 day incubation period. A) Raw data. B) Data transformed by a best-fit model based on exponential growth.

Chapter 5.0: Conclusions and Perspectives on Future Research

5.1 Conclusions and Perspectives on Future Research

This study is one of the first to investigate the effects of atmospheric mercury (Hg) deposition in pristine lakes of the Hudson Bay Lowlands (HBL) of Northern Ontario. Although the lakes are far removed from anthropogenic activities, the main source of Hg to the atmosphere, I recorded sediment mercury concentrations that compare to those of temperate lakes in urban environments. However, Hg concentrations in lake surface sediments from 13 lakes varied considerably, from 6.13 ± 0.7 ng g^{-1} to 125.4 ± 0.9 ng g^{-1}, underscoring the importance of post-depositional *in situ* processes in Hg cycling. The spatial analysis also revealed that total Hg concentrations are a poor predictor of methylmercury (MeHg) concentrations, the bioaccumulative neurotoxic form of Hg. MeHg concentrations were significantly correlated with organic carbon (OC), suggesting that MeHg formation may be limited by the availability of OC and not the availability of the Hg substrate. In the spatial analysis, Hg and OC were positively correlated in 3 sediment cores, supporting the hypothesis that Hg and OC, i.e. *in situ* productivity, are increasing in tandem. I also used Rock-Eval® analysis, carbon to nitrogen ratios (C:N) and carbon isotopic signatures ($\partial^{13}C$) to support the hypothesis of increasing productivity in lakes of the HBL due to climate warming.

In the second part of this study, I used a molecular approach to assess the impact of increasing Hg concentrations on the microbial populations of the lake sediments. I used the *merA* gene, which encodes the mercuric reductase enzyme capable of reducing ionic Hg (Hg(II)) to its volatile elemental form (Hg(0)), as a proxy of bacterial mercury resistance. In sediment cores from three different lakes, I detected an increase in the *merA* gene abundance in the bacterial genome of sediments deposited before ~1960. I propose that the decrease in merA gene abundance recorded in the uppermost intervals of the cores could be due to a selective pressure for functional forms of the *merA* gene as a response to increasing [Hg]. Further studies should focus on the metatranscriptome of the surface sediment to assess the expression of the *merA* gene by the autochthonous microbial populations of these lakes as my efforts were inconclusive.

The last chapter of this study consisted of experimental incubations to assess the potential for Hg(0) production form sediments of Aquatuk Lake. I used a combination of analytical and molecular tools to confirm that the production of Hg(0) recorded was of a biogenic nature. I performed several treatments to assess the impacts of nutrients, pH and ionic strength on Hg(0) production rates and concluded that ionic strength had the greatest influence on Hg(0) production, with increased Hg(0) production as ionic strength increased. The treatment with the highest ionic strength had a Hg(0) production rate of 4.5×10^{-3} and had transformed 0.21% of the Hg in the system into Hg(0). To put this into perspective, this rate, once corrected for temperature, corresponds to 4% of the Hg deposited annually onto Aquatuk Lake. This is the first report of such rates and I believe this data will be instrumental for Hg modeling and mass-balance studies, which have, until now, underestimated the potential contribution of microbial populations to the Hg redox cycle in lake sediments. Further studies should focus on other environmental variables that could potentially influence the biogenic production of Hg(0) in lake sediments. As ionic strength was shown to play a critical role in Hg(0) production rates, I believe that the impact of ion-rich snow melt runoff from roadways in temperate regions on lakes should be further investigated.

The effect of climate change on the mercury cycle in Arctic and subarctic regions, where temperature increases are predicted to be doubled that of the global average, is one of the most pressing questions of the 21st century. Some predicted changes include a shift in predominant winds, due to changing atmospheric pressure patterns, which will alter the transport of Hg into and out of northern regions (AMAP, 2011). The thawing glaciers and permafrost will release Hg that has been accumulated and stored over centuries and the accompanying organic matter stored in permafrost may stimulate MeHg by methylating bacteria. However, the predominant concern is the longer ice-free season and warmer water temperatures which will lead to increased productivity of lakes and wetlands where Hg methylation is highest (AMAP, 2011). Many indigenous peoples still have blood Hg concentrations exceeding the U.S. EPA's reference dose of 0.1μg kg^{-1} day^{-1} and this

is expected to increase with climate change as Hg availability increases and becomes mobilized in Arctic ecosystems and foodwebs (EPA, 2001; AMAP, 2011).

Methylmercury concentrations are primarily a function of methylation and demethylation rates, thus any reaction modulating the availability of the Hg template, Hg^{2+}, has the potential to directly affect MeHg concentrations and its toxicity (Morel *et al.*, 1998). In my thesis, I demonstrated the potential for Hg reduction by microbes in lakes of the Hudson Bay Lowlands of Ontario. These microbes have the potential to reduce Hg(II) to Hg(0) which then, presumably, leaves the immediate environment and is no longer available to methylating bacteria. I believe that the biological reduction of Hg(II) is of primordial importance when studying the Hg cycle in northern regions that are undergoing acute climate changes. The predicted pulse of Hg and organic matter combined with longer growing seasons and warmer waters of northern lakes and wetlands has the potential to increase Hg methylation but it could also be mitigated by a corresponding increase in bacterial reduction of Hg(II).

5.2 References

AMAP. 2011. Arctic pollution. Editor. Oslo.

EPA, U.S. 2001. Methylmercury (MeHg) (casrn 22967-92-6). Editor.

Morel, F.M.M., A.M.L. Kraepiel and M. Amyot. 1998. The chemical cycle and bioaccumulation of mercury. Annual Review of Ecology and Systematics, 29: 543-566.